Analysis of Kinase Signaling Pathways Regulating Filamentous Development in *Saccharomyces cerevisiae* and *Candida albicans*

by

Kaitlyn L. Norman

A dissertation submitted in partial fulfillment
of the requirements for the degree of
Doctor of Philosophy
(Molecular, Cellular and Developmental Biology)
in the University of Michigan
2017

Doctoral Committee:

Professor Anuj Kumar, Chair
Professor Robert S. Fuller
Professor Daniel J. Klionsky
Professor Laura J. Olsen

Kaitlyn L. Norman

knorm@umich.edu

ORCID iD: 0000-0003-0693-072X

DEDICATION

To my partner in life, Jeremiah, for keeping me grounded and always being the light at the end of a hard day. Without your love, support, sacrifices, silly faces, and comforting smile greeting me each and every day, I could not have succeeded. You were by my side through prelims, through rough days, through failing experiments, and through the end of this dissertation journey. Thank you for choosing me and allowing me to find my place in this world and continually walking beside me through this crazy journey.

To my parents, for instilling in me the value of hard work and self-sufficiency. For never letting me quit and always having the highest expectation of me while also being there to catch me when I inevitably fell. Without you both, I never would have made it in to a PhD program nonetheless finished one.

To my sister, who is one of my biggest inspirations and pillars of strength and courage. As a younger sister, I have always looked up to you. You are such a strong, passionate, and good human being. I strive to be more like you. I am proud of all of your accomplishments and the continuous example you set for always speaking up for what you believe in and being true to who you are.

To my fur babies, Moose (the cat) and Widget (the dog), both of whom I found on this journey through graduate school. For keeping me warm during prelim writing, for loving me unconditionally on my hardest of days, for making sure I don't take life too seriously, and

especially for always waking me promptly at 5 AM (even on the weekends) to make sure I always got my work done. Without your snuggles, licks, play times and unwavering love, my life would not be so bright.

ACKNOWLEDGEMENTS

I must extend my deepest and sincerest gratitude to a number of people whom without I would not have been able to complete this dissertation work. First and foremost, I would like to thank my advisor Dr. Anuj Kumar. Thank you for guiding me and allowing me to think critically about my own science. Even more so, thank you for allowing me to explore other opportunities and gain valuable skills outside of lab work and supporting me in my efforts to find a non-traditional job on completion of this PhD program.

I would also like to thank my committee members, Dr. Daniel J. Klionsky, Dr. Robert Fuller, and Dr. Laura Olsen for providing valuable feedback and ideas over the past several years. Additionally, I would like to thank Bob for generously lending me his HPLC, which ended up assisting in a large portion of data for my thesis work.

It is especially important for me to thank Dr. Adolfo Saiardi for welcoming me in to his lab for three weeks, teaching me new techniques which were essential to finishing my dissertation work, and guiding me through the wonderful culture of London.

I would like to thank my many lab members through the years for the stimulating conversation, ideas, and suggestions to my work. Finally, I would like to thank all of my friends and graduate students within MCDB for always being available for a beer on a good day or bad. I wouldn't have made it out half has sane without your company and shenanigans throughout the past five years.

PREFACE

This dissertation summarizes research that I have conducted over the past five years while working in Dr. Anuj Kumar's laboratory. Sections of this thesis have been previously published and are presented here with some modifications as outlined below.

Chapter two is work that has been previously published as follows: Shively CA, Kweon HK, Norman KL, Mellacheruvu D, Xu T, Sheidy DT, et al. (2015) Large-Scale Analysis of Kinase Signaling in Yeast Pseudohyphal Development Identifies Regulation of Ribonucleoprotein Granules. PLoS Genet 11(10): e1005564. https://doi.org/10.1371/journal.pgen.1005564. Shively CA, Kweon HK, and I are listed as co-first authors and contributed equally to the work and generated the vast majority of the data. Hye Kyong Kweon from Phil Andrews's laboratory conducted the mass-spectrometry experiment. Christian Shively and I contributed equally to the genetic analysis, pseudohyphal growth analysis, and characterization of all ribonucleoprotein granule components that were identified through the mass spectrometry dataset. Specifically, I contributed: Fig 2.1 B-D, Fig 2.3 B, Fig 2.4, Fig 2.6, Fig 2.7 D and F, Fig 2.8 A and C, Fig 2.10, and Fig 2.11.

All figures and data in Chapter 3 were created directly by me.

Chapter four contains portions of work, with modifications, from a paper in which I was second author and has been published in full as follows: Saputo S, Norman KL, Murante T,

Horton BN, De La Cruz Diaz J, DiDone L et al. (2016) Complex Haploinsufficiency-Based Genetic Analysis of the NDR/Lats Kinase Cbk1 Provides Insight into its Multiple Functions in *Candida albicans*. Genetics. 203(3): 1217-1233. https://doi.org/10.1534/genetics.116.188029. Saputo *et al*. conducted the large screen and my work encompassed validation and characterization of genetic interactions. As such, the portions of this paper relating to how the screen was conducted and initial findings have been excluded from this thesis. The results and all of the figures presented here were produced directly by me or with equal contribution from Sara Saputo.

TABLE OF CONTENTS

LIST OF FIGURES

LIST OF TABLES

ABSTRACT

Yeast pseudohyphal growth is a stress response characterized by elongated cell morphology, exaggerated polarized growth, and increased cell-cell adhesion. The signaling network that regulates the formation of pseudohyphal filaments has been the subject of intense research interest, as filament formation is required for virulence in numerous pathogenic fungi. Pseudohyphal growth is regulated through highly conserved kinase pathways, encompassing MAPK/ERK, PKA, and AMPK signaling modules; however, the full scope of these pathways has not been elucidated fully. To address this knowledge gap, quantitative phosphoproteomics was used in *Saccharomyces cerevisiae* to identify differentially phosphorylated proteins in kinase-deficient mutant strains surveyed under conditions inducing pseudohyphal growth. The use of stable isotope labeling of amino acids in cell culture (SILAC) and liquid chromatography-mass spectrometry/mass spectrometry (LC-MS/MS) analysis of phosphopeptide-enriched samples, identified 439 phosphoproteins and 539 novel phosphorylated residues dependent on a pseudohyphal growth kinase. This data set yielded two interesting results. First, the identified phosphoprotein set was significantly enriched for ribonucleoprotein (RNP) granule components, including P-bodies and stress granules. Through fluorescence microscopy of GFP-chimeras, co-localization of the MAPK cascade proteins Kss1p, Ste20p, Fus3p, and also PKA (Tpk2p) with the RNP component Igo1p was observed. Furthermore, Kss1p kinase activity was required for wild-type levels of mRNA localization in P-bodies. Second, the phosphoproteomic data set

indicated that a statistically significant set of kinases mediating inositol polyphosphate (IP) signaling undergoes pseudohyphal growth kinase-dependent phosphorylation. Deletion of kinases in the IP synthesis pathway resulted in aberrant pseudohyphal growth, and through metabolic labeling of IP species, striking changes in IP levels under pseudohyphal growth conditions were observed. In particular, a correlation between increased filamentous growth and the presence of high levels of the inositol pyrophosphate produced by Kcs1p, 5PP-IP_5 were found. Additionally, interesting changes in IP levels upon the deletion of key kinases involved in the pseudohyphal growth transition were observed. With the relevance of yeast pseudohyphal growth as a model of filamentous development in the pathogen *Candida albicans*, these studies investigated the role of the *C. albicans* cell wall integrity kinase Cbk1p in morphogenesis during hyphal development. In collaborative studies with Damian Krysan's group at the University of Rochester, this work indicated a mechanism where *Ca*Cbk1p regulates cross-talk between the RAM and PKA pathways. Taken together, the doctoral research presented here provides insight into the mechanisms through which conserved kinase signaling networks regulate filamentous growth, with particular relevance in understanding the mechanisms controlling RNP dynamics and regulated IP biogenesis.

CHAPTER 1

Introduction

1.1 *Saccharomyces cerevisiae* as a Genetic Model

The baker's yeast *Saccharomyces cerevisiae* has long been used as an important model for studying genetics and eukaryotic cellular mechanisms. *S. cerevisiae* is a small unicellular organism that divides by budding, an event in which a daughter cell grows from a mother cell and is eventually pinched off [1]. *S. cerevisiae* can exist as a haploid cell of one of two mating types (**a** and α). Two haploids with opposite mating types can then mate to form a diploid cell [1]. The commonly used S288c strain of *S. cerevisiae* (or genetic derivatives of this strain) has been instrumental in promoting genetic advances largely because it can exist as a stable heterothallic haploid while other strains are often homothallic diploids [2,3]. Both haploid and diploid cells divide rapidly in a laboratory setting under ideal conditions in rich media, making yeast inexpensive to culture and easy to maintain [4].

The ease of use of *S. cerevisiae*, along with the discovery in the 1950s that it could be crossed and traits could therefore be isolated over time, made it an ideal model organism, even before it became the first eukaryotic organism to have its entire genome sequenced in 1996 [5,6]. Additionally, the large collection of techniques discovered that can be used to easily and efficiently manipulate the genetic makeup of *S. cerevisiae*, such as the ability to "transform" yeast with foreign DNA and have them uptake it into the chromosome through homologous

recombination, has advanced *S. cerevisiae* as a genetically tractable organism [7,8]. The capability to manipulate the relatively small genome of *S. cerevisiae*, along with the availability of the entire genetic sequence, paved way for the completion of libraries of strains including a full deletion collection of non-essential genes [9] as well as several extensive overexpression libraries [10-13], all of which can be utilized for both small and large-scale analysis of genes (reviewed in [14]). A database of all *S. cerevisiae* genetic and functional information is easily found and referenced through the Saccharomyces Genome Database (SGD; http://www.yeastgenome.org) allowing researchers to quickly gather known information of any gene of interest. The continuing evolution and advancement of techniques in yeast biology has opened up new fields of research such as functional genomics and systems biology, which focus on the more expansive view of how networks of genes and proteins work together to accomplish cellular goals [15].

Experiments utilizing *S. cerevisiae* have been instrumental in advancing knowledge regarding yeast function and evolution, while also elucidating functions in higher eukaryotes. Not only are many genes, proteins, and pathways conserved from yeast to higher organisms, but also genetic techniques allow the expression of heterologous proteins from humans and other metazoans in a yeast cell [16]. This makes yeast an attractable model for studying human diseases or for elucidating pathogenic mechanisms of fungi such as *Candida albicans* and *Cryptococcus neoformans* [17-19].

1.2 General Stress Responses in Yeast

Organisms in their natural environment are often exposed to a variety of environmental stressors including temperature fluctuations, nutrient limitation, osmotic concentrations, and

oxidative stress. For example, *S. cerevisiae* encounters a large number of environmental changes during the production of dough in baking, as well as the fermentation processes involved in the production of wine and beer, including increased sugar content, oxidative stress, and increased alcohol levels. The majority of stressors are considered unfavorable, and, therefore, the cell must act appropriately in order to properly mitigate the stress for continued growth. *S. cerevisiae* has been utilized informatively to understand how cells react to different stresses and what cellular mechanisms are triggered under each particular stress.

S. cerevisiae undergoes a general stress response known as the environmental stress response (ESR). The ESR encompasses a group of roughly 900 genes that react in response to temperature, osmotic shock, hydrogen peroxide, amino acid starvation, nitrogen depletion, as well as various other environmental triggers [20]. Roughly two thirds of these genes are inhibited during ESR activation, while 300 of them are activated [21,22]. A large portion of the genes that are repressed during the ESR encode ribosomal proteins as well as those proteins involved in ribosomal assembly, since the cell largely shifts its focus away from cellular division and replication during stress [23,24]. While this collection of genes is generally affected by a large group of stressors, each environmental stress also produces its own specific response on the cell [22]. The specific response seen in a given condition often results from the activation of specific signaling pathways that are activated upon an environmental stimulus. The coordinated response between the ESR and this specific response often stems from the complex regulation of translation, transcription, and post-transcriptional modifications [25].

1.3 Filamentous Growth

One specific type of environmental stress is nitrogen depletion. Nitrogen stress is also

one of the main triggers that induce filamentous growth in *S. cerevisiae* [26]. In rich media and normal growth conditions, yeast develops as round budding cells, and this characteristic mode of morphology and division is often referred to as yeast-form growth. However, when stressed, yeast cells can undergo a growth change to form long, interconnected filaments. These elongated chains of cells that remain attached at the cell wall are known as pseudohyphae. This dramatic growth transition often occurs under environmental conditions of nutrient stress. The two most studied stressors, and those conditions most often used to induce filamentous growth in the lab, are nitrogen depletion [26] as well as growth on an alternate carbon source [27]. Since nutrient limitation typically causes filamentous growth, this growth transition is hypothesized to be a scavenging mechanism that yeast can utilize to spread out and search for nutrients when they are limiting [28]. It is important to note that most strains of *S. cerevisiae* (such as S288c) have lost the ability to undergo filamentous growth because of a mutation in the flocculence gene *FLO8*. This mutation was most likely selected for when choosing a strain whose cells were easy to separate [29]. Therefore, a "wild-type" filamentous strain, Σ1278b, that has a properly functioning *FLO8* gene and can undergo this growth transition, is most often used for experimental procedures exploring pseudohyphal growth [28,30].

1.3.1 Filamentous Growth in *S. cerevisiae* as a Model for Fungal Pathogenicity

Filamentous growth has been the focus of scientific studies for decades for two main reasons: 1) its connection with fungal pathogenicity and 2) the highly conserved signaling pathways that regulate the transition from yeast-form to pseudohyphal growth. Fungal pathogens can have a detrimental affect to our society, especially in those individuals that are immunocompromised or immunosuppressed. Invasive fungal infections increase the rate of

mortality and the length of hospitalization stays and therefore associated hospital costs [31,32]. Signaling pathways that regulate *S. cerevisiae* pseudohyphal growth are homologous to those used in other filamentous fungal pathogens, especially in the closely related opportunistic fungal pathogen *Candida albicans* [33]. Other pathogens that utilize the ability to switch between a yeast-form and a filamentous form are *Cryptococcus, Aspergillus*, and *Pneumocystis*. The ability of these pathogens to become virulent is heavily linked to their ability to transition back and forth between the two growth forms [34-36]. Since *S. cerevisiae* utilizes the same signaling pathways, is an easy and inexpensive organism to culture in the laboratory, and is a genetically tractable organism, it is an ideal model organism to study the mechanisms that control fungal virulence through the filamentous growth transition [19].

1.3.2 Phenotypic Assays for Visualization of Pseudohyphal Growth in *S. cerevisiae*

This growth transition can be phenotypically visualized using several experimental assays. One of the most commonly used assays is an invasive growth assay [37,38]. As *S. cerevisiae* begins to filament on solid media, it will start to invade the agar [37]. The surface colony can then be gently washed away and all that remains are those cells that have embedded below the surface of the agar [37]. While both haploid and diploid cells have the ability to invade agar, this assay is most commonly done in haploid cells. Another common assay used is to assess the surface spread filamentation of diploid cells [39]. This is done using low nitrogen media known as synthetic low ammonium dextrose (SLAD) that only contains 50 μM of ammonium sulfate [39]. After growing diploid cells on SLAD agar for four days, pseudohyphae can be visualized protruding from the edges of the colony in a wild-type strain using microscopy [26]. Some haploid strains have the ability to produce pseudohyphae and exhibit filamentous surface

spreading, but it is a phenotype predominately seen in diploid cells and therefore, is the most common technique used in diploid phenotypic assays for filamentous growth. Filamentous growth can be seen in liquid culture with the addition of 1% butonal, which is thought to mimic the response seen under nitrogen starvation. The regulatory machinery used during invasive growth, surface spread, and butonal induced filamentation has been found to be mostly similar [37,40].

1.3.3 Characteristics of Pseudohyphal Growth in *S. cerevisiae*

Pseudohyphal growth has three main and distinctive characteristics: change in polar budding pattern of diploids [26,41], an increased cell length and shape and increased cell-cell adhesion [42-45]. Yeast growth under ideal conditions exhibits a very distinctive budding pattern that is different between haploids and diploid. Haploids exhibit an axial budding pattern while diploids undergo bipolar budding [46]. However, upon induction of filamentous growth, both haploids and diploids switch to a distal-unipolar budding pattern in which new cells only form at the distal pole [37]. The change in polarity [47], along with an extension of the cell cycle [48], causes the increased length of filamentous cells. Cell-cell adhesion seen during filamentous growth is caused by several genes, including the well studied flocculence gene *FLO11* (also known as *MUC1)* [43,44], which is considered to be one of the master down stream effectors of filamentous growth signaling pathways and is necessary in order for yeast to undergo invasive filamentation on solid media [49] as well as biofilm formation [50]. While these changes occur in coordination with each other, they are largely regulated by separate mechanisms [41,51].

1.3.4 Kinase Signaling Pathways Involved in Pseudohyphal Growth

Over the past two and a half decades, research has been largely focused on understanding how this growth transition is initiated, regulated, and how each of the three characteristics are affected and in turn coordinated. Most extensively studied are three predominate signaling pathways: mitogen activated protein kinase (MAPK) pathway, protein kinase A (PKA), and the AMP activated kinase Snf1p (sucrose nonfermentable). All of these pathways sense stress through cell-membrane proteins and this information is relayed through multiple protein phosphorylation events that ultimately affect transcription of downstream effector genes, the most predominate being *FLO11* [28]. Though these pathways have been traditionally thought of as very independent and linear pathways, research is continually revealing that there is more cross-talk between these pathways than previously thought and still a large number of signaling targets that are unknown [52]. The majority of research presented later in this thesis is aimed at exploring previously unknown factors that contribute to the transition of yeast-form to filamentous growth through kinase signaling pathways.

1.3.4.1 Filamentous MAPK Pathway

Mitogen activated protein kinase (MAPK) pathways are highly conserved signaling pathways in eukaryotic organisms [53]. These pathways work through a common signaling mechanism that consists of a phosphorylation cascade that is initiated when a MAPK kinase kinase (MAPKKK) phosphorylates a MAPK kinase (MAPKK) that then finally phosphorylates a MAPK [53]. The downstream MAPK often affects nuclear components upon activation such as transcription factors that can then affect gene expression [53]. Yeast have multiple MAPK pathways that regulate responses during mating [54], osmotic tolerance [55], and filamentous growth [28]. During filamentous growth, the upstream sensors Msb2p, Ras2p, and Cdc42p sense

nutrient limitation. This sensory information is eventually relayed to the p21-activated kinase (PAK) family member Ste20p that becomes activated and phosphorylates the MAPKKK Ste11p, which in turn activates Ste7p (MAPKK). The MAPK that predominately acts during filamentous growth regulation is Kss1p [28,37,38,56,57]. Under normal growth conditions, Kss1p is inhibited but becomes activated by the phosphorylation of Ste7p [57]. This allows Kss1p to signal Ste12p and Tec1p toward filamentous growth genes containing a filamentous growth response element (FRE) or a Tec1 binding site, such as *FLO11* [58,59].

The Ste20p-Ste11p-Ste7p cascade is also the common core set of proteins used in the pheromone responsive MAPK mating pathway. How the cell distinguishes the different pathways when they share signaling proteins [60,61] but induce different physiological responses is still continually being studied. Research has found that the use of different MAPKs and transcription factors may be a contributing factor to specificity. Kss1p can also function in the mating pathways but it is thought to only occur in the absence of Fus3p, the MAPK used by the mating pathway. Interestingly, a *fus3*Δ strain exhibits increased pseudohyphal growth, suggesting it too plays some type of regulatory role during filamentous growth transition.

1.3.4.2 RAS/cAMP-Dependent Protein Kinase A (PKA)

While yeast contains two rat sarcoma (RAS) genes*, RAS1* and *RAS2*, it is *RAS2* that predominately works in filamentous growth regulation because of its control of adenylate cyclase, which produces cyclic adenosine monophosphate (cAMP) [62,63]. cAMP levels directly contribute to the ability of *S. cerevisiae* to filament [56]. cAMP binds Bcy1p, thus releasing PKA and activating it. In *S. cerevisiae* all three PKAs (Tpk1p, Tpk2, and Tpk3) have the ability to bind Bcy1p, but each PKA has a different effect on the regulation of filamentous growth [64,65].

Tpk3p has an inhibitory affect on filamentous growth, although the mechanism of this regulation and its cellular targets are still largely unknown [64]. Activation of Tpk2p leads to the phosphorylation of the transcription factor *FLO8*, which activates filamentous growth genes. Loss of Tpk2p leads to a loss of filamentous growth [65,66]. While the deletion of *TPK1* seems to have no phenotypic affect on filamentous growth, it phosphorylates Yak1p deactivating it so it can no longer regulate *FLO11* activity [67,68]. Upstream of Ras2, the G-protein coupled receptor Gpr1p is thought to sense glucose limitation and possibly sucrose and then signal through the G protein alpha subunit Gpa2 [69,70]. Gpa2 works at the same level as Ras2 and helps to regulate cAMP levels, which ultimately control PKA activation and filamentous growth response genes [71,72].

1.3.4.3 AMP Activated Kinase Snf1p

The AMP activated protein kinase Snf1p was found to regulate filamentous growth when it was determined that glucose depletion triggers filamentous growth [27]. Unlike the PKA pathway, which utilizes the G-protein coupled receptor Gpr1 to sense glucose levels, Snf1p works by the regulation of two repressors, Nrg1 and Nrg2, that bind the *FLO11* promoter [73,74]. Recently, Snf1p was also found to have a non-canoncical guanine-nucleotide exchange factor (GEF) domain that binds and activates the ADP-ribosylation factor Arf3p [75]. Arf3p is necessary for invasive growth, involved in cell polarity, and its activity is stimulated upon depletion of glucose [76,77]. Interestingly, Snf1p regulation of Arf3 is independent of its kinase activity and instead involves elements of the regulatory domain suggesting a Snf1p dependent regulatory mechanism of filamentous growth outside of its kinase ability [75].

1.3.5 Filamentous Growth in *Candida albicans*

As mentioned above, *Candida albicans* is an opportunistic fungal pathogen that causes serious health problems in immunocompromised individuals. Normally, *C. albicans* is a commensal fungus that lives in our mucosal membranes without causing an infection [78,79]. However, when an individual has a suppressed immune system such as during chemotherapy treatment or patients with AIDS, *C. albicans* can cause an infection [79]. *C. albicans* is the most common human fungal pathogen [80] acquired while in the hospital and can cause various diseases including easily treatable mucosal infections to a full systemic disease [81]. While *C. albicans* was first identified in the 1800s as the cause of oral flush, scientific advancements have been relatively slow [82]. Unlike *S. cerevisiae* that can exist as a stable haploid and diploid, *C. albicans* is considered an "obligate diploid" [83]. Additionally, homologous recombination occurs at a lower frequency, The CUG codon codes for Leucine instead of the standard Serine [84], there is no propagation of plasmids, and it is resistant to a large number of antibiotics [82]. These characteristics make *C. albicans* a difficult organism to study in the laboratory, although there has been an increase in the development and availability of relevant tools for *C. albicans* genetics, revitalizing efforts to study this organism in recent years.

C. albicans can transition from yeast-form to pseudohyphae much like *S. cerevisiae.* However, it is also able to form true multinucleated hyphae, which *S. cerevisiae* is incapable of forming [85]. Traditionally, the ability to filament was considered to be necessary for *C. albicans* pathogenicity because cells that were not able to filament were unable to cause an infection [86]. However, recently it has been shown the ability to switch between hyphae and yeast-form is what is most important for virulence, because if a cell is locked in the yeast-form it also cannot form an infection [86]. Therefore, the cell must be able to switch from one form to another and

back again in order for it to be virulent. Naturally, the filamentous growth transition is thought to be a scavenging mechanism much like that in *S. cerevisiae.* In the lab, this growth transition can be induced by growth in near body temperatures (37°C) along with molecules found in serum, Spider media, or Lee's media [87].

Complex signaling networks, including conserved kinase pathways also seen to regulate *S. cerevisiae* pseudohyphal growth, like the cAMP-dependent PKA pathway and the MAPK pathway, regulate filamentous growth in *C. albicans* [88-90]. Another pathway conserved in *S. cerevisiae* that regulates filamentous growth in *C. albicans* is the Regulation of Ace2 and Morphogenesis (RAM) pathway [91]. The RAM pathway does not induce the pseudohyphal growth transition in *S. cerevisiae* and is thought to regulate hyphal development outside of nutrient signaling.

In subsequent chapters, this thesis will consider signaling pathways and cellular processes that regulate pseudohyphal growth in *S. cerevisiae* and hyphal growth in *C. albicans*, particularly with respect to the RAM pathway in regards to the latter. The research in Chapters 2 and 3 identify roles for mRNP biogenesis and inositol polyphosphate signaling, respectively, in contributing to the wild-type *S. cerevisiae* filamentous growth response. The research collectively highlights the complex signaling interconnections driving filamentation, identifying new aspects of yeast cell biology involved in this important growth transition.

1.5 References

1. Herskowitz I (1988) Life cycle of the budding yeast Saccharomyces cerevisiae. Microbiol Rev 52: 536-553.

2. Mortimer RK (2000) Evolution and variation of the yeast (Saccharomyces) genome. Genome Res 10: 403-409.

3. Cubillos FA, Vasquez C, Faugeron S, Ganga A, Martinez C (2009) Self-fertilization is the main sexual reproduction mechanism in native wine yeast populations. FEMS Microbiol Ecol 67: 162-170.

4. Duina AA, Miller ME, Keeney JB (2014) Budding Yeast for Budding Geneticists: A Primer on the Saccharomyces cerevisiae Model System. Genetics 197: 33-48.

5. Dujon B (1996) The yeast genome project: what did we learn? Trends Genet 12: 263-270.

6. Mortimer RK, Johnston JR (1986) Genealogy of principal strains of the yeast genetic stock center. Genetics 113: 35-43.

7. Hinnen A, Hicks JB, Fink GR (1978) Transformation of yeast. Proc Natl Acad Sci U S A 75: 1929-1933.

8. Eckert-Boulet N, Rothstein R, Lisby M (2011) Cell Biology of Homologous Recombination in Yeast. Methods Mol Biol 745: 523-536.

9. Giaever G, Nislow C (2014) The yeast deletion collection: a decade of functional genomics. Genetics 197: 451-465.

10. Sopko R, Huang D, Preston N, Chua G, Papp B, et al. (2006) Mapping pathways and phenotypes by systematic gene overexpression. Mol Cell 21: 319-330.

11. Douglas AC, Smith AM, Sharifpoor S, Yan Z, Durbic T, et al. (2012) Functional analysis with a barcoder yeast gene overexpression system. G3 (Bethesda) 2: 1279-1289.

12. Jones GM, Stalker J, Humphray S, West A, Cox T, et al. (2008) A systematic library for comprehensive overexpression screens in Saccharomyces cerevisiae. Nat Methods 5: 239-241.

13. Gelperin DM, White MA, Wilkinson ML, Kon Y, Kung LA, et al. (2005) Biochemical and genetic analysis of the yeast proteome with a movable ORF collection. Genes Dev 19: 2816-2826.

14. Norman KL, Kumar A (2016) Mutant power: using mutant allele collections for yeast functional genomics. Brief Funct Genomics 15: 75-84.

15. Botstein D, Fink GR (2011) Yeast: An Experimental Organism for 21st Century Biology. Genetics 189: 695-704.

16. Mokdad-Gargouri R, Abdelmoula-Soussi S, Hadiji-Abbes N, Amor IY, Borchani-Chabchoub I, et al. (2012) Yeasts as a tool for heterologous gene expression. Methods Mol Biol 824: 359-370.

17. Miller-Fleming L, Giorgini F, Outeiro TF (2008) Yeast as a model for studying human neurodegenerative disorders. Biotechnol J 3: 325-338.

18. Smith MG, Snyder M (2006) Yeast as a model for human disease. Curr Protoc Hum Genet Chapter 15: Unit 15 16.

19. Goldstein AL, McCusker JH (2001) Development of Saccharomyces cerevisiae as a model pathogen. A system for the genetic identification of gene products required for survival in the mammalian host environment. Genetics 159: 499-513.

20. Gasch AP, Spellman PT, Kao CM, Carmel-Harel O, Eisen MB, et al. (2000) Genomic Expression Programs in the Response of Yeast Cells to. Mol Biol Cell 11: 4241-4257.

21. Gasch AP (2007) Comparative genomics of the environmental stress response in ascomycete fungi. Yeast 24: 961-976.

22. Causton HC, Ren B, Koh SS, Harbison CT, Kanin E, et al. (2001) Remodeling of yeast genome expression in response to environmental changes. Mol Biol Cell 12: 323-337.

23. Gasch AP (2003) The environmental stress response: a common yeast response to diverse environmental stresses. In: Hohmann S, Mager WH, editors. Yeast Stress Responses. Berlin, Heidelberg: Springer Berlin Heidelberg. pp. 11-70.

24. Gasch AP, Spellman PT, Kao CM, Carmel-Harel O, Eisen MB, et al. (2000) Genomic expression programs in the response of yeast cells to environmental changes. Mol Biol Cell 11: 4241-4257.

25. Ho YH, Gasch AP (2015) Exploiting the yeast stress-activated signaling network to inform on stress biology and disease signaling. Curr Genet 61: 503-511.

26. Gimeno CJ, Ljungdahl PO, Styles CA, Fink GR (1992) Unipolar cell divisions in the yeast *S. cerevisiae* lead to filamentous growth: regulation by starvation and RAS. Cell 68: 1077-1090.

27. Cullen PJ, Sprague GF, Jr. (2000) Glucose depletion causes haploid invasive growth in yeast. Proc Natl Acad Sci U S A 97: 13619-13624.

28. Cullen PJ, Sprague GF (2012) The Regulation of Filamentous Growth in Yeast. Genetics 190: 23-49.

29. Kron SJ (1997) Filamentous growth in budding yeast. Trends Microbiol 5: 450-454.

30. Liu H, Styles CA, Fink GR (1996) Saccharomyces cerevisiae S288C has a mutation in FLO8, a gene required for filamentous growth. Genetics 144: 967-978.

31. Menzin J, Meyers JL, Friedman M, Perfect JR, Langston AA, et al. (2009) Mortality, length of hospitalization, and costs associated with invasive fungal infections in high-risk patients. Am J Health Syst Pharm 66: 1711-1717.

32. Wilson LS, Reyes CM, Stolpman M, Speckman J, Allen K, et al. (2002) The direct cost and incidence of systemic fungal infections. Value Health 5: 26-34.

33. Yapar N (2014) Epidemiology and risk factors for invasive candidiasis. Ther Clin Risk Manag 10: 95-105.

34. Lo HJ, Kohler JR, DiDomenico B, Loebenberg D, Cacciapuoti A, et al. (1997) Nonfilamentous C. albicans mutants are avirulent. Cell 90: 939-949.

35. Wang L, Zhai B, Lin X (2012) The link between morphotype transition and virulence in Cryptococcus neoformans. PLoS Pathog 8: e1002765.

36. Fortwendel JR, Juvvadi PR, Rogg LE, Asfaw YG, Burns KA, et al. (2012) Plasma membrane localization is required for RasA-mediated polarized morphogenesis and virulence of Aspergillus fumigatus. Eukaryot Cell 11: 966-977.

37. Roberts RL, Fink GR (1994) Elements of a single MAP kinase cascade in Saccharomyces cerevisiae mediate two developmental programs in the same cell type: mating and invasive growth. Genes Dev 8: 2974-2985.

38. Madhani HD, Styles CA, Fink GR (1997) MAP kinases with distinct inhibitory functions impart signaling specificity during yeast differentiation. Cell 91: 673-684.

39. Gimeno CJ, Fink GR (1994) Induction of pseudohyphal growth by overexpression of PHD1, a Saccharomyces cerevisiae gene related to transcriptional regulators of fungal development. Mol Cell Biol 14: 2100-2112.

40. Lorenz MC, Cutler NS, Heitman J (2000) Characterization of alcohol-induced filamentous growth in Saccharomyces cerevisiae. Mol Biol Cell 11: 183-199.

41. Palecek SP, Parikh AS, Kron SJ (2000) Genetic analysis reveals that FLO11 upregulation and cell polarization independently regulate invasive growth in Saccharomyces cerevisiae. Genetics 156: 1005-1023.

42. Birkaya B, Maddi A, Joshi J, Free SJ, Cullen PJ (2009) Role of the cell wall integrity and filamentous growth mitogen-activated protein kinase pathways in cell wall remodeling during filamentous growth. Eukaryot Cell 8: 1118-1133.

43. Lambrechts MG, Bauer FF, Marmur J, Pretorius IS (1996) Muc1, a mucin-like protein that is regulated by Mss10, is critical for pseudohyphal differentiation in yeast. Proc Natl Acad Sci U S A 93: 8419-8424.

44. Lo WS, Dranginis AM (1998) The cell surface flocculin Flo11 is required for pseudohyphae formation and invasion by Saccharomyces cerevisiae. Mol Biol Cell 9: 161-171.

45. Guo B, Styles CA, Feng Q, Fink GR (2000) A Saccharomyces gene family involved in invasive growth, cell-cell adhesion, and mating. Proc Natl Acad Sci U S A 97: 12158-12163.

46. Chant J, Pringle JR (1991) Budding and cell polarity in Saccharomyces cerevisiae. Curr Opin Genet Dev 1: 342-350.

47. Pruyne D, Bretscher A (2000) Polarization of cell growth in yeast. J Cell Sci 113 (Pt 4): 571-585.

48. Kron SJ, Styles CA, Fink GR (1994) Symmetric cell division in pseudohyphae of the yeast Saccharomyces cerevisiae. Mol Biol Cell 5: 1003-1022.

49. Casalone E, Barberio C, Cappellini L, Polsinelli M (2005) Characterization of Saccharomyces cerevisiae natural populations for pseudohyphal growth and colony morphology. Res Microbiol 156: 191-200.

50. Reynolds TB, Fink GR (2001) Bakers' yeast, a model for fungal biofilm formation. Science 291: 878-881.

51. Cullen PJ, Sprague GF, Jr. (2002) The roles of bud-site-selection proteins during haploid invasive growth in yeast. Mol Biol Cell 13: 2990-3004.

52. Shively CA, Kweon HK, Norman KL, Mellacheruvu D, Xu T, et al. (2015) Large-Scale Analysis of Kinase Signaling in Yeast Pseudohyphal Development Identifies Regulation of Ribonucleoprotein Granules. PLoS Genet 11: e1005564.

53. Yang SH, Sharrocks AD, Whitmarsh AJ (2013) MAP kinase signalling cascades and transcriptional regulation. Gene 513: 1-13.

54. Bardwell L (2005) A walk-through of the yeast mating pheromone response pathway. Peptides 26: 339-350.

55. Saito H, Tatebayashi K (2004) Regulation of the osmoregulatory HOG MAPK cascade in yeast. J Biochem 136: 267-272.

56. Mosch HU, Roberts RL, Fink GR (1996) Ras2 signals via the Cdc42/Ste20/mitogen-activated protein kinase module to induce filamentous growth in Saccharomyces cerevisiae. Proc Natl Acad Sci U S A 93: 5352-5356.

57. Cook JG, Bardwell L, Thorner J (1997) Inhibitory and activating functions for MAPK Kss1 in the *S. cerevisiae* filamentous-growth signalling pathway. Nature 390: 85-88.

58. Zeitlinger J, Simon I, Harbison CT, Hannett NM, Volkert TL, et al. (2003) Program-specific distribution of a transcription factor dependent on partner transcription factor and MAPK signaling. Cell 113: 395-404.

59. Rupp S, Summers E, Lo HJ, Madhani H, Fink G (1999) MAP kinase and cAMP filamentation signaling pathways converge on the unusually large promoter of the yeast FLO11

gene. EMBO J 18: 1257-1269.

60. Liu H, Styles CA, Fink GR (1993) Elements of the yeast pheromone response pathway required for filamentous growth of diploids. Science 262: 1741-1744.

61. Posas F, Saito H (1997) Osmotic activation of the HOG MAPK pathway via Ste11p MAPKKK: scaffold role of Pbs2p MAPKK. Science 276: 1702-1705.

62. Kataoka T, Powers S, McGill C, Fasano O, Strathern J, et al. (1984) Genetic analysis of yeast RAS1 and RAS2 genes. Cell 37: 437-445.

63. Toda T, Uno I, Ishikawa T, Powers S, Kataoka T, et al. (1985) In yeast, RAS proteins are controlling elements of adenylate cyclase. Cell 40: 27-36.

64. Pan X, Heitman J (1999) Cyclic AMP-dependent protein kinase regulates pseudohyphal differentiation in Saccharomyces cerevisiae. Mol Cell Biol 19: 4874-4887.

65. Robertson LS, Fink GR (1998) The three yeast A kinases have specific signaling functions in pseudohyphal growth. Proc Natl Acad Sci U S A 95: 13783-13787.

66. Pan X, Heitman J (2002) Protein kinase A operates a molecular switch that governs yeast pseudohyphal differentiation. Mol Cell Biol 22: 3981-3993.

67. Malcher M, Schladebeck S, Mosch HU (2011) The Yak1 protein kinase lies at the center of a regulatory cascade affecting adhesive growth and stress resistance in Saccharomyces cerevisiae. Genetics 187: 717-730.

68. Deminoff SJ, Howard SC, Hester A, Warner S, Herman PK (2006) Using substrate-binding variants of the cAMP-dependent protein kinase to identify novel targets and a kinase domain important for substrate interactions in Saccharomyces cerevisiae. Genetics 173: 1909-1917.

69. Nakafuku M, Obara T, Kaibuchi K, Miyajima I, Miyajima A, et al. (1988) Isolation of a second yeast Saccharomyces cerevisiae gene (GPA2) coding for guanine nucleotide-binding regulatory protein: studies on its structure and possible functions. Proc Natl Acad Sci U S A 85: 1374-1378.

70. Lemaire K, Van de Velde S, Van Dijck P, Thevelein JM (2004) Glucose and sucrose act as agonist and mannose as antagonist ligands of the G protein-coupled receptor Gpr1 in the yeast Saccharomyces cerevisiae. Mol Cell 16: 293-299.

71. Kubler E, Mosch HU, Rupp S, Lisanti MP (1997) Gpa2p, a G-protein alpha-subunit, regulates growth and pseudohyphal development in Saccharomyces cerevisiae via a cAMP-dependent mechanism. J Biol Chem 272: 20321-20323.

72. Van de Velde S, Thevelein JM (2008) Cyclic AMP-protein kinase A and Snf1 signaling mechanisms underlie the superior potency of sucrose for induction of filamentation in Saccharomyces cerevisiae. Eukaryot Cell 7: 286-293.

73. Vyas VK, Kuchin S, Berkey CD, Carlson M (2003) Snf1 kinases with different beta-subunit isoforms play distinct roles in regulating haploid invasive growth. Mol Cell Biol 23: 1341-1348.

74. Kuchin S, Vyas VK, Carlson M (2002) Snf1 protein kinase and the repressors Nrg1 and Nrg2 regulate FLO11, haploid invasive growth, and diploid pseudohyphal differentiation. Mol Cell Biol 22: 3994-4000.

75. Hsu J-W, Chen K-J, Lee F-JS (2015) Snf1/AMP-activated protein kinase activates Arf3p to promote invasive yeast growth via a non-canonical GEF domain. 6: 7840.

76. Hsu JW, Lee FJ (2013) Arf3p GTPase is a key regulator of Bud2p activation for invasive growth in Saccharomyces cerevisiae. Mol Biol Cell 24: 2328-2339.

77. Huang CF, Liu YW, Tung L, Lin CH, Lee FJ (2003) Role for Arf3p in development of polarity, but not endocytosis, in Saccharomyces cerevisiae. Mol Biol Cell 14: 3834-3847.

78. Mora Carpio A, Climaco A (2017) Candidiasis, Fungemia. StatPearls. Treasure Island (FL): StatPearls Publishing
StatPearls Publishing LLC.

79. Tong Y, Tang J (2017) Candida albicans infection and intestinal immunity. Microbiol Res 198: 27-35.

80. Gullo A (2009) Invasive fungal infections: the challenge continues. Drugs 69 Suppl 1: 65-73.

81. Enoch DA, Ludlam HA, Brown NM (2006) Invasive fungal infections: a review of epidemiology and management options. J Med Microbiol 55: 809-818.

82. Noble SM, Johnson AD (2007) Genetics of Candida albicans, a diploid human fungal pathogen. Annu Rev Genet 41: 193-211.

83. Chakraborty U, Mohamed A, Kakade P, Mugasimangalam RC, Sadhale PP, et al. (2013) A stable hybrid containing haploid genomes of two obligate diploid Candida species. Eukaryot Cell 12: 1061-1071.

84. Santos MA, Tuite MF (1995) The CUG codon is decoded in vivo as serine and not leucine in Candida albicans. Nucleic Acids Res 23: 1481-1486.

85. Romani L, Bistoni F, Puccetti P (2003) Adaptation of Candida albicans to the host environment: the role of morphogenesis in virulence and survival in mammalian hosts. Curr Opin Microbiol 6: 338-343.

86. Noble SM, Gianetti BA, Witchley JN (2017) Candida albicans cell-type switching and functional plasticity in the mammalian host. Nat Rev Microbiol 15: 96-108.

87. Sudbery PE (2011) Growth of Candida albicans hyphae. Nat Rev Micro 9: 737-748.

88. Csank C, Schroppel K, Leberer E, Harcus D, Mohamed O, et al. (1998) Roles of the Candida

albicans mitogen-activated protein kinase homolog, Cek1p, in hyphal development and systemic candidiasis. Infect Immun 66: 2713-2721.

89. Saputo S, Kumar A, Krysan DJ (2014) Efg1 directly regulates ACE2 expression to mediate cross talk between the cAMP/PKA and RAM pathways during Candida albicans morphogenesis. Eukaryot Cell 13: 1169-1180.

90. Stoldt VR, Sonneborn A, Leuker CE, Ernst JF (1997) Efg1p, an essential regulator of morphogenesis of the human pathogen Candida albicans, is a member of a conserved class of bHLH proteins regulating morphogenetic processes in fungi. EMBO J 16: 1982-1991.

91. Saputo S, Chabrier-Rosello Y, Luca FC, Kumar A, Krysan DJ (2012) The RAM network in pathogenic fungi. Eukaryot Cell 11: 708-717.

Figure 1.1 Summarized version of important kinase signaling pathways that regulate filamentous growth

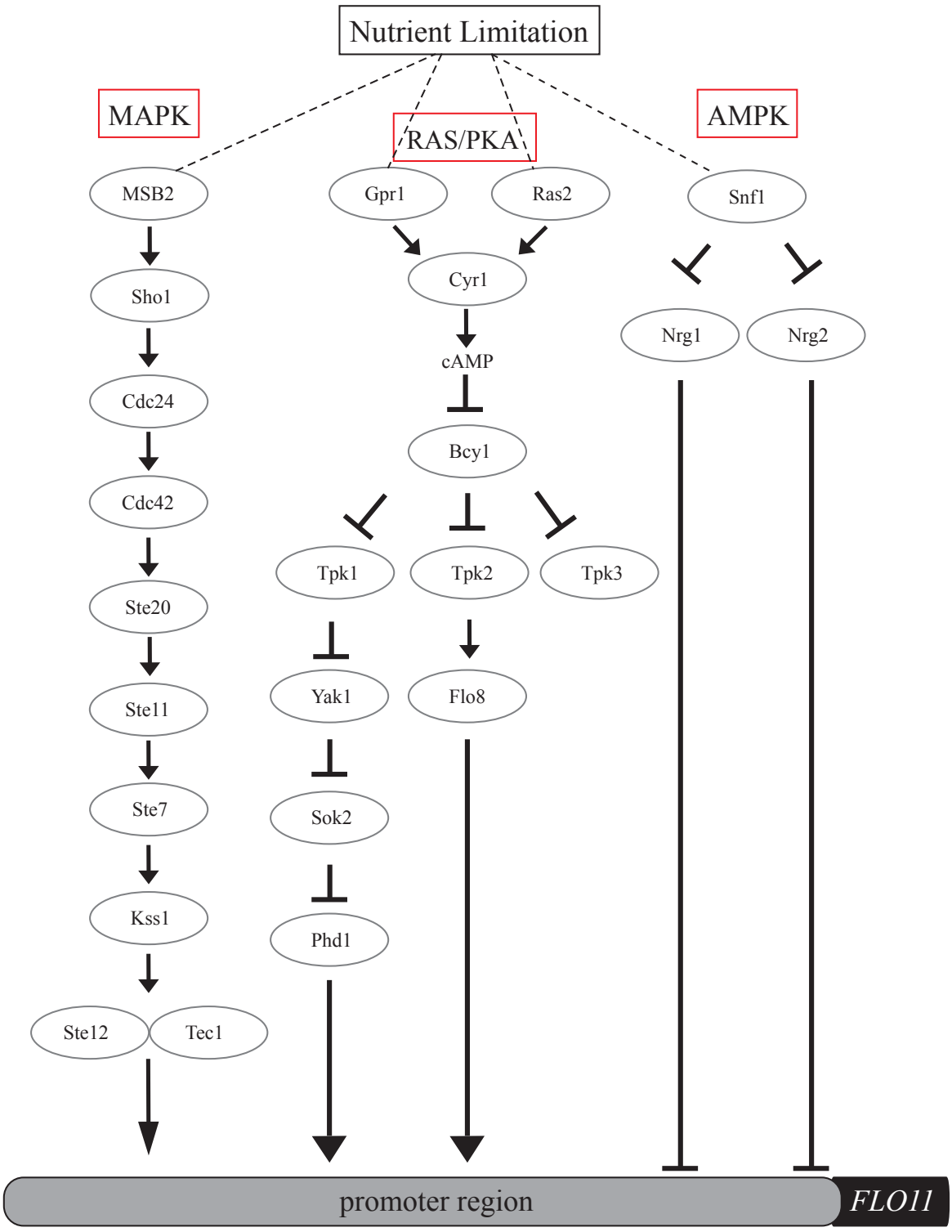

CHAPTER 2

Large-scale analysis of kinase signaling in yeast pseudohyphal development identifies regulation of ribonucleoprotein granules.

2.1 Abstract

Yeast pseudohyphal filamentation is a stress-responsive growth transition relevant to processes required for virulence in pathogenic fungi. Pseudohyphal growth is controlled through a regulatory network encompassing conserved MAPK (Ste20p, Ste11p, Ste7p, Kss1p, and Fus3p), protein kinase A (Tpk2p), Elm1p, and Snf1p kinase pathways; however, the scope of these pathways is not fully understood. Here, we implemented quantitative phosphoproteomics to identify each of these signaling networks, generating a kinase-dead mutant in filamentous *S. cerevisiae* and surveying for differential phosphorylation. By this approach, we identified 439 phosphoproteins dependent upon pseudohyphal growth kinases. We report novel phosphorylation sites in 543 peptides, including phosphorylated residues in Ras2p and Flo8p required for wild-type filamentous growth. Phosphoproteins in these kinase signaling networks were enriched for ribonucleoprotein (RNP) granule components, and we observe co-localization of Kss1p, Fus3p, Ste20p, and Tpk2p with the RNP component Igo1p. These kinases localize in puncta with GFP-visualized mRNA, and *KSS1* is required for wild-type levels of mRNA localization in RNPs. Kss1p pathway activity is reduced in *lsm1*Δ/Δ and *pat* Δ/Δ strains, and

these genes encoding P-body proteins are epistatic to *STE7*. The P-body protein Dhh1p is also required for hyphal development in *Candida albicans*. Collectively, this study presents a wealth of data identifying the yeast phosphoproteome in pseudohyphal growth and regulatory interrelationships between pseudohyphal growth kinases and RNPs.

2.2 Author Summary

Eukaryotic cells affect precise changes in shape and growth in response to environmental and nutritional stress, enabling cell survival and wild-type function. The single-celled budding yeast provides a striking example, undergoing a set of changes under conditions of nitrogen or glucose limitation resulting in the formation of extended cellular chains or filaments. Related filamentous growth transitions are required for virulence in pathogenic fungi and have been studied extensively; however, the full scope of signaling underlying the filamentous growth transition remains to be determined. Here, we used a combination of genetics and proteomics to identify proteins that undergo phosphorylation dependent upon kinases required for filamentous growth. Within this protein set, we identified novel sites of phosphorylation in the yeast proteome and extensive phosphorylation of mRNA-protein complexes regulating mRNA decay and translation. The data indicate an interrelationship between filamentous growth and these ubiquitously conserved sites of RNA regulation: the RNA-protein complexes are required for the filamentous growth transition, and a well studied filamentous growth signaling kinase is required for wild-type numbers of RNA-protein complexes. This interdependence is previously unappreciated, highlighting an additional level of translational control underlying this complex growth transition.

2.3 Introduction

The pseudohyphal growth response is a complex morphogenetic program in which fungal cells transition from a yeast-like growth form to a filamentous state, with cells remaining physically connected after cytokinesis in elongated structures [1-3]. This growth transition is evident in several strains of *S. cerevisiae* (e.g., Σ1278b and SK1)[4,5] and is triggered by numerous conditions, including nitrogen limitation, glucose limitation, the presence of starch as a sole carbon source, and elevated levels of fusel alcohols [1,6-9]. Since yeast pseudohyphal growth is principally induced in response to nutrient stress, it is widely presumed to be a nutritional foraging mechanism[10]. Pseudohyphal growth has been studied intensely in *S. cerevisiae* as an informative model of related processes of filamentous growth evident in many fungi. In particular, the pseudohyphal growth transition in *S. cerevisiae* is closely related to filamentous growth transitions enabling the formation of pseudohyphae and true hyphae with parallel-sided cell walls in the opportunistic human fungal pathogen *Candida albicans* [11-13]. Further, the ability to form hyphae and to transition between these growth forms is required for virulence in *C. albicans* [14-16].

The molecular basis of yeast pseudohyphal growth is extensive. Pseudohyphal formation in *S. cerevisiae* is enabled by changes in cell polarity, cytoskeletal organization, and cell adhesion controlled through a regulatory network encompassing a core set of strongly conserved signaling modules [17-20]. Yeast cells contain several mitogen-activated protein kinase (MAPK) pathways, and elegant studies in the mid-1990s identified the cascade of Ste11p, Ste7p, and Kss1p as a pseudohyphal growth activator [21-23]. Within this pseudohyphal growth MAPK pathway, the upstream p21-activated kinase Ste20p phosphorylates and activates Ste11p, and this phosphorylation signal is propagated through Kss1p to the heterodimeric transcription factor

Ste12p/Tec1p [24,25]. Ste11p and Ste7p are also components of a pheromone-responsive MAPK cascade containing the MAPK Fus3p [26,27]. Fus3p negatively regulates pseudohyphal growth by phosphorylating Tec1p Thr273, targeting Tec1p for degradation [28].

In addition to these MAPK pathways, cAMP-dependent protein kinase A (PKA) is a key regulator of pseudohyphal development. In *S. cerevisiae*, PKA consists of the Bcy1p regulatory subunit and one of three catalytic subunits, Tpk1p, Tpk2p, and Tpk3p [29,30]. Tpk2p phosphorylates the filamentous growth transcriptional activator Flo8p, and deletion of *TPK2* reduces pseudohyphal growth [31,32]. The AMP-activated kinase Snf1p is a well-studied transcription factor required for derepressed expression of glucose-repressible genes [33]. Snf1p represses the pseudohyphal growth negative regulators Nrg1p and Nrg2p, resulting in transcriptional activation of *FLO11*, among other targets [34]. *FLO11* encodes a GPI-anchored cell surface flocculin required for pseudohyphal growth, acting as a downstream effector of the Kss1p MAPK pathway through Ste12p/Tec1p, the PKA pathway through Flo8p, and Snf1p as described [35,36]. Snf1p Thr210 is phosphorylated by Elm1p, which regulates cellular morphogenesis and cytokinesis [37].

The core components of these signaling pathways are well established, but the set of targets of each signaling module are not as clearly defined with respect to the gene network contributing to pseudohyphal growth. Systematic analysis of loss-of-function mutants revealed that approximately 700 genes are required for wild-type pseudohyphal growth [38,39], and a partially overlapping set of 551 genes promotes invasive growth upon galactose-induced overexpression [40]. In particular, the regulation of stress-responsive processes during pseudohyphal growth is a point of ongoing study, indicating counterbalanced control of autophagy through Tor/PKA [41] and an extensive glucose-regulated signaling network

encompassing Snf1p and related pathways [34,42]. Pseudohyphal growth gene networks have been analyzed globally for regulatory control at the level of transcription [43,44], but kinase signaling networks regulating filamentous growth have been constructed predominantly from individual studies of a given kinase and target. Although kinase signaling in yeast has been analyzed effectively through mass spectrometry-based phosphoproteomics [45-48], these methods had not been applied to define kinase networks controlling pseudohyphal growth in a filamentous strain of *S. cerevisiae*. Here, we implemented quantitative phosphoproteomics to identify signaling networks for a set of kinases that regulate filamentation, with the results revealing a wealth of previously unknown phosphorylation sites, phosphorylated residues in Ras2p and Flo8p required for pseudohyphal growth, and MAPK regulation of ribonucleoprotein complexes via the Kss1p cascade.

2.4 Results

2.4.1 Identifying pseudohyphal growth kinase signaling networks by quantitative phosphoproteomics

To dissect kinase signaling networks regulating yeast pseudohyphal growth, we adopted a straightforward approach, generating a loss-of-function mutation in relevant pseudohyphal growth kinases and surveying the resulting changes in phosphorylation. For this study, we constructed catalytically impaired kinase-dead alleles in the filamentous Σ1278b strain of *S. cerevisiae* for each of the following kinases: Ste20p, Ste11p, Ste7p, Kss1p, Fus3p, Tpk2p, Elm1p, and Snf1p. The signaling context of each protein is indicated in Fig 2.1A. Mutant kinase alleles were generated by deletion of each kinase gene and introduction of a low-copy centromeric plasmid bearing the native gene promoter and mutated coding sequence encoding a

Lys-to-Arg substitution at the conserved residue in the catalytic loop of each respective kinase domain. Resulting filamentous growth phenotypes are presented in Table 2.1; images of these kinase-dead mutants as well as background deletion strains and isogenic strains carrying wild-type kinase genes are shown in Fig 2.1B-D.

Differential phosphorylation in the kinase-dead mutants relative to wild-type was assessed by quantitative phosphoproteomics using stable isotopic labeling of amino acids in cell culture (SILAC) [49]. To implement this SILAC-based approach, the wild-type and kinase mutant strains in Σ1278b were made auxotrophic for lysine and arginine by deletion of *LYS1* and *ARG4*. The resulting strains were cultured in triplicate under conditions inducing pseudohyphal growth in medium containing either isotopically labeled or unlabeled lysine and arginine. Protein extracts from the cultures were enriched for phosphopeptides, and the enriched fractions were analyzed by liquid chromatography coupled with tandem mass spectrometry to determine the identity and relative abundance of the phosphopeptides. This experimental design and workflow is summarized in Fig 2.2A.

2.4.2 An extensive phosphorylation network dependent upon pseudohyphal growth kinase activity

By SILAC-based phosphoproteomics, we identified 11,337 peptide-to-spectrum matches and filtered the peptides by criteria indicated in Materials and Methods. The resulting data indicate 3,699 unique phosphopeptides, corresponding to 1,111 proteins. In total, we observed 711 peptides that exhibited a change in phosphorylation (SILAC ratio $\geq$1.5 or $\leq$0.5 with statistical significance $\leq$0.05) in the respective kinase mutants relative to wild-type (Fig 2.2B).This differentially phosphorylated peptide set corresponds to 439 phosphoproteins. A full

listing of these data is provided in Table 2.2. In addition to Ser/Thr phosphorylation, we also identify 137 peptides with a phosphorylated tyrosine residue, corresponding to 110 yeast proteins. By our experimental design, the proteins identified in this study encompass both direct and indirect targets of the respective pseudohyphal growth kinases. These phosphoproteins encompass eighteen functionally uncharacterized proteins and 73 proteins whose corresponding genes yield pseudohyphal growth phenotypes upon deletion (Fig 2.2B) [38,39].

2.4.3 Previously unidentified phosphorylation sites in the proteome of the filamentous Σ1278b strain

These mass spectrometry studies provide a substantial catalog of previously unreported phosphorylation sites across the yeast proteome. Due to the lack of a centralized repository of previously identified phosphopeptides, novel sites were identified through a multi-step process: we first generated a compendium of known phosphorylation sites culled from phosphopeptide databases (Materials and Methods), and we subsequently mapped peptides and phosphorylation sites from each of these databases onto the yeast proteome along with phosphosites identified in our data. Allowing for inherent uncertainties in both our data and reported phosphorylation sites from the community databases, we identified sites that were well distinct from those previously reported. A listing of potentially novel phosphorylation sites can be accessed from Table 2.2. Interestingly, as indicated in Fig 2.3, we identified previously unreported phosphorylation sites in the GTP-binding protein Ras2p (Y165, T166) and the pseudohyphal growth transcription factor Flo8p (S587, S589, S590), both proteins being required for filamentous growth [50,51]. Mutation of these sites to encode non-phosphorylatable residues results in decreased invasive growth (Fig 2.4). A *flo8* mutant encoding alanine at residues 587, 589, and 590 (*flo8*-S3A)

results in decreased production of *lacZ* driven from a segment of the *FLO11* promoter containing Flo8p-binding sites ($P_{flo11\text{-}6/7}$). Additionally, the *flo8*-S3A allele yields decreased activity of a *lacZ* reporter driven by a filamentation-responsive element (FRE) recognized by the Kss1p-regulated Ste12p/Tec1p transcription factor [22] (Fig 2.3B). The *ras2*-Y165F/T166A and *flo8*-S3A alleles encode proteins that can be visualized as GFP chimeras exhibiting wild-type localization to the plasma membrane and nucleus, respectively (Fig 2.4).

2.4.4 The pseudohyphal growth kinase signaling network is enriched for proteins in RNP granules

To identify cellular processes involved in the pseudohyphal growth transition, we mined the collective set of proteins differentially phosphorylated in the kinase-dead mutants for statistically significant enrichment of associated Gene Ontology (GO) terms using the Biological Process, Molecular Function, and Cellular Component vocabularies. In addition to the expected identification of terms associated with pseudohyphal growth and polarized growth, this analysis indicated enrichment for proteins involved in translational regulation (Fig 2.5A). Using the DAVID bioinformatics suite, we identified a cluster of genes annotated with related GO terms involving the regulation of translation (GO ID:0006417), the regulation of cellular protein metabolic process (GO ID:0032268), and the posttranscriptional regulation of gene expression (GO ID:0010608). The gene set contains protein components of mRNA-protein granules, and gene sets annotated with the GO terms RNP granule (GO ID:00035770), cytoplasmic mRNA processing body (GO ID:0000932), and cytoplasmic stress granule (GO ID:0010494) are statistically enriched in the set of differentially phosphorylated proteins observed for many of the kinase-dead mutants (Fig 2.5B). It is noteworthy that the subset of identified proteins exhibiting

increased phosphorylation in the kinase-dead strains, presumably encompassing indirect kinase targets, is not enriched for GO terms associated with RNP granules. A listing of GO terms enriched in this hyper-phosphorylated protein subset is presented in Table 2.3.

Cytoplasmic stress granules and mRNA processing bodies (P-bodies) are two classes of RNPs observed in yeast, with compositional and presumed functional similarities to large families of RNP particles observed throughout eukaryotes. As reviewed in Buchan and Parker [52], the stress-induced RNPs contain non-translating mRNAs and function in an mRNP cycle, wherein mRNA may traffic between mRNPs that exhibit a dynamic protein makeup. Classically, P-bodies are thought to be aggregates of mRNA with proteins involved in translational repression, deadenylation, decapping, and 5'-to-3' exonucleolytic mRNA decay [53,54], while the protein composition of yeast stress granules encompasses translation initiation factors suggestive of associated RNAs stalled in translation initiation [55,56]. Our phosphoproteomic analysis identifies pseudohyphal growth (PHG) kinase-dependent phosphorylation of proteins localized in P-bodies (Dcp2p, Ded1p, Dhh1p, Edc3p, Pat1p, Sbp1p, and Xrn1p) and stress granules (Eap1p, Hrp1p, Pbp1p, and Ygr250cp), as well as proteins identified in both (Igo1p, Ngr1p, and Tif4632p) [57]. A listing of PHG kinase-dependent phosphorylation sites in these RNP granule proteins is indicated in Table 2.4.

As a further step towards identifying a regulatory link between pseudohyphal growth kinase signaling and RNP biology, we constructed a network connectivity map integrating physical interactions between: 1) RNP components and 2) proteins in signaling pathways/cell processes required for filamentation. Using annotations from the Kyoto Encyclopedia of Genes and Genomes (KEGG), we identified a fairly dense map between proteins localized to RNPs and the indicated KEGG pathways related to filamentous growth (Fig 2.5C). We did not observe

maps of similar density between RNP components and proteins in other filamentous growth-related KEGG pathways. The proteins used to generate this network and the database sources of the interactions are listed in Table 2.5.

2.4.5 A set of pseudohyphal growth kinases localizes with RNP particles

Since the phosphorylation of numerous RNP components is dependent upon pseudohyphal growth kinases, we examined the set of eight kinases selected here for co-localization with RNP particles. For this analysis, we generated carboxy-terminal GFP-fusions to each kinase and carboxy-terminal mCherry fusions to several RNP components (Dcp2p, Edc3p, Igo1p, and Pat1p) as chromosomal alleles in a strain of the filamentous Σ1278b genetic background. As indicated in Fig 2.6A, Fus3p, Kss1p, Ste20p (in the MAPK pathway) and Tpk2p (PKA) co-localized as GFP chimeras with Igo1p-mCherry. Igo1p is a RNP component of unknown function that has been identified as a Rim15p target required for proper initiation of G_0 [58]. Rim15p, acting downstream of PKA, phosphorylates Igo1p at S64; this phosphorylation site was also observed in the mass spectrometry studies reported here. Igo1p binds the P-body protein Dhh1p and the stress-granule protein Pbp1p as determined previously by co-immunoprecipitation [58]. We observe Igo1p-mCherry puncta and co-localization with Fus3p, Kss1p, Ste20p, and Tpk2p post-diauxic shift, upon 3 days growth in standard media (Fig 2.6A).

We further considered co-localization of pseudohyphal growth kinases with RNPs using the RNA visualization strategy of Brodsky and Silver [59]. By this method, RNA can be visualized in puncta by fluorescence microscopy of a U1A-GFP fusion bound to multiple U1A-binding sites introduced into the 3'-untranslated region of a target mRNA. For this study, we used *PGK1* mRNA modified with sixteen U1A-binding sites as a marker of bulk and stable

mRNAs (Fig 2.6B). As described in Sheth and Parker [60], this fluorescence-tagging strategy has been used to visualize RNPs as puncta, and we have co-localized Pbp1-GFP with U1A-mCherry-bound RNA puncta by this approach. Each pseudohyphal growth kinase tested in this study was analyzed for co-localization with *PGK1* RNA puncta, and, consistent with the results presented above, we observed substantial RNA puncta co-localization with mCherry fusions to Fus3p, Kss1p, Ste20p, and Tpk2p (Fig 2.6B). In contrast, mCherry chimeras with Elm1p, Snf1p, Ste7p, and Ste11p did not co-localize with the engineered *PGK1* RNA. Kinase puncta were evident under a short period of glucose limitation, with RNA co-localization persistent through at least two days. Transferring cells from media limited in glucose to media with normal levels of glucose resulted in a loss of observed puncta, indicating that punctate formation was responsive to glucose limitation.

2.4.6 RNP components are required for wild-type signaling through the pseudohyphal growth PKA and MAPK pathways

The RNP protein Igo1p is PKA-regulated, and we find that wild-type localization of the PKA catalytic subunit Tpk2p requires *IGO1* and its paralog *IGO2*. The *IGO1* and *IGO2* genes arose from a whole genome duplication event, with 58% identity between these proteins [58], suggesting that these genes are functionally redundant. Upon deleting both genes, complex colony morphology is exaggerated, consistent with perturbed PKA signaling [61] (Fig 2.7A). *IGO1* and *IGO2* are required for signaling through the Kss1p MAPK pathway and PKA pathway as assessed using *lacZ* reporters containing FRE sites responsive to Kss1p-regulated Ste12p/Tec1p and a segment of the *FLO11* promoter bound by PKA-regulated Flo8p, respectively (Fig 2.7B). Further, the punctate localization of a Tpk2p-GFP chimera is disrupted

in a strain deleted for *IGO1* and *IGO2* (Fig 2.7C). The subcellular distribution of Kss1p, Fus3p, and Ste20p is unaffected in an *igo1*Δ/*igo2*Δ mutant in the filamentous Σ1278b background (Fig 2.8C).

Numerous genes encoding RNP components are required for wild-type pseudohyphal growth. We identified strongly diminished pseudohyphal growth in strains of the filamentous Σ1278b background containing homozygous deletions of the mRNA decay/translational repressor genes *CCR4*, *DHH1*, *LSM1*, *PAT1*, *PBP1*, and *SBP1* (Fig 2.7D). To assess activity of the MAPK pathway in these mutants, we introduced the plasmid-based *FRE-lacZ* Kss1p reporter and assayed for β-galactosidase activity under conditions of nitrogen limitation. As indicated in Fig 2.7D, *lsm1*Δ/Δ and *pat1*Δ/Δ mutants were strongly decreased in MAPK pathway activity relative to wild-type, approaching levels observed in a homozygous diploid strain deleted for *STE12*. *LSM1* and *PAT1* both encode P-body proteins that function in mRNA decapping [60]; Lsm1p functions with a group of six other Lsm family proteins in a complex that associates with the Pat1p decapping enzyme, and, collectively, the proteins mediate mRNA decay through decapping [62]. Epistasis studies indicate that overactive alleles of *STE11* and *STE7 [63]* are suppressed by deletion of *LSM1* and *PAT1*, both morphologically and by *FRE-lacZ* reporter assay (Fig 2.7E). A hyperactive *KSS1* allele did not yield an exaggerated pseudohyphal growth phenotype. These results indicate that the core mRNA decapping proteins Lsm1p and Pat1p are required for wild-type pseudohyphal growth MAPK signaling, and that the genes act at or below the level of the MAPKK *STE7*.

2.4.7 The pseudohyphal growth MAPK Kss1p is required to achieve wild-type numbers of RNA puncta

In addition to the requirement for RNP components in wild-type Kss1p signaling, we find that *KSS1* is required to achieve wild-type levels of mRNA puncta. A strain of the filamentous Σ1278b background deleted for *KSS1* yields a significantly decreased amount of U1A-GFP-tagged *PGK1* mRNA localized in puncta under conditions of glucose limitation (Fig 2.7F). This phenotype was consistent in the *kss1*Δ strain from a brief 15-minute incubation under conditions of glucose limitation up to a period of at least eight hours. The percentage of cells exhibiting mRNA puncta decreased from 65% in wild-type cells to 15% in *kss1*Δ mutants, and, correspondingly, the maximum number of puncta observed in these cells decreased from maximally 16 in wild-type to no greater than four in the *kss1*Δ strain. Visible puncta were lost upon the introduction of media with normal levels of glucose. Profiling studies indicate that bulk RNA association with polyribosomes is not substantially altered in a strain of the Σ1278b background deleted for *KSS1* (Fig 2.9), although the translational processing of specific transcripts may still be perturbed in a *kss1*Δ strain.

2.4.8 The RNP-localized Dhh1p helicase is required for hyphal development in *Candida albicans*

To consider the likelihood of a conserved functional interrelationship between RNP components and filamentous growth, we assessed the contributions of the P-body protein Dhh1p towards hyphal development in the pathogenic fungus *Candida albicans*. We selected *DHH1* for study because it is a core component of P-bodies, and its localization has been confirmed in *C. albicans*. Further, in *S. cerevisiae*, a loss-of-function mutation in *DHH1* results in decreased pseudohyphal growth (Fig 2.7D), although its hyphal growth phenotype in *C. albicans* has not been clearly identified. The *C. albicans* ortholog of *DHH1* is presumed to

function similarly to *S. cerevisiae DHH1*, and the genes exhibit 91% sequence similarity at the encoded amino acid level. For this analysis, we generated a heterozygous deletion of *DHH1* in *C. albicans* by standard gene replacement and assayed for altered colony and cell morphology under conditions inducing hyphal development. As indicated in Fig 2.10A, the *dhh1*Δ/*DHH1* strain exhibits reduced surface wrinkling and peripheral hyphae relative to an isogenic wild-type strain. Deletion of *DHH1* resulted in cells that were less elongated than wild-type, and, correspondingly, hyphae were decreased in number under these conditions (Fig 2.10B).

2.5 Discussion

The phosphoproteomic analysis presented here is the first such study of kinase signaling networks in pseudohyphal growth, effectively complementing previous phosphoproteomic analyses of yeast kinases in a non-filamentous strain under standard growth conditions. Compared to data in the major phosphorylation databases (Experimental Procedures), this analysis identifies a large set of previously unreported phosphorylation sites. These sites encompass residues that are phosphorylated strictly in the Σ1278b proteome in response to the conditions employed here as well as phosphorylation sites that were not sampled in previous analyses. This suggests that the quantitative phosphoproteomic data collected here and elsewhere are not saturating. Consequently, there is benefit in continued analysis of the yeast phosphoproteome towards understanding kinase networks more fully.

Our mass spectrometry data identify 73 proteins that: 1) were differentially phosphorylated in a kinase-dead strain, and 2) result in a pseudohyphal growth phenotype upon deletion. Ryan *et al*. [39] reported 497 genes that result in diploid pseudohyphal growth defects

in *S. cerevisiae* under conditions of low nitrogen; thus, the kinase signaling network identified here encompasses a significant fraction of this gene set. The network contains both direct and indirect kinase targets. In a landmark study, Ptacek *et al*. [64] used a proteome microarray to identify in vitro substrates of most yeast kinases. We integrated the results from this microarray study for the kinases tested here with our own data, identifying in vitro substrates that also exhibited differential phosphorylation by mass spectrometry. The results are indicated in Table 2.6.

Further interpretation of the kinase-dependent phosphorylation data yields two observations. First, many of the identified phosphorylation sites were dependent on the presence of more than one pseudohyphal growth kinase. This observation holds true for kinases that are thought to function in distinct pathways. Of 311 unique proteins identified as undergoing differential phosphorylation in a strain carrying a kinase-dead mutation in the MAPK Kss1p, 188 of these proteins were also differentially phosphorylated in a strain carrying a kinase-dead allele of *ELM1*. We report 814 unique proteins differentially phosphorylated in *tpk2-K99R*, and 249 of these proteins were also differentially phosphorylated in a strain with a kinase-dead allele of *KSS1*. Collectively, this suggests that the respective kinases and pathways regulate partially overlapping signaling networks. Overlapping signaling networks further suggest a degree of functional redundancy, although mutant phenotypes are evident upon deletion of each individual kinase analyzed here. Second, the identification of new and functionally important phosphorylated residues in pseudohyphal growth proteins such as Flo8p underscores the utility in extending quantitative phosphoproteomic studies to the analysis of non-standard growth conditions and strains, as *FLO8* is an incompletely translated pseudogene in standard S288C laboratory strains of *S. cerevisiae*.

The functional interrelationship identified in this study between RNP components and pseudohyphal growth is supported by several lines of evidence obtained in the non-filamentous S288C genetic background. As reported in Yoon *et al*. [65], Ste20p phosphorylates Dcp2p at Ser 137, and this phosphorylation is required for Dcp2p localization in P-bodies. Shah *et al*. [66] found that overexpression of PKA isoforms inhibits P-body formation and that the Tpk1p and Tpk2p subunits of PKA are capable of phosphorylating the P-body protein Pat1p in vitro. Also in an S288C background under conditions of glucose depletion, Xrn1p undergoes Snf1p-dependent phosphorylation along with a subset of additional mRNA processing proteins [48]. In S288C, Fus3p co-localizes with P-bodies and stress granules as yeast cells enter stationary phase [67]. It is noteworthy that Kss1p is non-functional in the S288C strain [26] and presumably would not have been identified as a regulator of RNPs in previous studies undertaken in that genetic background.

In the filamentous Σ1278b strain, the kinases Kss1p, Fus3p, Tpk2p, and Ste20p co-localize with *PGK1* mRNA foci as well as with the P-body and stress-granule protein Igo1p. As presented in Buchan *et al*. [68], mRNAs are thought to traffic between P-bodies, stress granules, and other RNPs, with the composition of each particle being dynamic in response to the specific cell stress and duration of the stress. Since we do not at present understand the full composition of these particles in a filamentous strain under the observed growth conditions, we use the term RNP here to indicate co-localization with RNA/protein foci and specifically identify co-localization with Igo1p.

It is interesting that the upstream PAK Ste20p and the MAPK Kss1p co-localize with Igo1p and GFP-tagged mRNA, but neither the MAPKKK Ste11p nor the MAPKK Ste7p share this localization pattern. Three points are relevant in considering the localization of these

pathway components. First, prior literature supports the observation that MAPK pathway components may not be uniformly localized. For example, in the mating pathway, Ste7p and Fus3p have been identified at the bud tip, although Ste11p has not been similarly localized. Fus3p exists in several complexes affecting its localization [69]. Kss1p has been reported previously to localize to the nucleus [70], although neither Ste11p nor Ste7p are found predominantly in the nucleus. Second, this work and other studies [64,71] indicate that the respective MAPK pathway components do not exhibit strictly overlapping targets. The fact that these kinases recognize nonoverlapping sets of targets suggests that differential localization of subpopulations of the kinases is possible. Third, Kss1p and Fus3p as well as the pseudohyphal growth upstream PAK Ste20p are not exclusively identified in mRNPs, and the likelihood exists that a subset of these respective protein populations may indeed be colocalized.

RNPs are induced in response to numerous cell stresses, including glucose limitation, hyperosomotic stress, and high cell density [72-74]; however, we find that nitrogen stress, a classic inducer of pseudohyphal growth, is not a strong inducer of RNPs in the absence of additional cell stresses. The mechanisms of these inductions are unclear; consequently, it is also unclear as to why nitrogen limitation alone is insufficient to strongly induce this response. In this analysis, 1-butanol, rather than low-nitrogen media, was used as an inducer of filamentation because of its ability to yield a strong filamentous response in liquid cultures. Further, the cells necessitated growth to 10 doublings under conditions inducing pseudohyphal growth to achieve efficient labeling, which resulted in a mild degree of glucose stress. The presence of short-chain alcohols coupled with glucose limitation provides strong induction of filamentation in liquid. Notably, we observe RNP foci under these conditions for a growth period of at least 30 hours, representing a time point matching the endpoint of growth for quantitative phosphoproteomic

analysis. It should be noted that stress granules form post entry into stationary phase [66], and consequently, this analysis may be less effective in identifying post-translational modifications affecting stress granule components. In sum, however, the conditions present at the point of mass spectrometric analysis allow for the presence of RNPs, consistent with the identification of differentially phosphorylated RNP components in this study.

Interestingly, the requirement for *DHH1*, encoding a helicase involved in mRNA decapping, is conserved between *S. cerevisiae* and the related pathogenic fungus *C. albicans*. Signaling pathways in *S. cerevisiae* serve as effective models of related pathways in *C. albicans* [75], raising the possibility that RNPs and hyphal development are functionally linked in *C. albicans* as well. In support of this notion, P-bodies have been observed to form during hyphal development in *C. albicans*, and Dhh1p does co-localize to P-bodies in *Candida* [76]. Further, a strain of *C. albicans* deleted for *EDC3* exhibits a defect in filamentation [76]. The results here are consistent with regulatory feedback between RNP components and hyphal development in this opportunistic human pathogen.

In total, the data support an interrelationship between pseudohyphal growth kinase signaling and RNP biology. Deletion analyses and epistasis studies indicate that RNA processing proteins are required for wild-type Kss1p MAPK signaling, likely to regulate the translational state of particular transcripts important for pseudohyphal growth. In turn, the identified pseudohyphal growth kinases localize to RNPs, and the Kss1p pathway is required for wild-type RNP numbers in the filamentous *S. cerevisiae* strain. Thus, Kss1p MAPK signaling and RNP signaling feed back reciprocally. Similarly, PKA regulates Igo1/2p function through Rim15p, and Igo1/2p is in turn required for wild-type PKA localization. The data here collectively provide an important step towards identifying the mechanisms through which this reciprocal

signaling is mediated.

2. 6 Materials and Methods

2.6.1 Strains, plasmids, and media

Strains used in this study are listed in Table 2.7. *S. cerevisiae* strains were derived from the filamentous Σ1278b genetic background. Haploid strains were derived from Y825 and HLY337 [1,77]. Standard protocols and techniques were used for the propagation of budding yeast as described [78]. DNA was introduced by methods of yeast transformation incorporating lithium acetate treatment and heat shock [79]. Plasmids used in this study are listed in Table 2.8.

S. cerevisiae strains were cultured on YPD (1% yeast extract, 2% peptone, 2% glucose) or Synthetic Complete (SC) (0.67% yeast nitrogen base (YNB) without amino acids, 2% glucose, and 0.2% of the appropriate amino acid drop-out mix). Nitrogen deprivation and filamentous phenotypes were assayed using Synthetic Low Ammonium Dextrose (SLAD) medium (0.17% YNB without amino acids, 2% glucose, 50 μM ammonium sulfate and supplemented with appropriate amino acids) or by supplementing growth medium with 1% 1-butanol [9]. Glucose limitation was achieved using media lacking glucose as a carbon source according to standard protocols.

2.6.2 Generation of gene deletions and integrated site-directed mutants

Gene deletions and tags for chromosomal integration were generated through one-step PCR- mediated transformation and subsequent PCR-based verification [80,81]. N-terminal and C-terminal GFP tagging was performed using plasmid-based modules from Longtine *et al*. [82]. Carboxy-terminal mCherry tagging was performed by PCR-based amplification of the mCherry-

kanMX or *Hyg*^{R} cassette of pBS34 or pBS35 (Yeast Resource Center, Univ. of Washington). Integrated point mutations in *RAS2* (*Y165F*, *T166A*) and *FLO8* (*S587A*,*S589A*, and *S590A*) were generated by the *URA* "flip-out" method. In brief, the *URA3* cassette of pRS406 was amplified by PCR and used to disrupt local sequence at the intended site of mutation. A second transformation was then performed to replace the *URA3* marker with DNA sequence encoding the desired mutated allele [5].

2.6.3 Experimental design and cell labeling for phosphoproteomic analysis

ARG4 and *LYS1* were deleted in the haploid Y825 filamentous strain. Subsequently, protein kinase genes were individually deleted in the filamentous *arg4*Δ *lys1*Δ auxotrophic Y825 background. These arginine/lysine auxotrophic kinase null strains were then transformed with *LEU2*-containing yeast shuttle vectors carrying the respective kinase-dead alleles. SILAC was used to differentially label proteins synthesized by kinase-dead allele strains and wild-type (*arg4*Δ *lys1*Δ Y825). SILAC-based mass spectrometry experiments were multiplexed; each mass spectrometry experiment was conducted in triplex, with the light (natural) versions of L-arginine and L- lysine used to label the wild-type strain and medium (Lys-4/Arg-6) or heavy (Lys-8/Arg-10) L-arginine and L-lysine labeling two kinase-dead allele strains.

In each triplex experiment, three strains were cultured in parallel during filamentous growth-inducing conditions. Wild-type and two kinase-dead allele strains were cultured overnight in synthetic complete media containing arginine or lysine residues with light, medium, or heavy isotopes overnight at 30°C, to obtain actively growing log-phase cultures. Each culture was then diluted to a low starting optical density (OD_{600} of approximately 0.1) in SILAC media. To induce filamentous growth in these haploid strains, 1% (vol/vol) 1-butanol was added to each

culture. These diluted cultures were subsequently incubated at 30°C for approximately 10 doublings (approximately 26 hours). This prolonged labeling and culturing step was found to be necessary to ensure effective metabolic labeling of proteins, as well as to obtain a minimum abundance of labeled protein from each strain. Protein extractions and mass spectrometry were performed as described previously [42,83].

2.6.4 Mass spectrometry data analysis and network construction

We processed mass spectrometry data using maxQuant [84] and collated the list of phospho (STY) peptides. The data were filtered at 5% FDR; additionally, we excluded peptides exhibiting low Mascot scores (<3), high charge states (≥5), and long peptide lengths (>40). A normalized heavy:light or medium:light ratio with a significance score (Sig A) ≤ 0.05 was considered statistically significant. Predicted phosphorylation sites were screened for known kinase motifs and the results from this analysis are included in the "Motifs" column in Table 2.2.

To identify potentially novel phosphorylation sites, Exonerate was used to align peptides extracted from major phosphorylation databases (GPM DB, PhosphoPep, PHOSIDA, and Phospho.ELM) onto yeast protein sequence data from the Saccharomyces Genome Database. Phosphosites were marked on the protein sequences, yielding a compendium of phosphorylation sites. Inherent ambiguities in the localization of phosphorylation sites were annotated as such in the compendium. Phosphorylation sites identified in our data were subsequently mapped onto the annotated phosphoproteome.

Networks were constructed using background sets of protein interactions encompassing kinase-dependent differentially phosphorylated proteins in the mass spectrometry data generated here as well as interactions identified in the iRefIndex database. KEGG signaling pathways

relevant for pseudohyphal growth were downloaded and parsed using in-house scripts. The resulting network was expanded by including previously identified core components of stress granules and P-bodies [57,85]. The network was visualized using Cytoscape. The interactions used to construct this network and the database source of each interaction are provided in Table 2.4.

2.6.5 Visualization of mRNA and RNPs by fluorescence microscopy

RNA localization in RNP foci was visualized as described [57]. Live *S. cerevisiae* cells with these plasmids and/or fluorescent protein fusions to known mRNP components were imaged using an upright Nikon Eclipse 80i microscope with CoolSnap ES2 CCD (Photometrics). Images were acquired using the MetaMorph software package (Molecular Devices).

2.6.6 *C. albicans* strains and analysis of filamentous development

Candida albicans strains used in this study were derived from the CAI4 genetic background (*ura3*Δ::*imm434*/*ura3*Δ::*imm434*). The *DHH1*/*dhh1*Δ heterozygote was generated independently by two approaches: 1) by replacement of one endogenous *DHH1* allele with a *URA3* cassette, and 2) by allele replacement using a *HIS1* cassette. A transformant generated by each method was tested for filamentous development, and identical results were observed (Fig 2.10 and 2.11). To induce hyphal formation, strains were inoculated onto standard YEPD plates (2% glucose, 2% peptone, 1% yeast extract) supplemented with 80 mg/L uridine and 1% or 10% fetal calf serum (FCS) as indicated. Hyphal formation was also induced by growth on carbon-limiting Spider medium (10g nutrient broth, 10g mannitol, 2g K_2HPO_4 per liter media) [86].

2.7 References

1. Gimeno CJ, Ljungdahl PO, Styles CA, Fink GR (1992) Unipolar cell divisions in the yeast *S. cerevisia*e lead to filamentous growth: regulation by starvation and RAS. Cell 68: 1077-1090.

2. Lo WS, Dranginis AM (1996) FLO11, a yeast gene related to the STA genes, encodes a novel cell surface flocculin. J Bacteriol 178: 7144-7151.

3. Erdman S, Snyder M (2001) A filamentous growth response mediated by the yeast mating pathway. Genetics 159: 919-928.

4. Grenson M (1966) Multiplicity of the amino acid permeases in Saccharomyces cerevisiae. II. Evidence for a specific lysine-transporting system. Biochim Biophys Acta 127: 339-346.

5. Song Q, Johnson C, Wilson TE, Kumar A (2014) Pooled segregant sequencing reveals genetic determinants of yeast pseudohyphal growth. PLoS Genet 10: e1004570.

6. Dickinson JR (1996) 'Fusel' alcohols induce hyphal-like extensions and pseudohyphal formation in yeasts. Microbiology 142 (Pt 6): 1391-1397.

7. Lambrechts MG, Bauer FF, Marmur J, Pretorius IS (1996) Muc1, a mucin-like protein that is regulated by Mss10, is critical for pseudohyphal differentiation in yeast. Proc Natl Acad Sci U S A 93: 8419-8424.

8. Cullen PJ, Sprague GF, Jr. (2000) Glucose depletion causes haploid invasive growth in yeast. Proc Natl Acad Sci U S A 97: 13619-13624.

9. Lorenz MC, Cutler NS, Heitman J (2000) Characterization of alcohol-induced filamentous growth in Saccharomyces cerevisiae. Mol Biol Cell 11: 183-199.

10. Gancedo JM (2001) Control of pseudohyphae formation in Saccharomyces cerevisiae. FEMS Microbiol Rev 25: 107-123.

11. Argimon S, Wishart JA, Leng R, Macaskill S, Mavor A, et al. (2007) Developmental regulation of an adhesin gene during cellular morphogenesis in the fungal pathogen Candida albicans. Eukaryot Cell 6: 682-692.

12. Mitchell AP (1998) Dimorphism and virulence in Candida albicans. Curr Opin Microbiol 1: 687-692.

13. Sudbery P, Gow N, Berman J (2004) The distinct morphogenic states of Candida albicans. Trends Microbiol 12: 317-324.

14. Lo HJ, Kohler JR, DiDomenico B, Loebenberg D, Cacciapuoti A, et al. (1997) Nonfilamentous C. albicans mutants are avirulent. Cell 90: 939-949.

15. Braun BR, Johnson AD (1997) Control of filament formation in Candida albicans by the transcriptional repressor TUP1. Science 277: 105-109.

16. Saville SP, Lazzell AL, Monteagudo C, Lopez-Ribot JL (2003) Engineered control of cell morphology in vivo reveals distinct roles for yeast and filamentous forms of Candida albicans during infection. Eukaryot Cell 2: 1053-1060.

17. Ahn SH, Acurio A, Kron SJ (1999) Regulation of G2/M progression by the STE mitogen-activated protein kinase pathway in budding yeast filamentous growth. Mol Biol Cell 10: 3301-3316.

18. Miled C, Mann C, Faye G (2001) Xbp1-mediated repression of CLB gene expression contributes to the modifications of yeast cell morphology and cell cycle seen during nitrogen-limited growth. Mol Cell Biol 21: 3714-3724.

19. Cullen PJ, Sabbagh W, Jr., Graham E, Irick MM, van Olden EK, et al. (2004) A signaling mucin at the head of the Cdc42- and MAPK-dependent filamentous growth pathway in yeast. Genes Dev 18: 1695-1708.

20. Karunanithi S, Vadaie N, Chavel CA, Birkaya B, Joshi J, et al. (2010) Shedding of the mucin-like flocculin Flo11p reveals a new aspect of fungal adhesion regulation. Curr Biol 20: 1389-1395.

21. Liu H, Styles CA, Fink GR (1993) Elements of the yeast pheromone response pathway required for filamentous growth of diploids. Science 262: 1741-1744.

22. Madhani HD, Styles CA, Fink GR (1997) MAP kinases with distinct inhibitory functions impart signaling specificity during yeast differentiation. Cell 91: 673-684.

23. Buehrer BM, Errede B (1997) Coordination of the mating and cell integrity mitogen-activated protein kinase pathways in Saccharomyces cerevisiae. Mol Cell Biol 17: 6517-6525.

24. Cook JG, Bardwell L, Kron SJ, Thorner J (1996) Two novel targets of the MAP kinase Kss1 are negative regulators of invasive growth in the yeast Saccharomyces cerevisiae. Genes Dev 10: 2831-2848.

25. Bardwell L, Cook JG, Voora D, Baggott DM, Martinez AR, et al. (1998) Repression of yeast Ste12 transcription factor by direct binding of unphosphorylated Kss1 MAPK and its regulation by the Ste7 MEK. Genes Dev 12: 2887-2898.

26. Elion EA, Brill JA, Fink GR (1991) FUS3 represses CLN1 and CLN2 and in concert with KSS1 promotes signal transduction. Proc Natl Acad Sci U S A 88: 9392-9396.

27. Madhani HD, Fink GR (1997) Combinatorial control required for the specificity of yeast MAPK signaling. Science 275: 1314-1317.

28. Bao MZ, Schwartz MA, Cantin GT, Yates JR, 3rd, Madhani HD (2004) Pheromone-dependent destruction of the Tec1 transcription factor is required for MAP kinase signaling specificity in yeast. Cell 119: 991-1000.

29. Toda T, Cameron S, Sass P, Zoller M, Wigler M (1987) Three different genes in *S.*

cerevisiae encode the catalytic subunits of the cAMP-dependent protein kinase. Cell 50: 277-287.

30. Toda T, Cameron S, Sass P, Zoller M, Scott JD, et al. (1987) Cloning and characterization of BCY1, a locus encoding a regulatory subunit of the cyclic AMP-dependent protein kinase in Saccharomyces cerevisiae. Mol Cell Biol 7: 1371-1377.

31. Robertson LS, Fink GR (1998) The three yeast A kinases have specific signaling functions in pseudohyphal growth. Proc Natl Acad Sci U S A 95: 13783-13787.

32. Pan X, Heitman J (1999) Cyclic AMP-dependent protein kinase regulates pseudohyphal differentiation in Saccharomyces cerevisiae. Mol Cell Biol 19: 4874-4887.

33. Vyas VK, Kuchin S, Berkey CD, Carlson M (2003) Snf1 kinases with different beta-subunit isoforms play distinct roles in regulating haploid invasive growth. Mol Cell Biol 23: 1341-1348.

34. Kuchin S, Vyas VK, Carlson M (2002) Snf1 protein kinase and the repressors Nrg1 and Nrg2 regulate FLO11, haploid invasive growth, and diploid pseudohyphal differentiation. Mol Cell Biol 22: 3994-4000.

35. Rupp S, Summers E, Lo HJ, Madhani H, Fink G (1999) MAP kinase and cAMP filamentation signaling pathways converge on the unusually large promoter of the yeast FLO11 gene. EMBO J 18: 1257-1269.

36. van Dyk D, Pretorius IS, Bauer FF (2005) Mss11p is a central element of the regulatory network that controls FLO11 expression and invasive growth in Saccharomyces cerevisiae. Genetics 169: 91-106.

37. Sutherland CM, Hawley SA, McCartney RR, Leech A, Stark MJ, et al. (2003) Elm1p is one of three upstream kinases for the Saccharomyces cerevisiae SNF1 complex. Curr Biol 13: 1299-1305.

38. Jin R, Dobry CJ, McCown PJ, Kumar A (2008) Large-scale analysis of yeast filamentous growth by systematic gene disruption and overexpression. Mol Biol Cell 19: 284-296.

39. Ryan O, Shapiro RS, Kurat CF, Mayhew D, Baryshnikova A, et al. (2012) Global gene deletion analysis exploring yeast filamentous growth. Science 337: 1353-1356.

40. Shively CA, Eckwahl MJ, Dobry CJ, Mellacheruvu D, Nesvizhskii A, et al. (2013) Genetic networks inducing invasive growth in Saccharomyces cerevisiae identified through systematic genome-wide overexpression. Genetics 193: 1297-1310.

41. Ma J, Jin R, Jia X, Dobry CJ, Wang L, et al. (2007) An interrelationship between autophagy and filamentous growth in budding yeast. Genetics 177: 205-214.

42. Johnson C, Kweon HK, Sheidy D, Shively CA, Mellacheruvu D, et al. (2014) The yeast Sks1p kinase signaling network regulates pseudohyphal growth and glucose response. PLoS Genet 10: e1004183.

43. Madhani HD, Galitski T, Lander ES, Fink GR (1999) Effectors of a developmental mitogen-activated protein kinase cascade revealed by expression signatures of signaling mutants. Proc Natl Acad Sci U S A 96: 12530-12535.

44. Borneman AR, Leigh-Bell JA, Yu H, Bertone P, Gerstein M, et al. (2006) Target hub proteins serve as master regulators of development in yeast. Genes Dev 20: 435-448.

45. Gruhler A, Olsen JV, Mohammed S, Mortensen P, Faergeman NJ, et al. (2005) Quantitative phosphoproteomics applied to the yeast pheromone signaling pathway. Mol Cell Proteomics 4: 310-327.

46. Bodenmiller B, Wanka S, Kraft C, Urban J, Campbell D, et al. (2010) Phosphoproteomic analysis reveals interconnected system-wide responses to perturbations of kinases and phosphatases in yeast. Sci Signal 3: rs4.

47. Oliveira AP, Ludwig C, Zampieri M, Weisser H, Aebersold R, et al. (2015) Dynamic phosphoproteomics reveals TORC1-dependent regulation of yeast nucleotide and amino acid biosynthesis. Sci Signal 8: rs4.

48. Braun KA, Vaga S, Dombek KM, Fang F, Palmisano S, et al. (2014) Phosphoproteomic analysis identifies proteins involved in transcription-coupled mRNA decay as targets of Snf1 signaling. Sci Signal 7: ra64.

49. Ong SE, Blagoev B, Kratchmarova I, Kristensen DB, Steen H, et al. (2002) Stable isotope labeling by amino acids in cell culture, SILAC, as a simple and accurate approach to expression proteomics. Mol Cell Proteomics 1: 376-386.

50. Mosch HU, Roberts RL, Fink GR (1996) Ras2 signals via the Cdc42/Ste20/mitogen-activated protein kinase module to induce filamentous growth in Saccharomyces cerevisiae. Proc Natl Acad Sci U S A 93: 5352-5356.

51. Kobayashi O, Suda H, Ohtani T, Sone H (1996) Molecular cloning and analysis of the dominant flocculation gene FLO8 from Saccharomyces cerevisiae. Mol Gen Genet 251: 707-715.

52. Buchan JR, Parker R (2009) Eukaryotic stress granules: the ins and outs of translation. Mol Cell 36: 932-941.

53. Teixeira D, Sheth U, Valencia-Sanchez MA, Brengues M, Parker R (2005) Processing bodies require RNA for assembly and contain nontranslating mRNAs. RNA 11: 371-382.

54. Kedersha N, Stoecklin G, Ayodele M, Yacono P, Lykke-Andersen J, et al. (2005) Stress granules and processing bodies are dynamically linked sites of mRNP remodeling. J Cell Biol 169: 871-884.

55. Buchan JR, Yoon JH, Parker R (2011) Stress-specific composition, assembly and kinetics of stress granules in Saccharomyces cerevisiae. J Cell Sci 124: 228-239.

56. Mitchell SF, Jain S, She M, Parker R (2013) Global analysis of yeast mRNPs. Nat Struct Mol Biol 20: 127-133.

57. Buchan JR, Nissan T, Parker R (2010) Analyzing P-bodies and stress granules in Saccharomyces cerevisiae. Methods Enzymol 470: 619-640.

58. Talarek N, Cameroni E, Jaquenoud M, Luo X, Bontron S, et al. (2010) Initiation of the TORC1-Regulated G(0) Program Requires Igo1 and Igo2, which License Specific mRNAs to Bypass Degradation via the 5′-3′ mRNA Decay Pathway. Mol Cell 38: 345-355.

59. Brodsky AS, Silver PA (2000) Pre-mRNA processing factors are required for nuclear export. RNA 6: 1737-1749.

60. Sheth U, Parker R (2003) Decapping and decay of messenger RNA occur in cytoplasmic processing bodies. Science 300: 805-808.

61. Granek JA, Magwene PM (2010) Environmental and genetic determinants of colony morphology in yeast. PLoS Genet 6: e1000823.

62. Bouveret E, Rigaut G, Shevchenko A, Wilm M, Seraphin B (2000) A Sm-like protein complex that participates in mRNA degradation. EMBO J 19: 1661-1671.

63. Maleri S, Ge Q, Hackett EA, Wang Y, Dohlman HG, et al. (2004) Persistent activation by constitutive Ste7 promotes Kss1-mediated invasive growth but fails to support Fus3-dependent mating in yeast. Mol Cell Biol 24: 9221-9238.

64. Ptacek J, Devgan G, Michaud G, Zhu H, Zhu X, et al. (2005) Global analysis of protein phosphorylation in yeast. Nature 438: 679-684.

65. Yoon JH, Choi EJ, Parker R (2010) Dcp2 phosphorylation by Ste20 modulates stress granule assembly and mRNA decay in Saccharomyces cerevisiae. J Cell Biol 189: 813-827.

66. Shah KH, Zhang B, Ramachandran V, Herman PK (2013) Processing body and stress granule assembly occur by independent and differentially regulated pathways in Saccharomyces cerevisiae. Genetics 193: 109-123.

67. Shah KH, Nostramo R, Zhang B, Varia SN, Klett BM, et al. (2014) Protein kinases are associated with multiple, distinct cytoplasmic granules in quiescent yeast cells. Genetics 198: 1495-1512.

68. Buchan JR, Muhlrad D, Parker R (2008) P bodies promote stress granule assembly in Saccharomyces cerevisiae. J Cell Biol 183: 441-455.

69. Choi KY, Kranz JE, Mahanty SK, Park KS, Elion EA (1999) Characterization of Fus3 localization: active Fus3 localizes in complexes of varying size and specific activity. Mol Biol Cell 10: 1553-1568.

70. Ma D, Cook JG, Thorner J (1995) Phosphorylation and localization of Kss1, a MAP kinase

of the Saccharomyces cerevisiae pheromone response pathway. Mol Biol Cell 6: 889-909.

71. Zhu H, Klemic JF, Chang S, Bertone P, Casamayor A, et al. (2000) Analysis of yeast protein kinases using protein chips. Nat Genet 26: 283-289.

72. Jona G, Choder M, Gileadi O (2000) Glucose starvation induces a drastic reduction in the rates of both transcription and degradation of mRNA in yeast. Biochim Biophys Acta 1491: 37-48.

73. Hilgers V, Teixeira D, Parker R (2006) Translation-independent inhibition of mRNA deadenylation during stress in Saccharomyces cerevisiae. RNA 12: 1835-1845.

74. Benard L (2004) Inhibition of 5′ to 3′ mRNA degradation under stress conditions in Saccharomyces cerevisiae: from GCN4 to MET16. RNA 10: 458-468.

75. Berman J, Sudbery PE (2002) Candida Albicans: a molecular revolution built on lessons from budding yeast. Nat Rev Genet 3: 918-930.

76. Jung JH, Kim J (2011) Accumulation of P-bodies in Candida albicans under different stress and filamentous growth conditions. Fungal Genet Biol 48: 1116-1123.

77. Bharucha N, Ma J, Dobry CJ, Lawson SK, Yang Z, et al. (2008) Analysis of the yeast kinome reveals a network of regulated protein localization during filamentous growth. Mol Biol Cell 19: 2708-2717.

78. Xu T, Shively CA, Jin R, Eckwahl MJ, Dobry CJ, et al. (2010) A profile of differentially abundant proteins at the yeast cell periphery during pseudohyphal growth. J Biol Chem 285: 15476-15488.

79. Kumar A, des Etages SA, Coelho PS, Roeder GS, Snyder M (2000) High-throughput methods for the large-scale analysis of gene function by transposon tagging. Methods Enzymol 328: 550-574.

80. Xu T, Johnson CA, Gestwicki JE, Kumar A (2010) Conditionally controlling nuclear trafficking in yeast by chemical-induced protein dimerization. Nat Protoc 5: 1831-1843.

81. Ma J, Dobry CJ, Krysan DJ, Kumar A (2008) Unconventional genomic architecture in the budding yeast saccharomyces cerevisiae masks the nested antisense gene NAG1. Eukaryot Cell 7: 1289-1298.

82. Longtine MS, McKenzie A, 3rd, Demarini DJ, Shah NG, Wach A, et al. (1998) Additional modules for versatile and economical PCR-based gene deletion and modification in Saccharomyces cerevisiae. Yeast 14: 953-961.

83. Zhang Y, Kweon HK, Shively C, Kumar A, Andrews PC (2013) Towards systematic discovery of signaling networks in budding yeast filamentous growth stress response using interventional phosphorylation data. PLoS Comput Biol 9: e1003077.

84. Cox J, Matic I, Hilger M, Nagaraj N, Selbach M, et al. (2009) A practical guide to the MaxQuant computational platform for SILAC-based quantitative proteomics. Nat Protoc 4: 698-705.

85. Wiwatwattana N, Landau CM, Cope GJ, Harp GA, Kumar A (2007) Organelle DB: an updated resource of eukaryotic protein localization and function. Nucleic Acids Res 35: D810-814.

86. Bharucha N, Chabrier-Rosello Y, Xu T, Johnson C, Sobczynski S, et al. (2011) A large-scale complex haploinsufficiency-based genetic interaction screen in Candida albicans: analysis of the RAM network during morphogenesis. PLoS Genet 7: e1002058.

Figure 2.1 Kinase regulation of yeast pseudohyphal growth.
A) Kinase signaling pathways that regulate yeast pseudohyphal growth are indicated. Major kinase pathways are boxed. Arrows indicate positive regulation of protein activity, and negative regulation is indicated as interrupted lines. Kinases analyzed in this study are highlighted in red. B) Surface-spread pseudohyphal growth phenotypes are shown for strains carrying kinase-dead alleles of the indicated genes. The degree of surface-spread growth is indicated in the inset boxes, with "++" representing exaggerated filamentous growth and "-" indicating decreased surface-spread filamentation. Strains were grown on low-nitrogen medium (SLAD). Scale bar, 2 mm. C) Colony morphology of yeast strains carrying wild-type and kinase-dead alleles of *FUS3*. The exaggerated morphology of the *fus3* mutant is indicated in the inset box (++) relative to wild-type. D) Yeast invasive growth is diminished relative to wild-type in a strain with a kinase-dead allele of *KSS1*. Images pre- and post-washing of surface cells are shown.

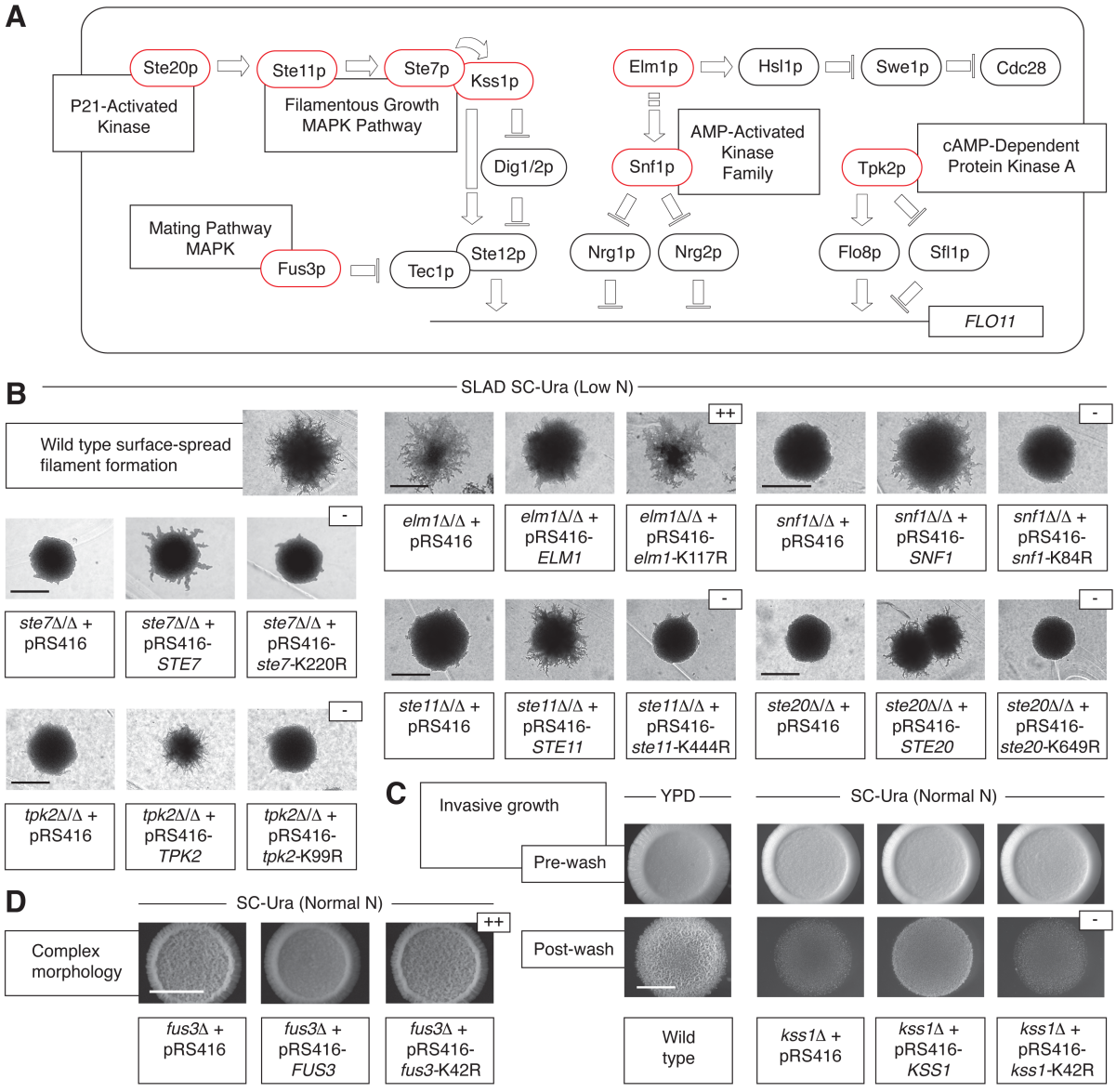

Figure 2.2 Quantitative phosphoproteomic analysis of pseudohyphal growth kinase signaling in a filamentous strain of *S. cerevisiae* by SILAC.
A) The diagram presents n overview of the major steps in protein labeling and mass spectrometry-based identification of kinase-dependent phosphorylation. The labeling scheme for a triplex experiment including strains with kinase-dead tpk2-K99R and snf1-K84R alleles is indicated as an example of the full study. B) Summary of mass spectrometry results.

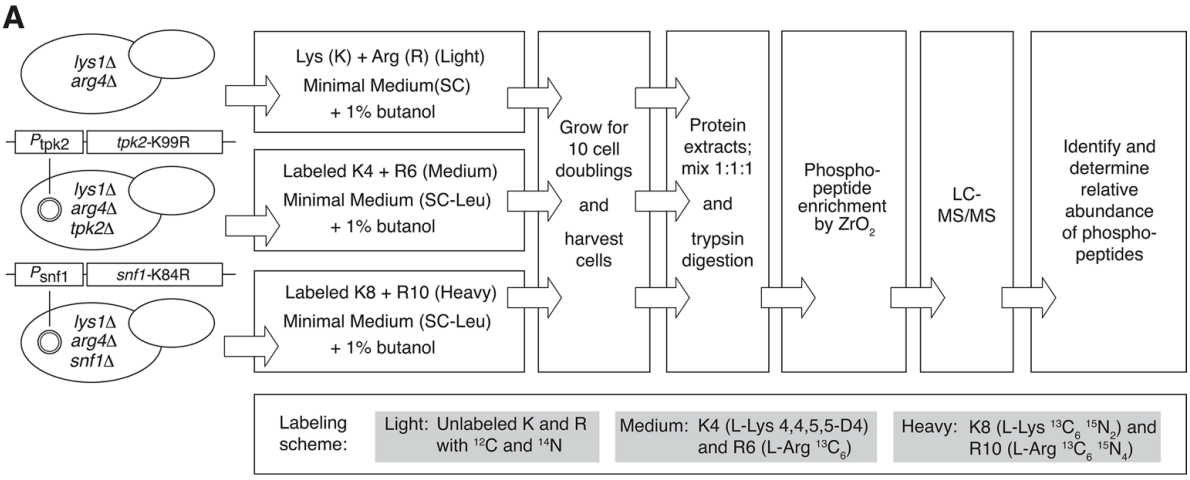

Fig 2.3 Newly identified phosphorylation sites in Ras2pm and Flo8p are required for wild-type yeast invasive growth.
A) Previously unreported phosphorylation sites in Ras2p are shown in red with indicated probability that the sites were correctly identified. Site-directed mutagenesis was used to generate an integrated allele of ras2 encoding Phe and Ala substitutions at Y165 and T166, respectively. The mutant exhibits diminished invasive growth ("-") on YPD medium. Invasive growth was scored quantitatively as mean pixel intensity of the spotted area post-washing relative to the mean pixel intensity before washing. Error bars indicate the standard deviation from three independent trials. B) Novel phosphorylation sites in Flo8p are shown in red. A mutant encoding alanine at each residue (flo8-S3A) yields decreased invasive growth and decreased transcriptional activity of lacZ reporters responsive to Ste12/Tec1p regulation (downstream of the Kss1p MAPK pathway, pFRE-lacZ) and Flo8p-binding (PKA-regulated, Pflo11-6/7), respectively.

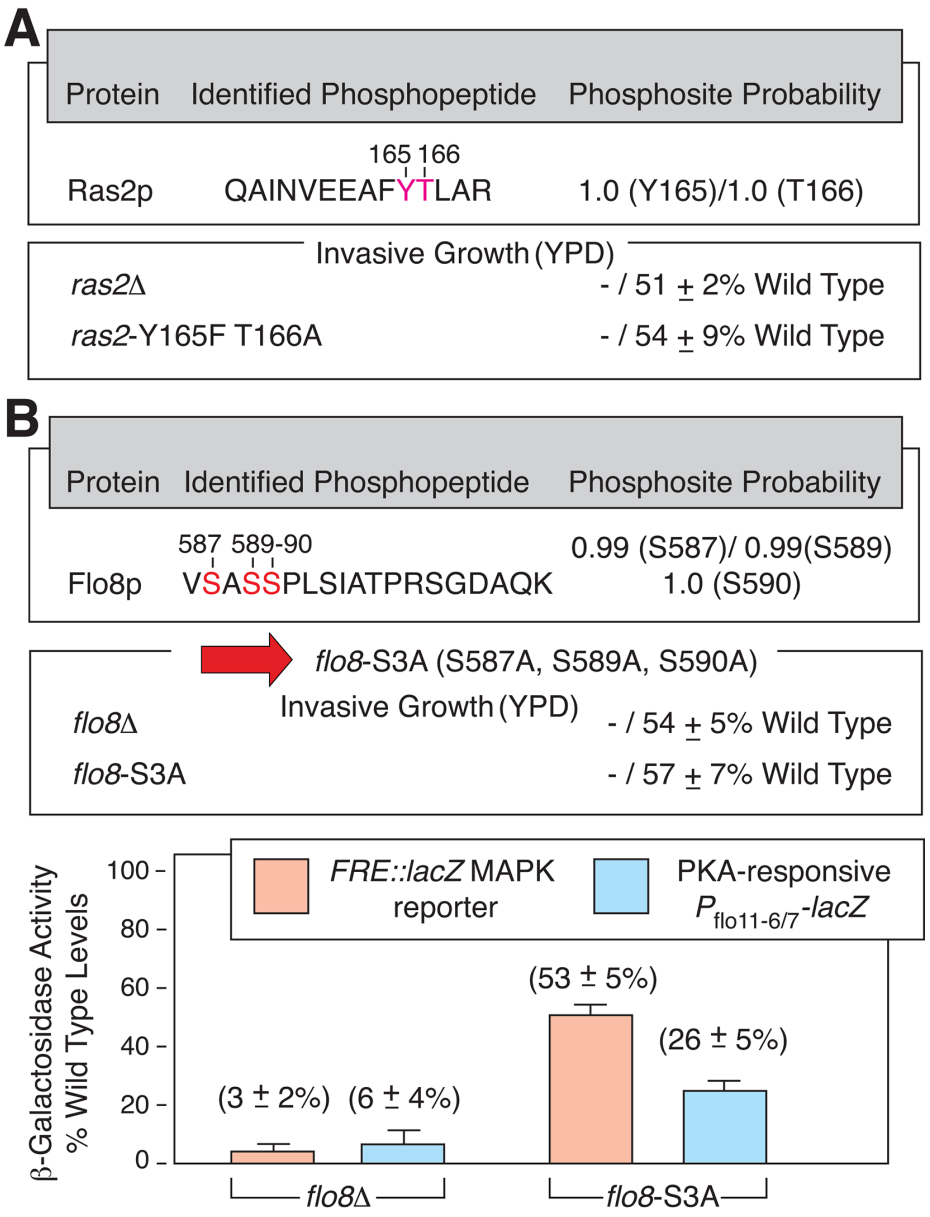

Figure. 2.4 Phenotypic analysis of site-directed mutants with non-phosphorylatable substitutions at newly identified phosphorylation sites in Ras2p and Flo8p.
A) The *ras2*-Y165F T166A mutant exhibits diminished invasive growth (-) on YPD medium relative to wild-type (+). Scale bar, 1 mm. GFP fusions to the amino terminus of wild-type Ras2p and the Ras2p-Y165F T166A mutant localize to the plasma membrane, indicating that the mutant protein is expressed and does localize properly. B) The *flo8*-S3A mutant undergoes decreased invasive growth relative to wild-type. A GFP fusion to the carboxy terminus of a Flo8p mutant with Ala substitutions at S587, S589, S590, and S593 (Flo8p-S4A) yields similar levels of fluorescence and nuclear localization patterns to wild-type Flo8p-GFP. The nucleus was visualized in these cells using a Mad1p-NLS-tDimer chimera. Merged images are shown to the right. Scale bar, 3 μm.

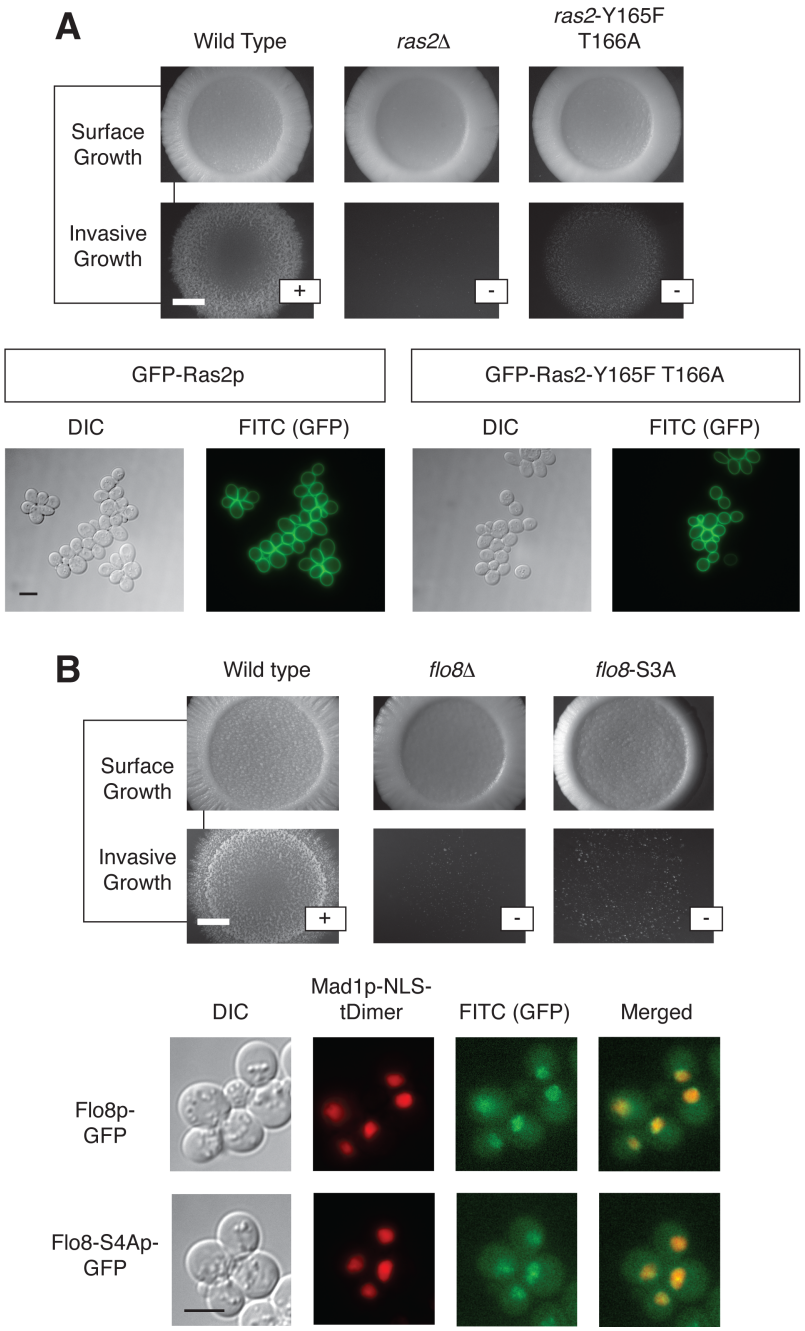

Figure 2.5 The yeast pseudohyphal growth kinase signaling network is enriched in proteins contributing to mRNP granule function.
A) Analysis of phosphoproteins identified as being dependent upon yeast pseudohyphal growth kinases indicates a cluster of proteins involved in translational regulation, encompassing protein components of RNPs. B) The diagram presents a heat map for the enrichment of indicated GO terms (columns) in the respective mass spectrometry data sets generated from the kinase mutants (rows). For convenience, GO IDs are listed below each GO term. Kinases are grouped as positive and negative regulators and presented as individual data sets. C) Connectivity map of proteins in KEGG pathways associated with pseudohyphal growth (MAPK signaling pathway sce04011, cell cycle sce04111, meiosis sce04113) and proteins identified as being components of either P-bodies or stress granules. Lines indicate interactions annotated in KEGG and iRefIndex. Dashed lines identify clusters of proteins involved in the indicated processes.

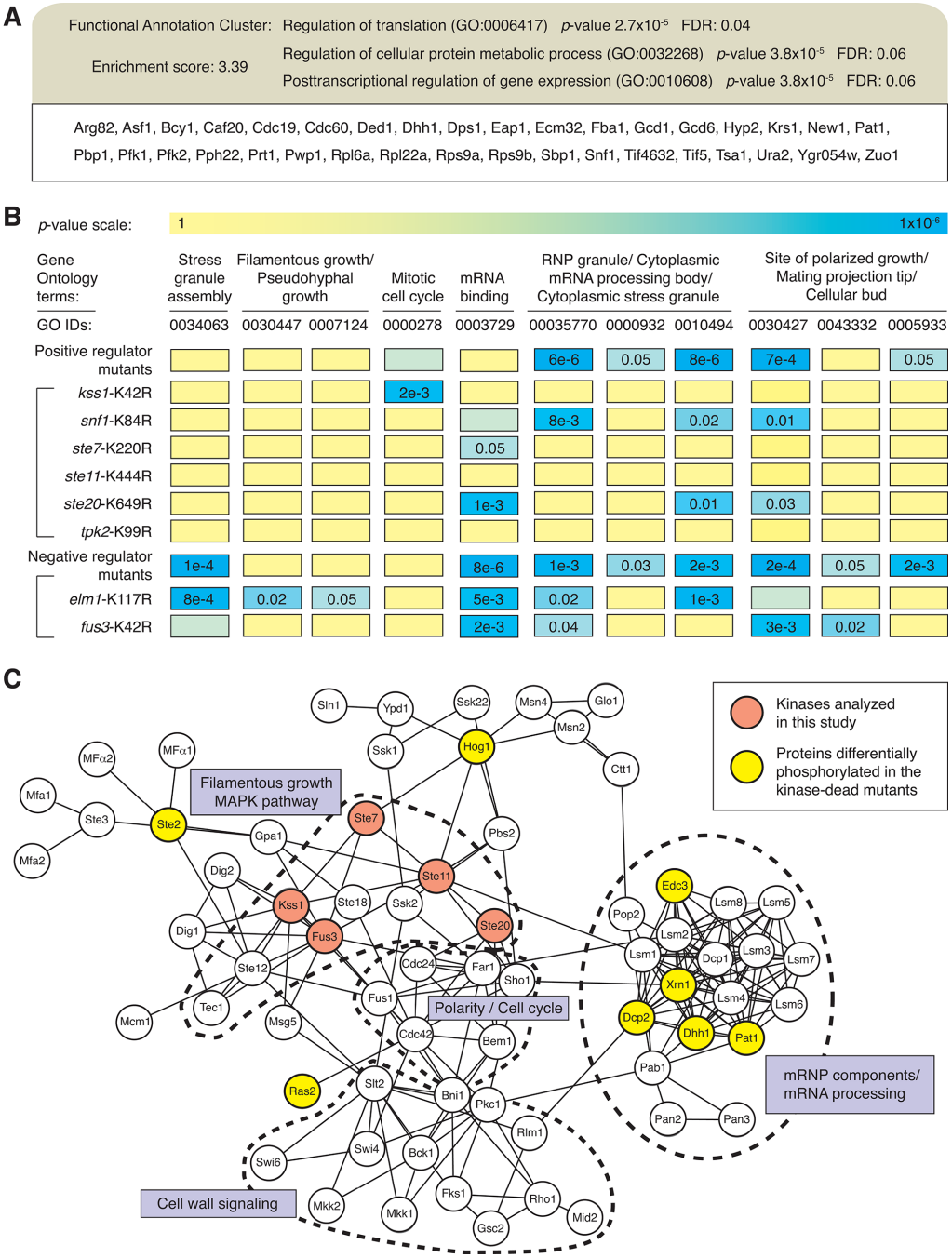

Figure 2.6 Co-localization of Fus3p, Kss1p, Ste20p, and Tpk2p with mRNPs.
A) The RNP component Igo1p was visualized as a carboxy-terminal mCherry fusion generated by integration of a mCherry cassette at the 3'-end of *IGO1*. GFP chimeras were constructed as integrated in-frame fusions to the 3'-ends of the indicated kinase genes. Cells were examined after three days of incubation with shaking in liquid cultures of minimal medium with normal levels of ammonium sulfate. Arrowheads indicate foci with the given kinase and Igo1p. Scale bar, 3 µm. Fluorescent protein fusions to the kinases Elm1p, Snf1p, Ste7p, and Ste11p did not localize significantly as puncta under identical conditions (Fig 2.8A), and were not tested further for co-localization with Igo1p. B) RNPs were visualized as foci using *PGK1* modified to contain 16 binding sites for U1A-GFP in its 3'-UTR. GFP-tagged RNA was analyzed for co-localization with kinase-mCherry fusions generated by integration of sequence encoding mCherry as an in-frame fusion to the 3'-end of the targeted kinase gene. Kinase localization was observed after 15 minutes of glucose stress in SC–Leu–Ura media lacking glucose. Arrowheads indicate kinase-mCherry puncta co-localized with GFP-tagged RNA foci. Quantification of puncta is provided.

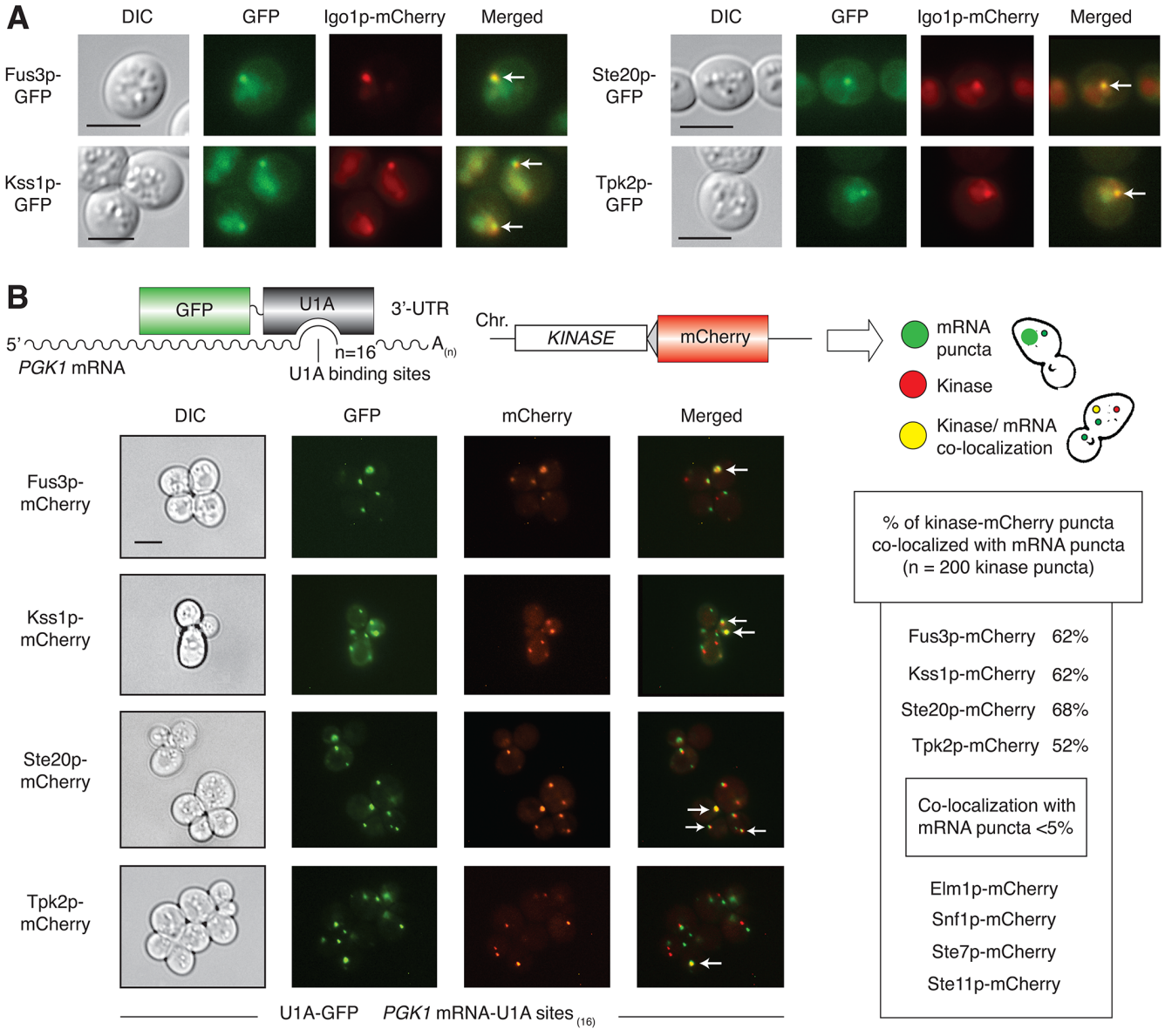

Figure 2.7 Interrelationship between mRNP components, PKA, and pseudohyphal growth MAPK signaling.
A) Morphology of a spotted culture of a haploid strain of the filamentous Σ1278b background deleted for *IGO1* and *IGO2*. Exaggerated wrinkling is evident in the *igo1*Δ*igo2*Δ strain grown on YPD medium. Images of the *igo1*Δ*igo2*0394 strain on low nitrogen SLAD media are presented in Fig 2.8B. B) FRE- and PKA-regulated ($P_{flo11\text{-}6/7}$) *lacZ* reporters indicate decreased signaling in a haploid *igo1*Δ*igo2*Δ mutant in normal media. Error bars indicate the standard deviation from three biological replicates.
C) *IGO1* and *IGO2* are required for wild-type localization of a Tpk2p-GFP fusion in puncta after three days growth in standard SC media. Sequence encoding GFP was fused to the 3'-end of *TPK2* at its native chromosomal locus. The arrowhead identifies a Tpk2p-GFP punctum. Puncta were observed in less than 15% of cells for the *igo1*Δ*igo2*Δ strain (n = 200 cells). Scale bar, 3 μm. D) Surface-spread pseudohyphal filamentation phenotypes are observed in homozygous diploid strains deleted for P-body genes involved in mRNA decay (*CCR4*, *DHH1*, *LSM1*, *PAT1*, *PBP1*, and *SBP1*). Surface spread filamentation was assayed on low nitrogen (SLAD) medium. Scale bar, 2 mm. The degree of filamentation is indicated as "++" (strong surface filamentation) or "-" (decreased surface filamentation). Activity of the pseudohyphal growth Kss1p MAPK signaling pathway is diminished in haploid strains deleted for P-body-localized mRNA decay genes. MAPK pathway activity was assessed using a plasmid-based FRE-*lacZ* reporter. Strains lacking the decapping proteins Lsm1p and Pat1p yielded particularly low levels of *lacZ* signal. Assays were performed on liquid cultures in log phase in standard growth medium. Error bars indicate the standard deviation from three independent trials. E) Epistasis studies of *PAT1* and *LSM1* with the *STE11* and *STE7* genes in the pseudohyphal growth MAPK pathway. Surface filamentation is shown for strains grown on synthetic complete medium. Scale bar, 2 mm. Activity of the pseudohyphal growth Kss1p MAPK pathway as determined using the *FRE*::*lacZ* reporter mirrored the observed colony morphology phenotypes, with the effect slightly lessened in the *STE7*-S368P mutants. The standard deviation in β-galactosidase levels from three independent trials is shown for each strain. F) The pseudohyphal growth MAPK Kss1p is required for wild-type numbers of GFP-tagged RNA puncta as visualized by U1A-GFP binding under conditions of glucose limitation. Arrowheads indicate RNA puncta. Scale bar, 3 μm.

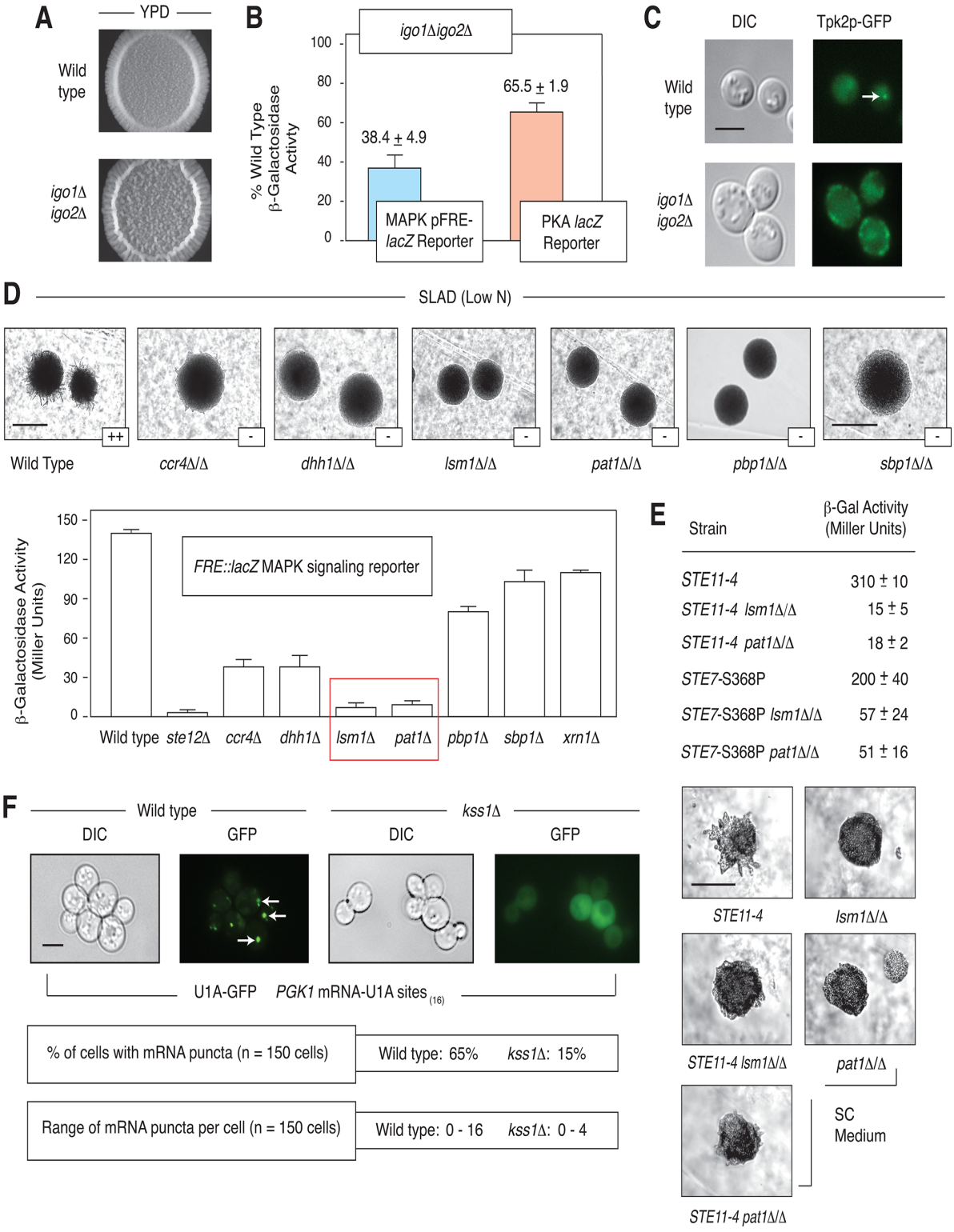
A
YPD
Wild type
igo1Δ igo2Δ
B
igo1Δigo2Δ
% Wild Type β-Galactosidase Activty
100
80
60
40
20
0
38.4 ± 4.9
65.5 ± 1.9
MAPK pFRE-lacZ Reporter
PKA lacZ Reporter
C
DIC
Tpk2p-GFP
Wild type
igo1Δ igo2Δ
D
SLAD (Low N)
++
-
Wild Type
ccr4Δ/Δ
dhh1Δ/Δ
lsm1Δ/Δ
pat1Δ/Δ
pbp1Δ/Δ
sbp1Δ/Δ
β-Galactosidase Activity (Miller Units)
150
120
90
60
30
0
FRE::lacZ MAPK signaling reporter
Wild type
ste12Δ
ccr4Δ
dhh1Δ
lsm1Δ
pat1Δ
pbp1Δ
sbp1Δ
xrn1Δ
E
Strain
β-Gal Activity (Miller Units)
STE11-4 310 ± 10
STE11-4 lsm1Δ/Δ 15 ± 5
STE11-4 pat1Δ/Δ 18 ± 2
STE7-S368P 200 ± 40
STE7-S368P lsm1Δ/Δ 57 ± 24
STE7-S368P pat1Δ/Δ 51 ± 16
STE11-4
lsm1Δ/Δ
STE11-4 lsm1Δ/Δ
pat1Δ/Δ
SC Medium
STE11-4 pat1Δ/Δ
F
Wild type
kss1Δ
DIC
GFP
DIC
GFP
U1A-GFP PGK1 mRNA-U1A sites (16)
% of cells with mRNA puncta (n = 150 cells)
Wild type: 65% kss1Δ: 15%
Range of mRNA puncta per cell (n = 150 cells)
Wild type: 0 - 16 kss1Δ: 0 - 4

Figure 2.8 PHG kinase localization and *IGO1/2* deletion phenotypes.
A) The Elm1p-mCherry, Snf1p-mCherry, Ste7p-GFP, and Ste11p-GFP chimeras do not exhibit significant numbers of puncta after 3 days growth. All chimeras were constructed as integrated in-frame fusions to the 3'-end of each indicated gene. Differential interference contrast (DIC) and fluorescent micrograph images are presented. Scale bar, 3 μm. B) Images of spotted cultures (scale bar, 1 mm) and liquid cultures (scale bar, 3 μm) of a haploid strain deleted for *IGO1* and *IGO2* in low nitrogen SLAD media. A wild-type haploid strain is shown for comparison. No changes in pseudohyphal filamentation or cell morphology are evident in the *igo1/2*Δ strain. C) The subcellular localization of the MAPKs Fus3-GFP and Kss1-GFP, as well as the distribution of the upstream PAK Ste20p-GFP are unaffected by deletion of *IGO1* and *IGO2*. Arrows indicate puncta for each kinase. Scale bar, 3 μm

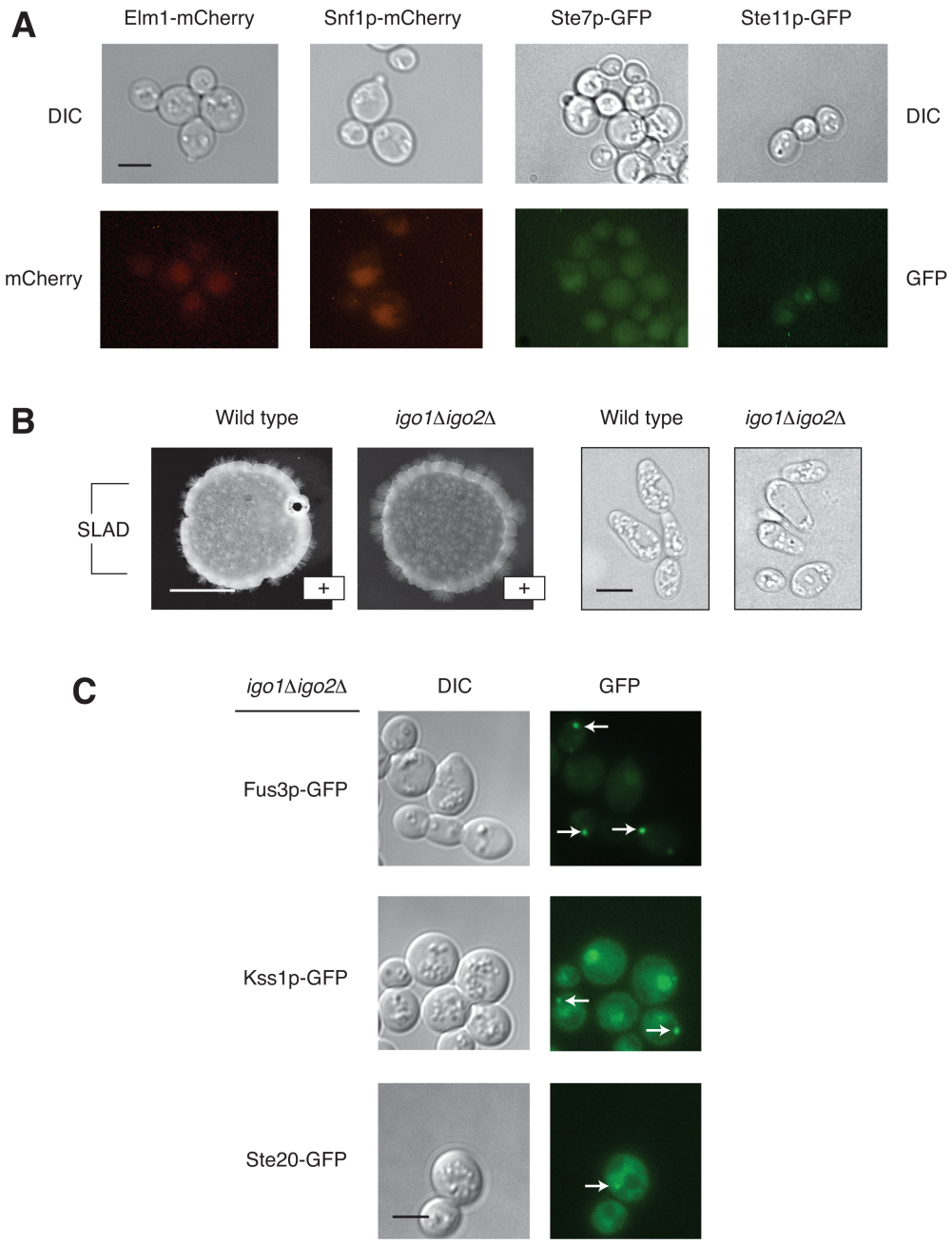

Figure 2.9 Polysome fractionation of lysate from yeast strains.
A) Analysis of a yeast strain with *RPL38-GFP*. Yeast cells were grown to log phase prior to the addition of cycloheximide at a final concentration of 0.1 mg/ml. The harvested cell pellets were resuspended in a slurry of 20 mM HEPES, 1.2% PVP40, 0.1 mg/ml cycloheximide, and Roche EDTA-free protease inhibitor cocktail prior to freezing in liquid nitrogen. Cell extracts were prepared from the frozen cells using a planetary ball mill under cryogenic conditions. The extracts were dissolved in polysome extraction buffer (20 mM HEPES, 140 mM KCl, 5 mM MgCl2, 0.1 mg/ml cycloheximide, 0.5 mM DTT, and protease inhibitor cocktail). The resulting lysates were centrifuged, and clarified lysates containing equivalent amounts of total RNA from treated cells were layered onto 12-ml continuous linear 7–50% (w/v) sucrose gradients in polysome buffer. Velocity sedimentation was performed by centrifuging the gradients at 35,000 rpm for 4 hours at 4 degrees C in a SW41 rotor. 500 µl fractions were manually collected from the top of the gradient to the bottom. Absorbance at 254 nm was measured for each fraction, and the fractions were analyzed for the presence of Rpl38p-GFP by Western blotting. Proteins were detected using Millipore Luminata Crescendo Western HRP Substrate and a BioRad ChemiDoc XRS imaging system with Image Lab software. In the polysome trace, peaks representing association of the large ribosomal subunit and monosome with mRNA are labeled 60S and 80S respectively. The heavier fractions containing polyribosomes are also identified. The polysome trace is from a single experiment representative of two biological replicates. Western blots of both biological replicates are located under the polysome trace. B) Analysis of the *kss1*Δ *RPL38-GFP* strain was carried out as described above.

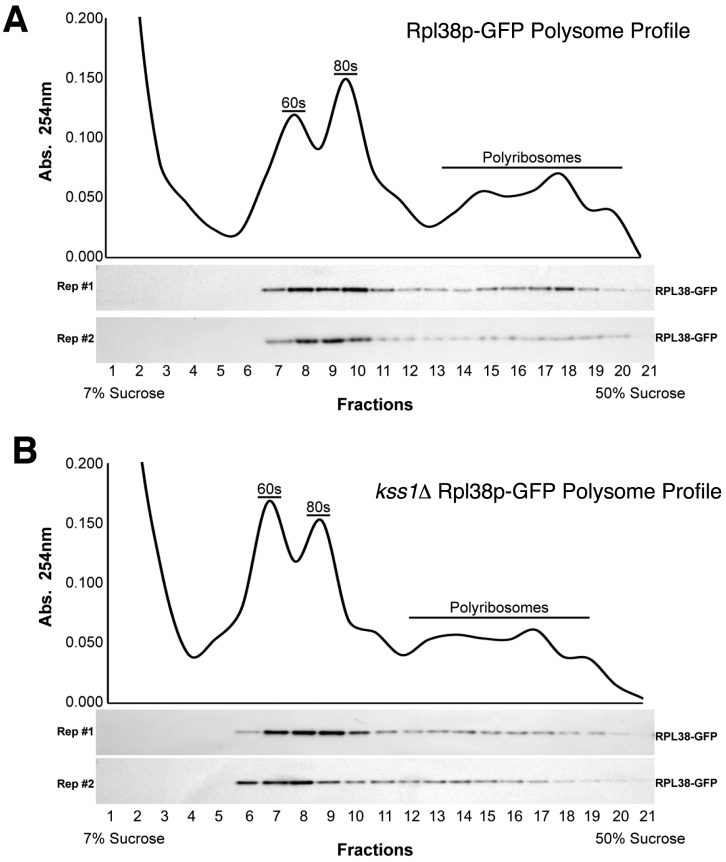

Figure 2.10 The P-body-localized mRNA decay gene *DHH1* is required for wild-type hyphal development in the opportunistic human fungal pathogen *Candida albicans*.
A) The colony morphology of a heterozygous dhh1Δ/DHH1 mutant exhibits diminished surface wrinkling and decreased peripheral filamentation relative to wild-type under conditions inducing hyphal growth (the presence of 10% serum or Spider Medium with 1% mannitol at 37°C). A mutant phenotype was not observed in the dhh1Δ/DHH1 mutant under conditions promoting yeast-form growth (YPD supplemented with uridine at 30°C). Scale bar, 1 mm. B) Cells of the dhh1Δ/DHH1 mutant are less elongated than wild-type under conditions inducing hyphal growth. Scale bar, 3 μm.

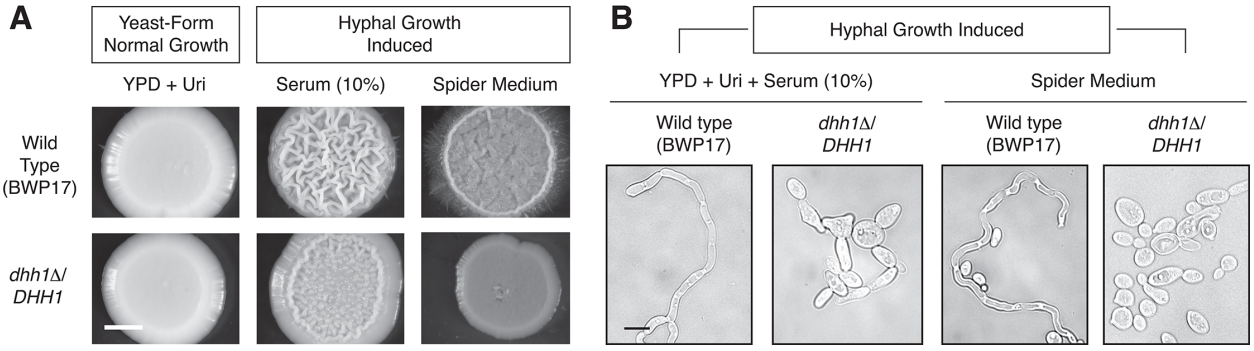

Figure 2.11 Independent construction of a heterozygous *dhh1Δ/DHH1* mutant using a *HIS1* cassette results in a consistent phenotype indicating decreased central wrinkling of a spotted culture.
Images were obtained on indicated media after two days growth. Scale bar, 1 mm.

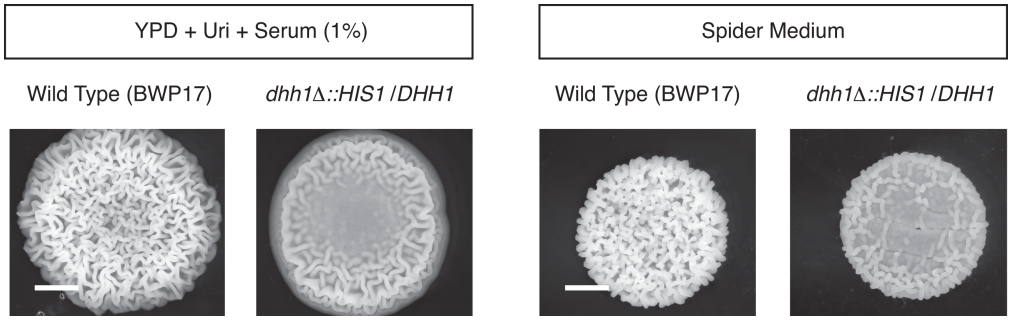

Table 2.1 Listing of pseudohyphal growth phenotypes of kinase-dead mutants studied in this work.

Kinase allele[a]	Kinase pathway/family	Filamentous growth phenotype
ste20-K649R	PAK	Decreased surface filamentation
ste11-K444R	MAPKKK	Decreased surface filamentation
ste7-K220R	MAPKK	Decreased surface filamentation
kss1-K42R	MAPK	Complex colony morphology
fus3-K42R	MAPK	Decreased invasive growth
tpk2-K99R	PKA	Decreased surface filamentation
snf1-K84R	AMP-activated kinase	Decreased surface filamentation
elm1-K117R	S/T Kinase regulating septins	Increased surface filamentation

[a].Kinase-dead mutants are diploid except for *kss1*-K42R and *fus3*-K42R

Table 2.2 Listing of proteins differentially phosphorylated in the kinase-dead mutants.
The "Kinase" column indicates the kinase-dead allele in which the differentially phosphorylated protein was identified. The PEP score, Mascot score, and PTM score for each protein record is indicated. The normalized ratio of phosphorylated peptide in kinase-dead mutant versus wild-type is provided, along with the significance of the ratio (SigA). Data from the constructed compendium of phosphorylation sites has been integrated as the "Known Site" column; blank indicates that we could not identify the phosphorylation site/peptide in the phosphorylation databases. IDs from the phosphorylation databases are provided in the "locEvi" and "pepEvi" columns when available. PepEvi provides evidence of a peptide match, while "locEvi" indicates the localization of phosphorylation to the indicated residue(s). Predicted phosphorylation sites matching a kinase family motif are indicated in the "Motifs" column; the "Best Motif" column indicates the motif that matches the peptide sequence most strongly.

This table can be accessed as a downloadable excel file here:
https://doi.org/10.1371/journal.pgen.1005564.s007

Table 2.3 Listing of Gene Ontology terms enriched in the set of proteins hyper-phosphorylated in one of the kinase-dead mutants tested here.
Indicated terms are enriched to a *p*-value of less than 0.001.

This table can be accessed as a downloadable excel file here:
https://doi.org/10.1371/journal.pgen.1005564.s008

Table 2.4 mRNP components differentially phosphorylated in kinase-dead mutants

Protein	Identified Phosphosite(s)[a]	KD/WT (normalized)[b]	Kinase-dead mutant
Dcp2p	S747/ S751/ S771/ S439	4.3/ 1.8/ 0.44/ 2.6	*kss1/ fus3/ ste20/ snf1*
Ded1p	S369	4.9	*ste20*
Dhh1p	S14	0.34	*elm1*
Eap1p	S30/ S282/ T391	0.31/ 0.12/ 0.28	*snf1*
Edc3p	S255	1.8	*fus3*
Hrp1p	S2, S3	2.7	*ste7*
Igo1p	S157	0.03/ 0.08	*snf1/ tpk2*
Ngr1p	S524	0.17	*snf1*
Pat1	S255	4.5	*ste20*
Pbp1	S106/ S436	0.32/ 2.9	*elm1/ kss1*
Sbp1	T91	3.2/ 2.6/ 3.1/ 5.1/ 8.1	*snf1/ ste7/ ste11/ ste20/ tpk2*
Tif4632p	S74/ T355	1.8/ 2.6	*fus3/ elm1*
Xrn1p	S1510	2.9	*kss1*
Ygr250cp	S482, T486/ S501/ T653	4.7/ 7.2/ 4.2	*ste20/ snf1/ ste20*

[a]Residues on distinct phosphopeptides are separated by slashes; residues on a single phosphopeptide are separated by commas. Phosphorylation sites were localized with $p>0.75$.

[b]Ratio of phosphopeptide in kinase-dead mutant relative to wild-type normalized to protein level. All results exhibit a statistical significance of ≤ 0.05.

doi:10.1371/journal.pgen.1005564.t001

Table 2.5 Listing of proteins and respective database sources used to construct the signaling network maps in Figure 2.5.
The relevant KEGG pathways for MAPK signaling in yeast (sce04011), cell cycle (sce04111), and meiosis (sce04113) are listed. Each constituent protein is shown with its systematic and common name; KEGG Ortholog group annotations and Enzyme Commission numbers are also listed in brackets. RNP components used to construct the network maps are also listed, with systematic name and common names indicated. The database source of each interaction in Fig 2.5C is listed as a separate sheet in this file.

This table can be accessed as a downloadable excel file here:
https://doi.org/10.1371/journal.pgen.1005564.s009

Table 2.6 Listing of in vitro substrates identified by proteome microarray for the kinases tested here that also exhibited differential phosphorylation in our study in the respective kinase-dead strains.

Each unique peptide identified in our analysis for each of these proteins is reported.

KINASE	TARGET	TARGET_STAN_NAME	PEPTIDE_SEQUENCE
ELM1	YIL033C	BCY1	_S(ph)RSSVMFK_
ELM1	YIL033C	BCY1	_SRS(ph)SVMFK_
ELM1	YIL033C	BCY1	_RT(ph)SVSGETLQPNNFDDWTPDHYK_
ELM1	YIL033C	BCY1	_RTSVSGET(ph)LQPNNFDDWTPDHYK_
ELM1	YIL033C	BCY1	_EKT(ph)S(ph)TPPLPMHFNAQR_
ELM1	YIL033C	BCY1	_EKT(ph)S(ph)TPPLPM(ox)HFNAQR_
ELM1	YIL033C	BCY1	_RT(ph)SVSGETLQPNNFDDWTPDHYK_
FUS3	YER122C	GLO3	_AIS(ph)SDQLFGR_
FUS3	YER122C	GLO3	_GNNNNSIDDINTQPDEFNDFLNDT(ph)SNSFDTTRK_
FUS3	YOL016C	CMK2	_S(ph)ALTKDAFVQIVK_
FUS3	YOR276W	CAF20	_KKGS(ph)GEDDEEETETTPTSTVPVATIAQETLK_
FUS3	YFL023W	BUD27	_ILENIS(ph)DDDYDDDDDGNKK_
FUS3	YNR019W	ARE2	_KSS(ph)PDAVDSVGK_
FUS3	YOL016C	CMK2	_NM(ox)YSLGDDGDNDIEENS(ph)LNESLLDGVTHSLDDLR_
FUS3	YOR276W	CAF20	_KKGSGEDDEEETET(ph)TPTSTVPVATIAQETLK_
FUS3	YKL064W	MNR2	_SFVDENS(ph)PTDR_
FUS3	YOR276W	CAF20	_KKGSGEDDEEETETTPT(ph)STVPVATIAQETLK_
FUS3	YOR276W	CAF20	_KKGSGEDDEEETETT(ph)PTSTVPVATIAQETLK_
FUS3	YNR019W	ARE2	_S(ph)SPDAVDSVGK_
FUS3	YDL153C	SAS10	_GMHDNNGADLDDKDY(ph)GSEDEAVSR_
KSS1	YGL061C	DUO1	_(ca)S(ph)T(ph)NS(ph)ILDSWINIHS(ph)QAGYIHK_
KSS1	YGR116W	SPT6	_VGDEGNAAESESDNVAAS(ph)R_
KSS1	YGR116W	SPT6	_EREEDDRLS(ph)EDDLDLLM(ox)ENAGVER_
KSS1	YLR324W	PEX30	_NEAESGVSEDNDNGS(ph)LEK_
KSS1	YGR116W	SPT6	_GGILDELDDFIEDDEFS(ph)DEDDETR_
KSS1	YGR116W	SPT6	_VGDEGNAAESES(ph)DNVAASR_
KSS1	YIL036W	CST6	_FGS(ph)DTDDDDIDLKPVEGGK_
KSS1	YNL272C	SEC2	_IGPLVEDDS(ph)DEDQNDAISVR_
KSS1	YIL036W	CST6	_FGSDT(ph)DDDDIDLKPVEGGK_
KSS1	YIL038C	NOT3	_IGS(ph)ALNT(ph)PK_
KSS1	YNL272C	SEC2	_IGPLVEDDS(ph)DEDQNDAIS(ph)VR_
KSS1	YGR116W	SPT6	_LEDFFS(ph)EDEEEEESGLR_
KSS1	YGR116W	SPT6	_VGDEGNAAES(ph)ESDNVAASR_
KSS1	YKR048C	NAP1	_GQEIVESLNETELLVDEEEKAQNDS(ph)EEEQVK_
KSS1	YIL038C	NOT3	_TPTTAAATTT(ph)SSNANSR_
KSS1	YFL023W	BUD27	_ILENIS(ph)DDDYDDDDDGNKK_

KSS1	YIL038C	NOT3	_TPTTAAATTTSS(ph)NANSR_
KSS1	YIL038C	NOT3	_TPTTAAATTTS(ph)SNANSR_
KSS1	YIL038C	NOT3	_TPTTAAAT(ph)TTSSNANSR_
KSS1	YDL153C	SAS10	_GMHDNNGADLDDKDY(ph)GSEDEAVSR_
SNF1	YAR014C	BUD14	_ENSSELPDSYDYS(ph)DSEFEDNLERR_
SNF1	YAR014C	BUD14	_ENSSELPDSYDYSDS(ph)EFEDNLERR_
SNF1	YBR130C	SHE3	_TNVTHNNDPSTS(ph)PTISVPPGVTR_
SNF1	YDL025C	RTK1	_KNTDS(ph)DQEDQIK_
SNF1	YDL051W	LHP1	_RNS(ph)FAVIEFTPEVLDR_
SNF1	YDL051W	LHP1	_EESKEDSS(ph)AIADDDEEHKE_
SNF1	YDL051W	LHP1	_EESKEDS(ph)SAIADDDEEHKE_
SNF1	YDL225W	SHS1	_FLNS(ph)PDLPER_
SNF1	YDL225W	SHS1	_NDTYTDLASIAS(ph)GRD_
SNF1	YDL225W	SHS1	_NDT(ph)YTDLASIASGRD_
SNF1	YDL225W	SHS1	_LNGS(ph)SSS(ph)INSLQQSTR_
SNF1	YDL225W	SHS1	_LNGSS(ph)SSINSLQQSTR_
SNF1	YDL225W	SHS1	_KNDT(ph)YTDLASIASGRD_
SNF1	YDL225W	SHS1	_KNDTYT(ph)DLASIASGRD_
SNF1	YDL225W	SHS1	_ENEY(ph)EDNGEHDSAENEQEMSPVR_
SNF1	YDL225W	SHS1	_NQVSGNFKENEYEDNGEHDS(ph)AENEQEMSPVR_
SNF1	YDR293C	SSD1	_NNEYS(ph)PGINSNWR_
SNF1	YDR293C	SSD1	_NQSQQPQQQLS(ph)PFR_
SNF1	YDR293C	SSD1	_S(ph)STINNDSDSLSSPTK_
SNF1	YDR293C	SSD1	_SSTINNDSDS(ph)LSSPTK_
SNF1	YDR293C	SSD1	_SSTINNDSDSLS(ph)SPTK_
SNF1	YDR293C	SSD1	_SSTINNDSDSLSS(ph)PTK_
SNF1	YDR293C	SSD1	_SST(ph)INNDSDSLSSPTK_
SNF1	YER024W	YAT2	_KTSS(ph)SSQVNLNR_
SNF1	YER122C	GLO3	_AIS(ph)SDQLFGR_
SNF1	YER122C	GLO3	_EAQQEKEDEFTNSSSS(ph)TK_
SNF1	YER122C	GLO3	_EAQQEKEDEFTNSSS(ph)STK_
SNF1	YER122C	GLO3	_AISSDQLFGRGS(ph)FDEAANR_
SNF1	YER122C	GLO3	_AISS(ph)DQLFGRGSFDEAANR_
SNF1	YER122C	GLO3	_GNNNNS(ph)IDDINTQPDEFNDFLNDTSNSFDTTRK_
SNF1	YGL023C	PIB2	_KNS(ph)AEENVR_
SNF1	YGL035C	MIG1	_S(ph)LTDFQGLNNANPNNNGSLR_
SNF1	YGL208W	SIP2	_VTELS(ph)LNK_
SNF1	YHR073W	OSH3	_TST(ph)QQDMLFR_
SNF1	YHR117W	TOM71	_RQS(ph)EAFAGQNEDEADLKDDGSVVSGSNK_
SNF1	YHR133C	NSG1	_LGS(ph)ASFTAINTLTKPALFSFYDDDITKNEGNVYDK_
SNF1	YHR133C	NSG1	_LGSASFT(ph)AINTLTKPALFSFYDDDITKNEGNVYDK_
SNF1	YHR205W	SCH9	_S(ph)SSQLDQLNSCSSVTDPSKR_
SNF1	YIL107C	PFK26	_S(ph)SFASDFLSR_

SNF1	YIL107C	PFK26	_RYSVIPT(ph)APPS(ph)AR_
SNF1	YIL107C	PFK26	_S(ph)NPTSASSSQSELSEQPK_
SNF1	YIL107C	PFK26	_RYS(ph)VIPTAPPS(ph)AR_
SNF1	YJL080C	SCP160	_KPT(ph)PLPS(ph)LK_
SNF1	YJL080C	SCP160	_DLPSLGS(ph)NAAFANVK_
SNF1	YJL080C	SCP160	_LTYEPIDLS(ph)SILSDGEEKEVTK_
SNF1	YJL080C	SCP160	_LTYEPIDLSSILS(ph)DGEEKEVTK_
SNF1	YJL080C	SCP160	_LTYEPIDLSS(ph)ILSDGEEKEVTKDTSNDSAK_
SNF1	YJL080C	SCP160	_LTYEPIDLSSILSDGEEKEVTKDT(ph)SNDSAK_
SNF1	YJL084C	ALY2	_TLS(ph)DNETITSR_
SNF1	YJL084C	ALY2	_T(ph)LSDNETITSR_
SNF1	YKR071C	DRE2	_VVDDLIEDS(ph)DDDDFSSDSSK_
SNF1	YLR192C	HCR1	_ALLDIDT(ph)LDEK_
SNF1	YML062C	MFT1	_DGLLNEAEGDNIDEDYES(ph)DEDEERKER_
SNF1	YML111W	BUL2	_SAS(ph)TTNLDR_
SNF1	YML111W	BUL2	_IDDTASQS(ph)PSYDSK_
SNF1	YMR165C	PAH1	_TNTSMVPGS(ph)PPNR_
SNF1	YMR205C	PFK2	_VHS(ph)YTDLAYR_
SNF1	YMR205C	PFK2	_S(ph)SPDENSTLLSNDSISLK_
SNF1	YMR290C	HAS1	_SRDS(ph)ESTEEPVVDEK_
SNF1	YNL227C	JJJ1	_GLQT(ph)DDDEDWSTK_
SNF1	YNL272C	SEC2	_IGPLVEDDS(ph)DEDQNDAISVR_
SNF1	YNR013C	PHO91	_RPS(ph)NTFNLDADR_
SNF1	YNR013C	PHO91	_RPSNT(ph)FNLDADR_
SNF1	YNR013C	PHO91	_INNDENS(ph)SGNEEDEDGNRQEVLDFQDAER_
SNF1	YOR123C	LEO1	_KQNS(ph)PTTYGASR_
SNF1	YOR123C	LEO1	_KQNSPT(ph)TYGASR_
SNF1	YOR123C	LEO1	_KFYGEDANNFS(ph)DQDETTHTFKEENVELVR_
SNF1	YOR123C	LEO1	_KFYGEDANNFSDQDET(ph)THTFKEENVELVR_
SNF1	YOR198C	BFR1	_VVADDLVLVT(ph)PK_
SNF1	YOR216C	RUD3	_MSTDPEADGIVAS(ph)PDDEGKDLSEGVDK_
SNF1	YOR216C	RUD3	_MSTDPEADGIVAS(ph)PDDEGKDLSEGVDKQK_
SNF1	YOR340C	RPA43	_IVFDDEVS(ph)IENK_
SNF1	YPR115W	RGC1	_RGS(ph)DLSPFEMESPLFEENR_
SNF1	YPR156C	TPO3	_QIDGASSPSSNEDALES(ph)DNNEKGK_
STE11	YJR059W	PTK2	_NFSAPNVS(ph)SSSNSLR_
STE11	YJR059W	PTK2	_NFSAPNVSS(ph)S(ph)SNSLR_
STE11	YJR059W	PTK2	_NFSAPNVSSS(ph)SNS(ph)LR_
STE11	YJR059W	PTK2	_NFSAPNVSSS(ph)SNSLR_
STE11	YJR059W	PTK2	_KRPT(ph)S(ph)PSISGSGSGGNSPSSSAGAR_
STE11	YJR059W	PTK2	_KRPT(ph)SPSISGSGSGGNSPSSSAGAR_
STE20	YBL085W	BOI1	_YGNLNDS(ph)ASNIGK_
STE20	YBR086C	IST2	_FDEDGKS(ph)IR_

STE20	YBR086C	IST2	_SSAES(ph)SNATNNNTLGTESK_
STE20	YBR086C	IST2	_S(ph)SAESSNATNNNTLGTESK_
STE20	YBR086C	IST2	_VPT(ph)VGS(ph)YGVAGATLPETIPTSK_
STE20	YBR086C	IST2	_VPT(ph)VGSYGVAGATLPETIPTSK_
STE20	YBR086C	IST2	_AVDNDT(ph)AGS(ph)AGKKPLATESTEK_
STE20	YBR086C	IST2	_DANIKPVVNAAVNDNQSKVS(ph)VATEQTK_
STE20	YBR086C	IST2	_AVDNDTAGS(ph)AGKKPLATESTEK_
STE20	YBR108W	AIM3	_DS(ph)SPVPSDLDEK_
STE20	YBR108W	AIM3	_VKDSSPVPS(ph)DLDEK_
STE20	YBR108W	AIM3	_EAT(ph)GQDEVLNSITNELSHIK_
STE20	YBR108W	AIM3	_SQS(ph)SNSSDSSYTIDGPEANHGR_
STE20	YDL153C	SAS10	_LNELQNS(ph)EDS(ph)DAEDGGK_
STE20	YDL153C	SAS10	_GM(ox)HDNNGADLDDKDYGS(ph)EDEAVSR_
STE20	YDL153C	SAS10	_GM(ox)HDNNGADLDDKDY(ph)GSEDEAVSR_
STE20	YDR293C	SSD1	_NQSQQPQQQLS(ph)PFR_
STE20	YDR293C	SSD1	_SSTINNDSDS(ph)LSSPTK_
STE20	YDR293C	SSD1	_SSTINNDSDSLSS(ph)PTK_
STE20	YDR293C	SSD1	_SST(ph)INNDSDSLSSPTK_
STE20	YDR293C	SSD1	_RSSTINNDSDSLSS(ph)PTK_
STE20	YDR330W	UBX5	_VNDMFDEGRPES(ph)IFNQR_
STE20	YER122C	GLO3	_AIS(ph)SDQLFGR_
STE20	YNL027W	CRZ1	_SIS(ph)PDEKAK_
STE20	YNL173C	MDG1	_SIFSQEVVELPDS(ph)EDETQQVNK_
STE20	YNL173C	MDG1	_SEGYVTDGLGKTQS(ph)SESR_
STE20	YNL173C	MDG1	_SIFS(ph)QEVVELPDSEDETQQVNK_
STE20	YNL272C	SEC2	_IGPLVEDDS(ph)DEDQNDAISVR_
STE20	YNR019W	ARE2	_S(ph)SPDAVDSVGK_
STE20	YOL139C	CDC33	_KFEENVSVDDTTAT(ph)PK_
STE20	YOL139C	CDC33	_TVLSDS(ph)AHFDVKHPLNTK_
STE20	YOR092W	ECM3	_TNHVDAQS(ph)VSELNDPTYR_
STE20	YPL217C	BMS1	_IYGKPVQEEDADIDNLPS(ph)DEEPYTNDDDVQDSEPR_
STE20	YPR091C	NVJ2	_WYKDNVGNS(ph)SDTEDMDEIDVQDKK_
STE20	YPR091C	NVJ2	_WYKDNVGNSS(ph)DTEDMDEIDVQDKK_
TPK2	YBR059C	AKL1	_QS(ph)SDPTISEQSPR_
TPK2	YBR059C	AKL1	_QSSDPTISEQS(ph)PR_
TPK2	YBR059C	AKL1	_S(ph)TSYGAATIGSDEALANEK_
TPK2	YBR059C	AKL1	_STSYGAATIGS(ph)DEALANEK_
TPK2	YBR059C	AKL1	_IPS(ph)QNVGQELEEEKESQSDQR_
TPK2	YBR059C	AKL1	_IPSQNVGQELEEEKES(ph)QSDQR_
TPK2	YFR014C	CMK1	_VCS(ph)SDSDLPGSDIK_
TPK2	YFR014C	CMK1	_VSEKES(ph)SPKQTEEDSEGK_
TPK2	YFR017C	IGD1	_S(ph)TNYMDALNSR_
TPK2	YFR017C	IGD1	_MTDPHLNTPQVSTS(ph)PTFER_

TPK2	YFR017C	IGD1	_TTNDSDLSHAGVDMGDSIS(ph)HTPICSR_
TPK2	YIL033C	BCY1	_T(ph)STPPLPMHFNAQR_
TPK2	YIL033C	BCY1	_TST(ph)PPLPMHFNAQR_
TPK2	YIL033C	BCY1	_EKTS(ph)T(ph)PPLPMHFNAQR_
TPK2	YIL033C	BCY1	_NIVLFPEPEES(ph)FSRPQSAQSQSR_
TPK2	YIL033C	BCY1	_NIVLFPEPEESFSRPQS(ph)AQSQSR_
TPK2	YIL033C	BCY1	_NIVLFPEPEESFSRPQSAQS(ph)QS(ph)R_
TPK2	YIL033C	BCY1	_RTS(ph)VSGETLQPNNFDDWTPDHYK_
TPK2	YIL033C	BCY1	_T(ph)SVSGETLQPNNFDDWTPDHYKEK_
TPK2	YIL033C	BCY1	_RT(ph)SVSGETLQPNNFDDWTPDHYKEK_
TPK2	YIL107C	PFK26	_S(ph)SFASDFLSR_
TPK2	YIL107C	PFK26	_S(ph)NPTSASSSQSELSEQPK_
TPK2	YIL107C	PFK26	_RYSVIPT(ph)APPS(ph)AR_
TPK2	YIL107C	PFK26	_RYS(ph)VIPTAPPS(ph)AR_
TPK2	YJL141C	YAK1	_TVYT(ph)YIQSR_
TPK2	YJL141C	YAK1	_NDLQPVLNAT(ph)PK_
TPK2	YJR001W	AVT1	_PEQEPLS(ph)PNGR_
TPK2	YKL064W	MNR2	_SFVDENSPT(ph)DR_
TPK2	YKL064W	MNR2	_SFVDENS(ph)PTDRR_
TPK2	YKL166C	TPK3	_TETT(ph)PDNVGQDIPVNAHSVHEECSSNTPVEINGR_
TPK2	YKL166C	TPK3	_YVPDVTYT(ph)LCGTPDYIAPEVVSTKPYNK_
TPK2	YKL166C	TPK3	_TET(ph)TPDNVGQDIPVNAHSVHEECSSNTPVEINGR_
TPK2	YOL016C	CMK2	_NMYSLGDDGDNDIEENSLNES(ph)LLDGVTHSLDDLR_
TPK2	YOL016C	CMK2	_NMYSLGDDGDNDIEENS(ph)LNESLLDGVTHSLDDLR_

Table 2.7 Listing of strains used in this study.

Strain	Genotype	Source
Y825	*ura3-52 leu2Δ0 MAT***a**	M. Snyder (Stanford, CA)
HLY337	*ura3-52 trp1-1 MAT*α	G. Fink (MIT, MA)
BWP17	*ura3::Δimm434/ura3::Δimm434 his1::hisG/his1::hisG arg4::hisG/arg4::hisG*	FGSC (UMKC, MO)
yCAS1	*ura3-52/ura3-52 leu2Δ0/leu2Δ0 MAT***a**/*MAT*α pRS426	This study
yCAS2	*ura3-52/ura3-52 leu2Δ0/leu2Δ0 MAT***a**/*MAT*α pRS416	This study
yCAS3	*ura3-52 leu2Δ0 arg4*Δ *lys1*Δ *MAT***a**	This study
yCD1	*ura3-52 leu2Δ0 arg4*Δ *lys1*Δ *elm1*Δ *MAT***a**	This study
yCD2	*ura3-52 leu2Δ0 arg4*Δ *lys1*Δ *fus3*Δ *MAT***a**	This study
yCD3	*ura3-52 leu2Δ0 arg4*Δ *lys1*Δ *kss1*Δ *MAT***a**	This study
yCD4	*ura3-52 leu2Δ0 arg4*Δ *lys1*Δ *ste7*Δ *MAT***a**	This study
yCD5	*ura3-52 leu2Δ0 arg4*Δ *lys1*Δ *ste11*Δ *MAT***a**	This study
yCD6	*ura3-52 leu2Δ0 arg4*Δ *lys1*Δ *ste20*Δ *MAT***a**	This study
yCD7	*ura3-52 leu2Δ0 arg4*Δ *lys1*Δ *snf1*Δ *MAT***a**	This study
yCD8	*ura3-52 leu2Δ0 arg4*Δ *lys1*Δ *tpk2*Δ *MAT***a**	This study
yTX1	*ura3-52 leu2Δ0 arg4*Δ *lys1*Δ *elm1*Δ *MAT***a** + pDEST-*ELM1*-KD	This study
yTX2	*ura3-52 leu2Δ0 arg4*Δ *lys1*Δ *fus3*Δ *MAT***a** + pDEST-*FUS3*-KD	This study
yTX3	*ura3-52 leu2Δ0 arg4*Δ *lys1*Δ *kss1*Δ *MAT***a** + pDEST-*KSS1*-KD	This study
yTX4	*ura3-52 leu2Δ0 arg4*Δ *lys1*Δ *snf1*Δ *MAT***a** + pDEST-*SNF1*-KD	This study
yTX5	*ura3-52 leu2Δ0 arg4*Δ *lys1*Δ *ste7*Δ *MAT***a** + pDEST-*STE7*-KD	This study
yTX6	*ura3-52 leu2Δ0 arg4*Δ *lys1*Δ *ste11*Δ *MAT***a** + pDEST-*STE11*-KD	This study
yTX7	*ura3-52 leu2Δ0 arg4*Δ *lys1*Δ *ste20*Δ *MAT***a** +	This study

	pDEST-*STE20*-KD	
yTX8	*ura3-52 leu2*Δ*0 arg4*Δ *lys1*Δ *ste20*Δ *MAT***a** + pDEST-*TPK2*-KD	This study
yCAS4	*ras2*Δ*::KanMX6*/*ras2*Δ*::KanMX6 ura3-52/ura3-52 leu2*Δ*0/LEU2 TRP1/trp1-1 MAT***a**/*MAT*α	This study
yCAS5	*ras2*Δ*::KanMX6*/*ras2*Δ*::KanMX6 ura3-52/ura3-52 leu2*Δ*0/LEU2 TRP1/trp1-1 MAT***a**/*MAT*α + pRS416-*RAS2*-Y165F/T166A	This study
yKN1	*flo8*-S3A *ura3-52 leu2*Δ*0 MAT***a**	This study
yCAS7	*flo8*Δ*::KanMX6 ura3-52 leu2*Δ*0 MAT***a** + pFRE-*lacZ*	This study
yKN2	*flo8*-S3A *ura3-52 leu2*Δ*0 MAT***a** + pFRE-*lacZ*	This study
yCAS923	*flo8*-S3A-GFP-*KanMX6 ura3-52 leu2*Δ*0 MAT***a**	This study
yCAS101	*KSS1*-GFP-*KanMX6 ura3-52 trp1-1 MAT*α	This study
yCAS102	*FUS3*-GFP-*KanMX6 ura3-52 trp1-1 MAT*α	This study
yCAS103	*STE20*-GFP-*KanMX6 ura3-52 trp1-1 MAT*α	This study
yCAS840	*TPK2*-GFP-*TRP1 ura3-52 trp1-1 MAT*α	This study
yCAS855	*TPK2*-GFP-*TRP1 IGO1*-mCherry-*KanMX6 ura3-52 trp1-1 MAT*α	This study
yCAS757	*FUS3*-GFP-*KanMX6 IGO1*-mCherry-*HphMX4 ura3-52 trp1-1 MAT*α	This study
yCAS758	*KSS1*-GFP-*KanMX6 IGO1*-mCherry-*HphMX4 ura3-52 trp1-1 MAT*α	This study
yCAS759	*STE20*-GFP-*KanMX6 IGO1*-mCherry-*HphMX4 ura3-52 trp1-1 MAT*α	This study
yCAS819	*igo1*Δ*::KanMX6*/*igo1*Δ*::KanMX6 igo2::URA3/igo2::URA3 ura3-52/ura3-52 leu2_0/LEU2 TRP1/trp1-1 MAT***a**/*MAT*α	This study
yCAS909	*igo1*Δ*::KanMX6 igo2*Δ*::URA3 TPK2*-GFP-*TRP1 ura3-52 trp1-1 MAT*α	This study
yCAS794	*ura3-52/ura3-52 leu2*Δ*0/LEU2 TRP1/trp1-1 igo1*Δ*::KanMX6*/*igo1*Δ*::KanMX6 MAT***a**/*MAT*α	This study
yCAS255	*ura3-52/ura3-52 leu2*Δ*0/LEU2 TRP1/trp1-1 dhh1*Δ*::KanMX6*/*dhh1*Δ*::KanMX6 MAT***a**/*MAT*α	This study

yCAS682	*ura3-52/ura3-52 leu2Δ0/LEU2 TRP1/trp1-1 dhh1Δ::KanMX6/dhh1Δ::KanMX6 MAT***a***/MATα*	This study
yCAS176	*ura3-52/ura3-52 leu2Δ0/LEU2 TRP1/trp1-1 pat1Δ::KanMX6/pat1Δ::KanMX6 MAT***a***/MATα*	This study
yCAS177	*ura3-52/ura3-52 leu2Δ0/LEU2 TRP1/trp1-1 pbp1Δ::KanMX6/pbp1Δ::KanMX6 MAT***a***/MATα*	This study
yCAS175	*ura3-52/ura3-52 leu2Δ0/LEU2 TRP1/trp1-1 sbp1Δ::KanMX6/sbp1Δ::KanMX6 MAT***a***/MATα*	This study
yCAS452	*ste12Δ::KanMX6 ura3-52 trp1-1 MATα* + pFRE-*lacZ*	This study
yCAS810	*ccr4Δ::KanMX6 ura3-52 trp1-1 MATα* + pFRE-*lacZ*	This study
yCAS454	*dhh1Δ::KanMX6 ura3-52 trp1-1 MATα* + pFRE-*lacZ*	This study
yCAS941	*lsm1Δ::KanMX6 ura3-52 trp1-1 MATα* + pFRE-*lacZ*	This study
yCAS943	*pat1Δ::KanMX6 ura3-52 trp1-1 MATα* + pFRE-*lacZ*	This study
yCAS537	*pbp1Δ::KanMX6 ura3-52 trp1-1 MATα* + pFRE-*lacZ*	This study
yCAS538	*sbp1Δ::KanMX6 ura3-52 trp1-1 MATα* + pFRE-*lacZ*	This study
yCAS540	*xrn1Δ::KanMX6 ura3-52 trp1-1 MATα* + pFRE-*lacZ*	This study
yCAS969	*ura3-52/ura3-52 leu2Δ0/LEU2 TRP1/trp1-1 lsm1Δ::KanMX6/lsm1Δ::KanMX6 MAT***a***/MATα* + *STE11-4*-pRS416	This study
yCAS971	*ura3-52/ura3-52 leu2Δ0/LEU2 TRP1/trp1-1 pat1Δ::KanMX6/pat1Δ::KanMX6 MAT***a***/MATα* + *STE11-4*-pRS416	This study
yCAS968	*ura3-52/ura3-52 leu2Δ0/LEU2 TRP1/trp1-1 lsm1Δ::KanMX6/lsm1Δ::KanMX6 MAT***a***/MATα* + *STE7*-S368P-pRS416	This study
yCAS970	*ura3-52/ura3-52 leu2Δ0/LEU2 TRP1/trp1-1 pat1Δ::KanMX6/pat1Δ::KanMX6 MAT***a***/MATα* + *STE7*-S368P-pRS416	This study
yCAS636	*ura3-52 leu2Δ0 FUS3*-mCherry-*KanMX6 MAT***a**	This study
yCAS637	*ura3-52 leu2Δ0 KSS1*-mCherry-*KanMX6 MAT***a**	This study
yCAS635	*ura3-52 leu2Δ0 STE20*-mCherry-*KanMX6 MAT***a**	This study
yCAS688	*ura3-52 leu2Δ0 TPK2*-mCherry-*KanMX6 MAT***a**	This study
yKN1	*ura3-52 leu2Δ0 FUS3*-mCherry-*KanMX6 MAT***a** +	This study

	pRP1194 + pPS2037	
yKN2	*ura3-52 leu2*Δ*0 KSS1*-mCherry-*KanMX6 MAT***a** + pRP1194 + pPS2037	This study
yKN3	*ura3-52 leu2*Δ*0 STE20*-mCherry-*KanMX6 MAT***a** + pRP1194 + pPS2037	This study
yKN4	*ura3-52 leu2*Δ*0 TPK2*-mCherry-*KanMX6 MAT***a** + pRP1194 + pPS2037	This study
yKN5	*ura3-52 leu2*Δ*0 kss1*Δ*::KanMX6 MAT***a** + pRP1194 + pPS2037	This study
yKN6	*ura3-52 leu2*Δ*0 FUS3*-GFP-*KanMX6 MAT***a** + pRP1194 + pDS7	This study
yKN7	*ura3-52 leu2*Δ*0 KSS1*-GFP-*KanMX6 MAT***a** + pRP1194 + pDS7	This study
yKN8	*ura3-52 leu2*Δ*0 STE20*-GFP-*KanMX6 MAT***a** + pRP1194 + pDS7	This study
yKN9	*ura3-52 leu2*Δ*0 TPK2*-GFP-*KanMX6 MAT***a** + pRP1194 + pDS7	This study
yKN11	*dhh1*Δ*::CdHIS1/DHH1 ura3::*Δ*imm434/ura3::*Δ*imm434 his1::hisG/his1::hisG arg4::hisG/arg4::hisG*	This Study

Table 2.8 Listing of plasmids used in this study.

Plasmid	Description	Source
pFRE-LacZ	$P_{FRE(TEC1)}$::*lacZ*, *URA3*, 2μ, Amp^r	Madhani and Fink, 1997
pRS415	*LEU2*, Cen, Amp^r	Sikorski and Hieter, 1989
pRS416	*URA3*, Cen, Amp^r	Sikorski and Hieter, 1989
p426GPD	P_{GPD3}, *URA3*, 2μ, Amp^r	Mumberg *et al*, 1995
pRS416-*ELM1*	P_{ELM1}-*ELM1*, *URA3*, Cen, Amp^r	This study
pRS416-*FUS3*	P_{FUS3}-*FUS3*, *URA3*, Cen, Amp^r	This study
pRS416-*KSS1*	P_{KSS1}-*KSS1*, *URA3*, Cen, Amp^r	This study
pRS416-*SNF1*	P_{SNF1}-*SNF1*, *URA3*, Cen, Amp^r	This study
pRS416-*STE7*	P_{STE7}-*STE7*, *URA3*, Cen, Amp^r	This study
pRS416-*STE11*	P_{STE11}-*STE11*, *URA3*, Cen, Amp^r	This study
pRS416-*STE20*	P_{STE20}-*STE20*, *URA3*, Cen, Amp^r	This study
pRS416-*TPK2*	P_{TPK2}-*TPK2*, *URA3*, Cen, Amp^r	This study
pRS416-*ELM1*-K117R	P_{ELM1}-*ELM1*-K117R, *URA3*, Cen, Amp^r	This study
pRS416-*FUS3*-K42R	P_{FUS3}-*FUS3*-K42R, *URA3*, Cen, Amp^r	This study
pRS416-*KSS1*-K42R	P_{KSS1}-*KSS1*-K42R, *URA3*, Cen, Amp^r	This study
pRS416-*SNF1*-K84R	P_{SNF1}-*SNF1*-K84R, *URA3*, Cen, Amp^r	This study
pRS416-*STE7*-K220R	P_{STE7}-*STE7*-K220R, *URA3*, Cen, Amp^r	This study
pRS416-*STE11*-K444R	P_{STE11}-*STE11*-K444R, *URA3*, Cen, Amp^r	This study
pRS416-*STE20*-K649R	P_{STE20}-*STE20*-K649R, *URA3*, Cen, Amp^r	This study
pRS416-*TPK2*-K99R	P_{TPK2}-*TPK2*-K99R, *URA3*, Cen, Amp^r	This study
pDEST-*ELM1*-KD	P_{ELM1}-*ELM1*-K117R-HA, *LEU2*, Cen, Amp^r	This study
pDEST-*FUS3*-KD	P_{FUS3}-*FUS3*-K42R-HA, *LEU2*, Cen, Amp^r	This study
pDEST-*KSS1*-KD	P_{KSS1}-*KSS1*-K42R-HA, *LEU2*, Cen, Amp^r	This study
pDEST-*SNF1*-KD	P_{SNF1}-*SNF1*-K84R-HA, *LEU2*, Cen, Amp^r	This study
pDEST-*STE7*-KD	P_{STE7}-*STE7*-K220R-HA, *LEU2*, Cen, Amp^r	This study
pDEST-*STE11*-KD	P_{STE11}-*STE11*-K444R-HA, *LEU2*, Cen, Amp^r	This study
pDEST-*STE20*-KD	P_{STE20}-*STE20*-K649R-HA, *LEU2*, Cen, Amp^r	This study
pDEST-*TPK2*-KD	P_{TPK2}-*TPK2*-K99R-HA, *LEU2*, Cen, Amp^r	This study
p*RAS2*-Y165F/T166A	P_{RAS2}-*RAS2*-Y165F/T166A, *URA3*, Cen, Amp^r	This study
pRS415-*STE11-4*	P_{STE11}-*STE11-4 LEU2*, Cen, Amp^r	This study

pRS416-*STE7*-S368P	P_{STE11}-*STE7*-S368P *URA3*, Cen, Amp^r	This study
pRP1194	P_{GPD3}-U1A-GFP, *LEU2*, Amp^r	Brengues *et al*, 2005
pDS7	P_{GPD3}-U1A-mCherry, *LEU2*, Amp^r	This study
pPS2037	P_{PGK1}-*PGK1*-16x U1A binding sites, *URA3*, Amp^r	Brodsky and Silver, 2000

CHAPTER 3

Inositol polyphosphate regulation of filamentous growth in *Saccharomyces cerevisiae*

3.1 Abstract

Inositol polyphosphates are important eukaryotic second messengers with diverse roles in chromatin remodeling, telomere maintenance, mRNA export, and regulation of the phosphate starvation response. Despite strong research interest, relatively little is known regarding the regulation of inositol polyphosphate signaling in yeast or metazoans. Through studies incorporating quantitative phosphoproteomic analysis of kinase signaling pathways required for yeast pseudohyphal growth, we report here an unexpected regulatory interrelationship between inositol polyphosphate signaling and the cellular response to nitrogen stress. *S. cerevisiae* exhibits a dramatic growth response to nitrogen limitation, characterized by the transition from a vegetative yeast-form to a filamentous form with chains of elongated pseudohyphal cells. Pseudohyphal growth is regulated through signaling networks encompassing MAPK and Snf1p pathways. Our previous studies have found that kinase-dead mutants of Ste11p, Ste7p, Kss1p, and Snf1p exhibit differential phosphorylation of the inositol polyphosphate kinases Arg82p, Vip1, and Kcs1p. Homozygous mutants deleted for the inositol polyphosphate kinases display distinct pseudohyphal growth phenotypes under conditions of nitrogen limitation. Profiling of inositol polyphosphates upon growth in media with limited nitrogen reveals striking increases in

the abundance of several inositol polyphosphate species as well as the appearance of different inositol polyphosphate species not normally seen under nitrogen rich conditions. In particular, we see a strong correlation of the *KCS1* made IP_7 isomer 5PP-IP_5 with filamentous growth. When large portions of 5PP-IP_5 accumulate, we observe hyper-filamentous phenotypes. Further, deletion mutants of the pseudohyphal growth MAPK *KSS1*, *FUS3,* and *SNF1* exhibit altered inositol polyphosphate profiles under nitrogen limitation. In sum, we present data indicating regulatory control of inositol polyphosphates by upstream filamentous growth regulatory kinases, as well as results identifying regulatory control of pseudohyphal growth through inositol polyphosphate signaling.

3.2 Introduction

In response to certain environmental stressors, particularly nitrogen limitation, the budding yeast *Saccharomyces cerevisiae* exhibits a dramatic growth response characterized by the transition from a vegetative yeast-like form to a filamentous form with chains of elongated cells referred to as pseudohyphae. The pseudohyphal growth response consists of changes in cell morphology and polarized growth regulated through a complex signaling network encompassing evolutionarily conserved signaling pathways including the Kss1p MAPK cascade, the Ras/PKA signaling pathway, and the AMPK Snf1p pathway (see Chapter 1). While these pathways have been studied and characterized rather expansively, the full molecular basis for pseudohyphal growth is still largely unknown. In particular, the metabolite profile of pseudohyphal growth has yet to be determined. Classically, signaling pathways and metabolic pathways have been viewed separately; however, further research has revealed that regulation of these two types of pathways is most likely coordinated, and, furthermore, both types of pathways may be involved in the

regulation of each other [1,2]. In particular, the inositol polyphosphate signaling pathways has been shown to bridge the gap between signal transduction pathways and metabolic pathways by acting as central communicators [2,3]. Our data presented here, suggest a role for the inositol polyphosphate pathway in the regulation of pseudohyphal growth within *S. cerevisiae* by possibly acting as signaling molecules between the conserved kinase pathways and downstream effectors.

Inositol polyphosphates (IPs) and inositol pyrophosphates (PP-IPs) are ubiquitous eukaryotic molecular second messengers with phosphate groups attached to a six-carbon *myo*-inositol backbone [4-6]. To date, over 40 IP molecules have been detected in eukaryotic organisms [7]. In the yeast *S. cerevisiae*, soluble IPs are generated through a phosphorylation cascade that begins once the yeast phospholipase CI, Plc1p, cleaves phosphatidylinositol 4,5-bisphosphate (PIP_2) and releases inositol 1,4,5-trisphosphate (IP_3) [8,9]. IP_3 is then further phosphorylated by four IP kinases: Arg82p (also known as IPK2p), Ipk1p, Vip1p, and Kcs1p (Pathway summarized in Fig 3.1) [10]. Once IP_3 has been released from PIP_2, Arg82p further phosphorylates IP_3 to inositol 1,4,5,6-tetrakisphosphate (IP_4) and then again to produce 1,3,4,5,6-pentakisphosphate (IP_5) [4,6,11-13]. IP_5 is then phosphorylated by IPk1p to generate inositol 1,2,3,4,5,6-hexakisphosphate (IP_6), which is a fully mono-phosphorylated *myo*-inositol molecule [14]. IP_6 is the most abundant inositol polyphosphate with levels ranging from 10 to 100 μM in eukaryotic organisms outside of plants, which have substantially increased levels because of the use of IP_6 by seeds to store phosphate [15,16].

Pyrophosphates are high-energy molecules that consist of two phosphate groups attached to a single carbon. The most well-known and abundant PP-IPs in yeast are produced from IP_6 [5,17,18]. There are two evolutionarily conserved types of enzymes that produce PP-IPs: IP_6-

kinases and PP-IP_5-kinases [11,19]. In yeast, the IP_6-kinase Kcs1p has the ability to add a pyrophosphate group to the monophosphate group at position 5. Kcs1p uses IP_6 as a substrate to produce an IP_7 isoform known as 5PP-IP_5 [13,20-22]. In yeast, the PP-IP_5-kinase Vip1p utilizes 5PP-IP_5 as a substrate and adds a second phosphate group on position one to produce IP_8 (1,5$(PP)_2$-IP_4) [21]. *In vitro*, Vip1p can also pyrophosphorylate position one on IP_6 to produce the second isoform of IP_7, 1PP-IP_5 [21]. Kcs1p can then in turn phosphorylate 1PP-IP_5 at position five to also produce IP_8. While IP_7 and IP_8 are the most characterized pyrophosphates in yeast, Kcs1p also has the ability to produce pyrophosphate molecules from IP_5 forming 5PP-IP_4 which can then be further phosphorylated by Vip1p to produce $(PP)_2$-IP_3 [22].

The pyrophosphate pools are rapidly overturned with up to 50% of the human IP_6 pool being cycled through PP-IPs every hour. Due to this quick turnover, the accumulation of any one PP-IP is low and only makes up 1-5% of IP_6 levels [23,24]. As a result of the rapid turnover and low levels of PP-IPs, current techniques may be limited in their ability to identify other pyrophosphate molecules that may never accumulate to detectable levels under standard growth conditions. Therefore, it is theorized that more pyrophosphate molecules could exist and be produced from lower energy IP molecules. The high turnover rate of PP-IPs is in large part due to quick phosphorylation and then dephosphorylation of these molecules. Currently, there are three known inositol phosphatases: Ddp1p, Siw14p, and a potential phosphatase domain located in Vip1p itself [25]. Current studies suggest that Ddp1p has the least amount of specificity for PP-IPs and largely prefers inorganic polyphosphate. However, *in vitro*, Ddp1p has the capability to remove the β-phosphate at the 1 position in both 1PP-IP_5 and IP_8 [26]. Siw14p was the most recently discovered inositol phosphatase and has only been shown to dephosphorylate the β-phosphate added at the 5-carbon position by Kcs1p [25]. While Vip1p contains a catalytic kinase

domain that allows it to pyrophosphorylate IPs at the 1-position, it also possesses a phosphatase-like domain that can potentially dephosphorylate the β-phosphate group on position one, thereby removing the pyrophosphate that its own kinase domain produces [27,28]. The phosphatase activity of Vip1p has been largely debated and it was found that the human orthologue of Vip1p contains a catalytically inactive phosphatase domain [29]. However, when the phosphatase domain is removed in *S. cerevisiae, Schizosaccharomyces pombe*, and even in human Vip1 variants, more inositol pyrophosphates are generated suggesting the phosphatase-like domain acts against the activity of the N-terminal kinase domain [30-32].

While the main role of some IPs is to act as precursor metabolites for the production of higher energy IPs and PP-IPs [33], many IPs themselves are utilized as active signaling molecules, such as IP_3, which is noted for its well characterized role in activating the release of calcium from intracellular stores in humans [34]. Since many IPs are thought to be predominately transient molecules that act as precursor metabolites, evolving research has focused more strongly on the PP-IPs, which have been implicated in a various number of cellular processes. In particular, the deletion of *KCS1*, and therefore loss of many PP-IPs, has uncovered important functions in the regulation of telomere length [35], cell wall integrity [36], transcriptional control [37], and autophagy [20], to name a few affected processes. PP-IPs have been found to control energetic metabolism in yeast, and removal of these molecules causes an increase in ATP metabolites, suggesting PP-IPs control many chemical processes within the cell [38]. PP-IPs have been implicated in many cellular stress responses, including the environmental stress response [39], salt stress and vacuolar morphogenesis [36], cell damage caused by reactive oxygen species [40], and the response to heat-shock [41].

Since IPs and predominately PP-IPs are involved in many stress responses within the cell,

it is reasonable to believe that they would be involved in the regulation of nutrient stress, particularly nitrogen starvation, which also induces pseudohyphal growth in *S. cerevisiae.* In this study, we found that inositol polyphosphate kinases and the resulting inositol polyphosphates are essential for wild-type pseudohyphal growth. Changes in the IP profiles of IP kinase deletion strains correlates with either an increase or decrease in pseudohyphal growth depending on the levels of each polyphosphate species, most noticeably the levels of PP-IPs.

3.3 Results

3.3.1 Inositol polyphosphate kinases are required for wild-type pseudohyphal growth

While much is known about the main kinases involved in the three major pathways that regulate filamentous growth, targets of these pathways and in turn how these targets affect pseudohyphal growth is still largely unknown. To further investigate complex signaling interactions and the role that metabolites have on pseudohyphal growth, we previously conducted and reported a large-scale phosphoproteomic study that identified targets of the known filamentous signaling pathways [42].

Our mass spectrometry data set revealed enrichment for many interesting networks, including one encompassing components of ribonucleoprotein complexes, which we identified as being regulated through the Kss1p MAPK cascade [42]. Our phosphoproteomic studies also revealed enrichment for differentially phosphorylated inositol polyphosphate kinases. In particular, kinase-deficient mutations in the MAPK Kss1p and the AMPK Snf1p led to differential phosphorylation of the inositol polyphosphate kinases Arg82p, Vip1p, and Kcs1p under pseudohyphal growth conditions compared to phosphorylation levels observed in a wild-type strain (Table 3.1). Because of this enrichment, we sought to determine if IP kinases are

involved in the pseudohyphal growth transition. To examine this, we first utilized straightforward genetic and phenotypic assays to test the effect on pseudohyphal growth of deleting the four IP kinases from the chromosome in the filamentous *S. cerevisiae* background strain Σ1278b. These strains were tested for haploid invasive growth after two days on YPD agar and diploid surface spread filamentation after four days on synthetic low ammonium dextrose (SLAD) agar, commonly used to present conditions of nitrogen limitation and to induce filamentous growth.

We found that deletion of the most upstream protein in the IP signaling pathway, *ARG82*, and therefore deletion of all downstream IPs and PP-IPs, led to a decrease in invasive growth as well as surface spread pseudohyphal growth (Fig 3.2). Interestingly, deletion of *IPK1*, which produces IP_6, the most abundant inositol polyphosphate as well as the precursor molecule for pyrophosphates IP_7 and IP_8, leads to hyper-invasiveness and increased surface spread filamentation (Fig 3.2). Deletion of *VIP1*, the kinase involved in the production of 1PP-IP_5 and IP_8, also leads to hyper–invasiveness and increased pseudohyphal growth; however, deletion of *KCS1*, encoding the kinase involved in the production of the additional IP_7 isomer (5PP-IP_5), IP_8 and pyrophosphates produced from IP_5, produced the opposite phenotype from that observed in a *VIP1* null strain and showed a decrease in invasion and pseudohyphal growth (Fig 3.2). Therefore, our data indicate that the each inositol polyphosphate kinase is necessary for wild-type pseudohyphal growth. However, the appearance of both hyper- and hypo-filamentous phenotypes suggests a complex interaction of both promoting and inhibitory roles.

3.3.2 Pseudohyphal growth conditions modulates inositol polyphosphate profiles *in vivo*

While our phenotypic assays suggest that the inositol polyphosphate signaling pathway is

necessary for wild-type levels of pseudohyphal growth, we wanted to determine if filamentous growth conditions lead to actual changes in inositol polyphosphate levels. To measure inositol polyphosphate levels, we utilized a technique established by Azevedo C. and Saiardi A. [43] in which we take advantage of the strong preference in *S. cerevisiae* to uptake inositol from the environment rather than producing the molecule itself. Even extremely low levels of inositol lead to suppression of endogenous inositol synthesis [44]. Therefore, by using media lacking inositol and instead adding tritiated inositol, cells are forced to uptake the tritiated inositol and eventually metabolize it to downstream IPs and PP-IPs that can be measured by HPLC analysis; the radioactivity in each collected fraction was measured by scintillation counting. Positioning of the peaks was determined by using standard deletion strains that have been shown to have consistent positioning of peaks: IP_3, IP_5, PP-IP_4, IP_6, IP_7, and IP_8 [43].

When a wild-type filamentous strain is given tritiated inositol to metabolize in synthetic complete liquid media lacking inositol (SC–inositol), we observe a peak for IP_5, a large peak for IP_6, and a small peak for IP_7. However, when cells are grown in SC-inositol and then shifted to growth in liquid SLAD (Low Nitrogen) for 8 hours, we observe nearly a complete loss of IP_5, an increase in IP_7, the appearance of a second IP_7 isoform peak, and an increase in IP_8 (Fig 3.3 A). Interestingly, we not only see a large increase in the IP_3 peak but a broadening of this peak, adopting a "hump"-like shape. To determine if these profile changes are dependent upon the ability of the strain to undergo pseudohyphal growth or rather represent a response to conditions of nitrogen limitation, we analyzed a diploid non-filamentous strain of *S. cerevisiae*, the commonly used laboratory strain BY4743, grown in SLAD media. Under these conditions, BY4743 exhibited a less dramatic drop in IP_5 as compared to the Σ1278b strain, but there was still an increase and broadening of the IP_3 peak, along with an increase in IP_7 and the presence of

a second IP_7 isoform (Fig 3.3 A).

3.3.3 IP_7 isoforms, 1PP-IP_5 and 5PP-IP_5, can be separated under low nitrogen conditions

Due to the presence of the two IP_7 isomers under pseudohyphal growth conditions, we were interested to determine the role played by the two inositol pyrophosphate kinases, Vip1p and Kcs1p, on the production of each of these peaks. We further wondered if either one of these peaks correlated to an increase or decrease in pseudohyphal growth, especially since *vip1*Δ/Δ and *kcs1*Δ/Δ strains exhibit opposite pseudohyphal growth phenotypes.

After further HPLC analysis with the *vip1*Δ/Δ and *kcs1*Δ/Δ strains under conditions of low nitrogen, we see a loss of each peak depending on the kinase that has been deleted (Fig 3.3 B). The *vip1*Δ/Δ strain analyzed under low nitrogen conditions results in a strikingly large increase in IP_7 isoform peak two. We almost completely lose both peaks of IP_7 in a *KCS1* null strain; however, under low nitrogen conditions, there is a small, repeatable, peak that forms at a position consistent with IP_7 peak one (Fig 3.3 C). Due to the loss of peak one and the increase of peak two in a *vip1*Δ/Δ strain, we will consider peak one the Vip1p-made IP_7 isomer 1PP-IP_5 for the remainder of this study. Since we completely lose peak two in a *kcs1*Δ/Δ strain and also see the increase of peak two in a *vip1*Δ/Δ strain under low nitrogen, we will consider peak two the Kcs1p made IP_7 isomer 5PP-IP_5 for the remainder of this study. Additionally, data indicated in later results further strengthen the identification of these two peaks as each particular IP_7 isomer.

While a *vip1*Δ/Δ strain shows a large increase in 5PP-IP_5, and an even larger hump of IP_3 compared to a wild-type strain under low nitrogen conditions, we see no other noticeable changes in the IP profile. The *kcs1*Δ/Δ mutant strain has a more complex IP profile. Under low nitrogen conditions, there is an almost identical increase in the IP_3 hump compared to that of

*vip1*Δ/Δ, but with two additional peaks evident that are not observed in the profiles generated previously from other mutants. One peak appears as a sharp increase within the IP_3 hump region. The other peak is observed in several fractions prior to IP_5 and may possibly constitute an IP_5 isomer. It remains unclear as to the identity of these peaks since they do not coincide with any of our standards (data not shown). The *kcs1*Δ/Δ mutant also exhibits an increase of PP-IP_4 (Fig 3.3 B).

3.3.4 The kinase domain of Vip1p suppresses pseudohyphal growth

Vip1p contains two enzymatically important domains: an N-terminal rimK/ATP-grasp domain responsible for phosphorylating the 1 position of IP_6 and a C-terminal phosphatase-like domain (Fig 3.4 A). The C-terminal phosphatase-like domain has been shown to specifically de-phosphorylate molecules produced by Vip1p itself [27] .Our phenotypic assays showed that a *VIP1* null strain is hyper-filamentous but it was unclear if this was due to the loss of its phosphatase activity or its kinase activity. To test this, chromosomal point mutations were generated, yielding two strains, one being kinase-defective (*vip1*-D487A) and the other phosphatase-defective (*vip1*-H548A). Both strains were constructed by mutating the amino acids that have previously been shown to provide kinase catalytic activity or phosphatase catalytic activity. In the kinase domain, the important residue is a conserved aspartic acid at position 487. In the phosphatase domain the conserved histidine necessary for phosphatase activity resides at position 548. Both of these residues were mutated to an alanine to disturb catalytic activity. We then tested these strains for both invasive growth and diploid pseudohyphal growth. Haploid *vip1*-D487A and diploid *vip1*-D487A/D487A strains showed an increase in invasive growth along with an increase in surface spread filamentation, while the *vip1*-H548A strains showed no

obvious changes in phenotype compared to a wild-type strain (Fig 3.3 B&C). When analyzed for inositol polyphosphate profiles, *vip1*-D487A/D487A exhibited an almost identical increase in 5PP-IP_5 as compared to the *vip1*Δ/Δ mutant. The *vip1*-H548A/H548A mutant exhibited a very similar profile to that observed from a WT strain under conditions of low nitrogen except for a substantial increase in IP_8 levels. Neither point mutant produced the large increase in IP_3 observed in a *vip1*Δ/Δ strain, exhibiting instead wild-type levels of IP_3 (Fig 3.4 D).

3.3.5 Overexpression of *KCS1* or *VIP1* affects pseudohyphal growth

Because of the phosphate groups attached to the *myo*-inositol backbone, IPs cannot be exogenously added for efficient uptake in yeast. With this lack of techniques to introduce IPs inside the yeast cell, it is difficult to determine which specific IP or PP-IP species promote or inhibit filamentous growth. Another obstacle that makes it difficult to study PP-IPs in particular is the presence of Siw14p, Ddp1p, and the phosphatase-like domain of Vip1p, that work in coordination to continuously dephosphorylate PP-IPs, and are a large factor as to why PP-IPs do not naturally accumulate in high concentrations within the cell during normal growth conditions. Since PP-IPs cannot be increased by the exogenous addition of purified PP-IP species, we attempted to increase PP-IP levels by first deleting the phosphatases within the IP pathway and second by overexpressing *KCS1* and *VIP1* as a means of promoting high levels of selected PP-IPs.

As indicated in Figure 3.4 B & C, mutation of the *VIP1* phosphatase domain alone does not cause a change in pseudohyphal growth phenotypes compared to wild-type or a drastic change in inositol polyphosphate profiles except for a large increase seen in IP_8. We hypothesized that this could be due to the redundant activity of *DDP1*, which also has the ability

to remove the β-phosphate group from the position one of PP-IPs. Therefore, in an attempt to increase the levels of 1PP-IP_5 we created a *ddp1*Δ/Δ mutant along with a *ddp1*Δ/Δ VIP1$^{H548A/H548A}$ double mutant., Upon examination of the HPLC IP profiles in these mutants, elevated levels of endogenous 1PP-IP_5 are present in a *ddp1Δ/Δ* strain. We also observe a drastic drop in IP_6 levels and virtually no IP_8 in this mutant. In the double mutant (*ddp1*Δ/Δ VIP1$^{H548A/H548A}$) we observe a combination of the two profiles seen in each single mutant alone: a decrease in IP_6, an increase in 1PP-IP_5, and an increase in IP_8 (Fig 3.5 A). Interestingly, all three mutants appeared to exhibit no change in surface spread filamentation compared to wild-type (Fig 3.5 B). Upon deletion of *SIW14*, the phosphatase responsible for removing the β-phosphate at position 5, we are able to increase the levels of 5PP-IP_5 and IP_8 (Fig 3.5 A). Unlike mutation of the other two phosphatases, deletion of *SIW14* causes a hyper-filamentous phenotype under low nitrogen conditions (Fig 3.5 B). Additionally, deletion of *SIW14* is enough to induce filamentous growth even on rich media without nitrogen stress (Fig 3.6 C)

To increase levels of PP-IPs by another means, *KCS1* and *VIP1* were overexpressed in a diploid background by cloning the respective genes under the transcriptional control of a constitutively active *ADH2* promoter in the high copy plasmid pSGP47. When analyzing the inositol polyphosphate profiles of a wild-type strain carrying pSGP47-*KCS1*, we see a large increase in 5PP-IP_5 and an increased amount of IP_8 (Fig 3.6 A). Conversely, when a wild-type strain carrying pSGP47-*VIP1* is examined through HPLC analysis, we do not see the expected increase in 1PP-IP_5. We do, however, observe almost the exact same level of increase in IP_8 as observed upon overexpression of *KCS1* or *VIP1* (Fig 3.6 A). In a wild-type background, overexpression of *KCS1* through the introduction of pSGP47-*KCS1* results in increased pseudohyphal growth relative to a wild-type strain carrying an empty vector with matching

auxotrophic marker (Fig 3.6 B). Like *siw14*Δ/Δ, overexpression of *KCS1* is sufficient to induce filamentous growth under normal conditions (Fig 3.6 C). Overexpression of pSGP47-*VIP1* results in decreased pseudohyphal growth relative to wild-type (Fig 3.6 B). A mutant strain overexpressing *KCS1* and deleted for *VIP1* exhibits exaggerated pseudohyphal growth relative to wild-type, consistent with other strains exhibiting elevated levels of 5PP-IP_5 (Fig 3.6 B). Conversely, a homozygous diploid *kcs1* deletion mutant carrying pSGP47-*VIP1* is deficient in pseudohyphal growth relative to a corresponding wild-type strain. The phenotypic patterns seen upon overproduction of *KCS1* and *VIP1* in a wild-type background are also evident in a homozygous diploid background deleted for *SIW14* as indicated in Figure 3.6 B & C. A *siw14*Δ/Δ mutant carrying pSGP47-*VIP1* still exhibits increased levels of filamentous growth compared to the wild-type carrying an empty vector. However, this mutant exhibits decreased filamentous growth with respect to *siw14*Δ/Δ alone (Figure 3.5 B and Fig 3.6 B). Interestingly, when analyzing the IP profile of a *siw14*Δ/Δ mutant carrying pSGP47-*VIP1* we see roughly the same amount of 5PP-IP_5 but almost twice as much IP_8 compared to a *siw14*Δ/Δ mutant alone (Fig 3.6 D). Deletion of *IPK1,* which leads to a loss of all IP_7 and IP_8, results in exaggerated pseudohyphal growth (Fig 3.2 A & B), and this phenotype is unaffected upon overexpressing *KCS1* or *VIP1* (Fig 3.6 B).

In summary, our data indicate that the respective ratios of IP_7 isomers and IP_8 species correlate strongly with pseudohyphal growth phenotypes, with elevated levels of 5PP-IP_5 relative to these other PP-IP species, associated with hyper-filamentous growth.

3.3.6 Deletion of the key pseudohyphal growth kinases, *SNF1*, *KSS1* and *FUS3*, alters inositol polyphosphate profiles

Since the inositol polyphosphate kinases Arg82p, Kcs1p, and Vip1p are differentially phosphorylated in strains defective for a kinase required for wild-type pseudohyphal growth [42], we set out to determine if deletion of the respective pseudohyphal growth kinase genes, *SNF1* and *KSS1*, would alter inositol polyphosphate profiles under conditions of nitrogen stress. Homozygous diploid *kss1*Δ/Δ and *snf1*Δ/Δ strains exhibit decreased pseudohyphal growth relative to wild-type [42]. In a *kss1*Δ/Δ mutant, IP_3 and IP_8 levels are elevated in SLAD media relative to wild-type (Fig 3.7 A). Upon removal of *SNF1* we see a more drastic change in the resulting IP profile. Notably, deletion of *SNF1* results in the largest levels of IP_3 observed in any strain under conditions of low nitrogen in this study. We also observe very slight increases in levels of both IP_7 isoforms in *snf1*Δ/Δ, along with an increase in IP_8 abundance to levels comparable to those observed in the *kss1*Δ/Δ strain (Fig 3.7 A). Interestingly, if we overlay the inositol polyphosphate traces detected in *snf1*Δ/Δ and *kcs1*Δ/Δ strains, we observe similar levels of increased PP-IP_4 along with the presence of another peak just before IP_5 (data not shown). Lastly, though we did not see enrichment for differentially phosphorylated IP kinases in a *FUS3* kinase defective strain, we nonetheless analyzed a homozygous diploid strain deleted for *FUS3* to determine if this kinase holds any regulatory control over IP levels. Fus3p is the mating pathway MAPK in *S. cerevisiae*, and contrary to the phenotypes observed in *kss1* and *snf1* mutants, *fus3* deletion mutants exhibit exaggerated pseudohyphal growth [42,45]. As a negative regulator of filamentation, *FUS3* is of interest, particularly since hyper- and hypo-filamentous phenotypes are evident upon manipulating IP kinases. Similar to other hyper-filamentous strains tested, we detect an increase in the levels of 5PP-IP_5 upon deletion of *FUS3* when grown under conditions of low nitrogen. We also observe a large increase in the levels of IP_8 in the *fus3*Δ/Δ mutant (Fig 3.7 B).

The most striking of these three results was obtained from analysis of *snf1*Δ/Δ. The changing levels of IPs in *snf1*Δ/Δ, along with the fact that a kinase defective allele of *SNF1* causes a decrease in phosphorylation of both Vip1p and Kcs1p (Table 3.1), led us to consider the possibility that Snf1p is interacting with either Vip1p or Kcs1p. Interestingly, *snf1*Δ/Δ*vip1*Δ/Δ diploid strain regains some ability to undergo pseudohyphal growth if grown on low nitrogen for an extended period, though not at wild-type levels (Fig 3.7 D). This may be due to the large increase in 5PP-IP_5 seen in *snf1*Δ/Δ*vip1*Δ/Δ mutants, which is nearly double the amount of 5PP-IP_5 observed in the *snf1*Δ/Δ mutant alone (Fig 3.7 C). Other than this large increase in 5PP-IP_5, the double mutant does not show significant differences as compared against the *snf1*Δ/Δ strain.

3.4 Discussion

Our results strongly suggest that IP kinases are necessary for wild-type pseudohyphal growth and that inositol polyphosphate signaling plays a role in proper regulation of filamentation. Furthermore, the ability to remove particular IP kinases and observe either increased or decreased pseudohyphal growth suggests a possible complex regulation system involving inhibitory and activating roles between different IP and PP-IP molecules. It is possible that several IPs and/or PP-IPs can act as a fine tuning system and are required in particular ratios in order to promote wild-type filamentous growth. PP-IPs, particularly those produced by Kcs1p, have been previously implicated in fine-tuning systems such as the regulation of inositol metabolism [46], and proper positioning of the second germ tube in the filamentous ascomycete *Aspergillus nidulans* [27].

We found that simply switching a wild-type strain to growth under low nitrogen for 8 hours causes a change in the inositol polyphosphate profile, indicating there is a shift in the IPs

and PP-IPs that contribute to cell signaling under conditions of nitrogen limitation. It is important to note that in the non-filamentous strain of *S. cerevisiae*, BY4743, we observed an IP profile that was a combination of peaks and peak sizes seen in both the filamentous wild-type strain, Σ1278b, under normal media and under low nitrogen conditions, suggesting that this profile results from a combination of filamentous growth-specific factors along with effects from general nitrogen stress. Thus, the use of Σ1278b in this work affords us a detectable phenotypic read-out to study the impact of inositol polyphosphates on filamentous growth, while also informing our understanding of the cellular processes employed in *S. cerevisiae* to manage nitrogen stress.

The data presented here, largely suggests that PP-IPs play the most important role in regulating pseudohyphal growth. We do, however, see a change in IP_3 and IP_5 levels after nitrogen starvation for 8 hours in wild-type strains. The large broadening peak of IP_3 is consistently present under low nitrogen conditions. It is reasonable to believe that the lack of sharpness within this peak is a result of a mixture of IP_3 and possibly IP_4 isomers, though further characterization of these fractions would need to be completed in order to elucidate conclusively the polyphosphate species present within this hump. The role of increased IP_3 levels in proper regulation of pseudohyphal growth remains unclear, but large fluctuations of the observed peak are evident upon deleting *KCS1* or *VIP1,* and *SIW14*. Additionally, an increase in this hump is seen when the key pseudohyphal growth regulatory kinases *KSS1* and *SNF1* are deleted, implicating the MAPK and SNF1/AMPK pathways as necessary factors for proper regulation of IP_3 levels under conditions of low nitrogen.

The most significant observation in our low nitrogen IP profiles was the appearance of two separate IP_7 isoform peaks. Current IP HPLC analysis techniques have been unable to

distinguish differing IP_7 isoforms in yeast and have only observed one peak for IP_7. However, in our HPLC profiles, we are able to visualize both Kcs1p-produced 5PP-IP_5 and the Vip1p-generated 1PP-IP_5 under low nitrogen conditions. Our ability to see two peaks most likely stems from the combination of employing a 15-minute extended separation gradient along with our study design of profiling strains under conditions of low nitrogen. The wild-type strain used in this study only exhibits one peak under normal growth conditions as has been previously reported. We believe that the transition to low nitrogen necessitates the need for higher levels of both IP_7 isoforms and therefore, they accumulate at high enough levels that they can both be detected. Furthermore, previous research suggests that the IP_7 peak seen in a wild-type non-filamentous strain under normal growth conditions represents Kcs1p-generated 5PP-IP_5, because deletion of *KCS1* led to a loss of this peak. While a *kcs1*Δ/Δ mutant in the filamentous Σ1278b background does exhibit a loss of all IP_7 peaks under standard growth conditions (data not shown), this strain under low nitrogen conditions presents a very small, but repeatable, peak that coincides with IP_7 peak one, aligning at the same position seen in a wild-type strain under normal growth conditions. While this was previously thought to be 5PP-IP_5 produced by Kcs1p, our data suggests IP_7 peak one is most likely Vip1p-produced 1PP-IP5, as Vip1p is the only available protein capable of adding a pyrophosphate group to IP_6 in a strain deleted for *KCS1*. Moreover, *vip1*Δ/Δ presents a very large peak at IP_7 peak two, which, by similar logic, most likely represents Kcs1p-produced 5PP-IP_5. This same peak is seen in a homozygous diploid strain deleted for *SIW14*, in which the Kcs1p-generated IP_7 isomer has previously been shown to accumulate, as this isomer cannot be dephosphorylated in the absence of *SIW14* [25]. Therefore, our data strongly suggest that we are able to efficiently separate IP_7 isomers under low nitrogen conditions as long as an extended gradient is used, with 1PP-IP_5 separating just ahead of 5PP-

IP_5.

Importantly, our results strongly suggest that loss of *VIP1* and, therefore, build up of 5PP-IP_5, leads to a hyper-filamentous phenotype. As part of a study centering on the *S. pombe* Asp1p inositol polyphosphate kinase, a member of the Vip1p 1/3 family, Pohlmann and Fleig [30] previously reported decreased surface-spread filamentation in a heterozygous *vip1*Δ/*VIP1 S. cerevisiae* mutant grown on SLAHD (SLAD supplemented with Histidine). Our data, gathered through phenotypic analysis of deletion and overexpression of *VIP1*, as well as through analysis of *vip1*Δ/Δ inositol polyphosphate profiles leads us to conclude that Vip1p plays an inhibitory role during filamentous growth. Point mutations of both the kinase domain and the phosphatase domain of Vip1p suggest that it exerts regulatory control of filamentous growth through its kinase domain. Upon mutation of the Vip1p kinase domain, invasive growth and surface-spread filamentation is exaggerated, accompanied by consistent increases in 5PP-IP_5 levels and, as expected, the complete loss of 1PP-IP_5. The increase in 5PP-IP_5 is almost identical to that seen in *vip1*Δ/Δ. Mutation of the phosphatase catalytic site of Vip1p, however, results in near wild-type levels of filamentation. We believe this is most likely due to redundant functions between Vip1p and Ddp1p, as Ddp1p has the ability to dephosphorylate PP-IPs produced by Vip1p. When we delete *DDP1* alone or assess the resulting phenotype in combination with a phosphatase-deficient Vip1p mutant, we see a strikingly large increase in 1PP-IP_5. This occurs with a decrease in IP_6, presumably resulting from a shift in IP_6 to later PP-IPs, without replenishment of the stock of IP_6 due to loss of phosphatase function. Interestingly, this increase in 1PP-IP_5 does not correlate with any change in filamentous growth.

Conversely, elevated levels of the IP_7 isomer, 5PP-IP_5, correlate strongly with hyper-filamentous growth phenotypes. In this study, the vast majority of hyper-filamentous mutant

strains (i.e., *vip1*Δ/Δ, *VIP1*-D487A, *siw14*Δ/Δ, strains carrying pSGP47-*KCS1*) exhibited a large increase in 5PP-IP_5. An exception to this was an *ipk1*Δ/Δ strain in which neither IP_6 nor any downstream PP-IPs are produced. The *ipk1*Δ/Δ strain under low nitrogen looks similar to previously reported non-filamentous strains under normal conditions with large increased peaks appearing at IP_5, two PP-IP_4 isomers, and $(PP)_2$-IP_3 (data not shown) [40]. It is possible that one of the lower energy PP-IPs produced from IP_5 could also play a role in causing hyper filamentation when present at such high levels as seen in *ipk1*Δ/Δ. However, this is most likely not the predominant form of regulation because the PP-IPs produced in *ipk1*Δ/Δ were not seen in any other hyper-filamentous strain tested here. The other exception was seen in a *siw14*Δ/Δ mutant carrying pSGP47-*VIP1*, which had a decrease in filamentous growth compared to *siw14*Δ/Δ alone but still elevated levels of filamentous growth compared to a wild-type strain. While this strain maintained high levels of 5PP-IP_5, most likely causing the increased filamentous growth above that observed in a wild-type strain under low nitrogen, it also accumulated nearly double the amount of IP_8, possibly adding to the decreased filamentous growth compared to *siw14*Δ/Δ alone. We hypothesize that the control over filamentous growth by PP-IPs is most likely not caused by a singular PP-IP species, but rather ratios of PP-IPs to each other.

From our data, we hypothesize that regulation of pseudohyphal growth is fine-tuned by the relative levels of inositol pyrophosphate species and that particular ratios of relevant PP-IPs are necessary to maintain wild-type levels of filamentation. If the relative abundance of these species fall or increase above standard levels, pseudohyphal growth is impacted. In particular, elevated levels of 5PP-IP_5 respective to other PP-IPs are associated with hyperactive filamentous growth. In a wild-type cell under conditions of low nitrogen, some amount of 5PP-IP_5 is

necessary for pseudohyphal growth, but overproduction is most likely combated by phosphorylation of 5PP-IP_5 to IP_8 by Vip1p and by dephosphorylation of 5PP-IP_5 to IP_6 by Siw14p. Consistent with the notion that PP-IP levels impact filamentation, pseudohyphal growth signaling pathways, such as the Snf1p pathway, may play an important role in regulating inositol polyphosphate biogenesis. It remains unclear if Snf1p is targeting Kcs1p, Vip1p, or Siw14p, or some intermediate molecule, but our previous studies show that removal of Snf1p kinase activity leads to lower phosphorylation levels of Kcs1p and Vip1p. We are currently unsure if Snf1p-mediated regulation of inositol polyphosphate signaling occurs through direct or indirect control of inositol polyphosphate kinase phosphorylation. Further studies will be necessary to determine the mechanism through which the Snf1p kinase pathway controls IP signaling and, in turn, the mechanism through which IP signaling regulates filamentous growth.

3.5 Materials and Methods

3.5.1 Strains. plasmids, and media

Strains used in this study are listed in Table 3.2. Filamentous *S. cerevisiae* strains were derived from the genetic background, Σ1278b. Haploid filamentous strains were derived from HLY337 and Y825 [42]. The diploid non-filamentous strain, BY4743, was used in these studies, and is derived from the genetic background S288C. Standard protocols for proper growth and maintenance of yeast are as previously described [47]. DNA was introduced into yeast cells by standard transformation protocols involving lithium acetate treatment and heat shock [48]. Plasmids used in this study are listed in Table 3.3.

S. cerevisiae strains were cultured on YPD (1% yeast extract, 2% peptone, 2% glucose) or Synthetic Complete (SC) media (0.67% yeast nitrogen base (YNB) without amino acids, 2%

glucose, and 0.2% of the appropriate amino acid drop-out mix). Nitrogen starvation and pseudohyphal growth phenotypic assays were conducted in synthetic low ammonium dextrose (SLAD) medium (0.17% YNB without amino acids and without ammonium sulfate, 2% glucose, 50 μM ammonium sulfate and supplemented with appropriate amino acids if necessary). Inositol polyphosphate profiles were conducted by first growing cells in SC-inositol (0.17% YNB without inositol, 2 % glucose, 0.5% ammonium sulfate and supplemented with appropriate amino acids) and when necessary further growth in SLAD-inositol (0.17% YNB without amino acids , ammonium sulfate and inositol, 2% glucose, 50 μM ammonium sulfate, and supplemented with amino acids as appropriate).

3.5.2 Gene deletions and integrated point mutations

Genes were deleted in the chromosome and replaced with either KanMX6 or HphMX6 antibiotic resistance cassettes of pFA6a-KanMX6 or pAG32. Deletions were conducted by standard PCR and homologous recombination techniques. Strains were then checked for incorporation of the marker in the correct genomic location by PCR. For diploid strains, deletions were typically made individually in both Y825 and HLY337 haploid backgrounds and then mated to form a diploid cell. The sterile *kss1*Δ/Δ and *fus3*Δ/Δ mutants were made in a diploid cell where each gene copy was deleted by allelic replacement with an antibiotic resistance marker. Overexpression plasmids were created by ligation independent cloning techniques [49]. Integrated point mutants in *VIP1* (D487A and H548A) were created using the *URA* flip-out method. In brief, *URA3* was amplified from pRS406 by PCR, and, utilizing homologous recombination, the resulting PCR product was integrated at its target destination site corresponding to the site of the desired point mutation. A second transformation was performed

to replace the *URA* cassette with a double-stranded piece of DNA homologous to the region of the intended mutation except for the desired single-site mutation. Point mutations were checked for removal of *URA* by PCR and further validated by sequencing.

3.5.3 Pseudohyphal growth assays

For invasive growth assays, haploid strains were grown to stationary phase overnight in YPD at 30°C with shaking at 250 rpm, harvested, and adjusted to cell density of 1 OD_{600} in sterile water. 5 µl of density-adjusted culture was spotted on YPD and allowed to invade the agar for two days. Plates were photographed for surface growth and then gently washed with a light stream of water and photographed again to visualize invasive growth. For surface spread assays, diploid strains were grown overnight in SC media with appropriate dropouts to maintain diploids. Saturated cultures were spot platted on SLAD medium and incubated at 30°C for four days. Colonies were imaged using an upright Nikon Eclipse 80i microscope with CoolSnap ES2 CCD (Photometrics), and images were acquired using MetaMorph software (Molecular Devices).

3.5.4 HPLC analysis of inositol polyphosphates

HPLC analysis of inositol polyphosphate levels was conducted as previously described with some modifications [43]. In brief, cultures are grown overnight at 30°C with shaking at 250 rpm until fully saturated in rich media. 5 µl of saturated culture is added to 5 ml of SC-inositol supplemented with 25 µl of *myo*[1,2-^{3}H]inositol 1 mCi/ml 30 Ci/mmol (American Radiolabeled Chemicals cat. no. ART02611MC) and allowed to grow overnight at 30°C with shaking at 250 rpm until reaching an OD_{600} of 0.9. At this point, cells are either harvested and frozen at -80°C

until further use or harvested and washed with H_2O and resuspended in 5 ml of SLAD-inositol and grown for 8 hours at 30°C at 250rpm. These cultures are then harvested and frozen at -80°C until further use. Inositol polyphosphates are extracted by resuspending the pellet in 300 µl of 1M perchloric acid with 3mM EDTA and bead beating at 4°C for five minutes. Samples are spun down and the resulting supernatant is saved and allowed to neutralize with the addition of 1 M potassium carbonate and 3 mM EDTA until a pH of 6.0-8.0 is reached, and allowed to sit on ice for two hours. The sample is again centrifuged and the clear supernatant is run on the HPLC (Hewlett Packard Series 1100) connected to a Partisphere 5 µm SAX cartridge column 125 x 4.6 mm (HiCHROM cat. no. 4621-0505). Inositol polyphosphates are eluted from the column with a gradient from mixing buffer A (1 mM EDTA) and buffer B (1.3 M $(NH_4)_2HPO_4$, 1 mM EDTA, pH to 3.8 with H_3PO_4). The gradient used is as follows: 0-5 min, 0% buffer B; 5-10 min, 0-10% buffer B; 10-90 min, 10-100% Buffer B; 90-100 min, 100% Buffer B; 100-101 min, 0% buffer B; 101-110 min 0% buffer B. The gradient is run at a flow rate of 1 ml/min and one-1ml fractions are collected every minute for the first 90 minutes. Fractions are mixed with 4 ml of Ultima-Flo AP liquid scintillation cocktail (Perkin-Elmer cat. no. 6013599) and counted using a scintillation counter.

3.6 References

1. Wellen KE, Thompson CB (2012) A two-way street: reciprocal regulation of metabolism and signalling. Nat Rev Mol Cell Biol 13: 270-276.

2. Wu M, Chong LS, Perlman DH, Resnick AC, Fiedler D (2016) Inositol polyphosphates intersect with signaling and metabolic networks via two distinct mechanisms. Proc Natl Acad Sci U S A 113: E6757-6765.

3. Wilson MS, Livermore TM, Saiardi A (2013) Inositol pyrophosphates: between signalling and metabolism. Biochem J 452: 369-379.

4. Tsui MM, York JD (2010) ROLES OF INOSITOL PHOSPHATES AND INOSITOL PYROPHOSPHATES IN DEVELOPMENT, CELL SIGNALING AND NUCLEAR PROCESSES. Advances in Enzyme Regulation 50: 324-337.

5. Bennett M, Onnebo SMN, Azevedo C, Saiardi A (2006) Inositol pyrophosphates: metabolism and signaling. Cellular and Molecular Life Sciences 63: 552.

6. Lee J-Y, Kim Y-r, Park J, Kim S (2012) Inositol polyphosphate multikinase signaling in the regulation of metabolism. Annals of the New York Academy of Sciences 1271: 68-74.

7. Saiardi A (2016) Functions of Inositol Polyphosphate and Inorganic Polyphosphate in Yeast and Amoeba. In: Kulakovskaya T, Pavlov E, Dedkova EN, editors. Inorganic Polyphosphates in Eukaryotic Cells. Cham: Springer International Publishing. pp. 61-78.

8. Coccetti P, Tisi R, Martegani E, Souza Teixeira L, Lopes Brandao R, et al. (1998) The PLC1 encoded phospholipase C in the yeast Saccharomyces cerevisiae is essential for glucose-induced phosphatidylinositol turnover and activation of plasma membrane H+-ATPase. Biochim Biophys Acta 1405: 147-154.

9. Flick JS, Thorner J (1993) Genetic and biochemical characterization of a phosphatidylinositol-specific phospholipase C in Saccharomyces cerevisiae. Molecular and Cellular Biology 13: 5861-5876.

10. Monserrate JP, York JD (2010) Inositol phosphate synthesis and the nuclear processes they affect. Curr Opin Cell Biol 22: 365-373.

11. Saiardi A, Erdjument-Bromage H, Snowman AM, Tempst P, Snyder SH (1999) Synthesis of diphosphoinositol pentakisphosphate by a newly identified family of higher inositol polyphosphate kinases. Curr Biol 9: 1323-1326.

12. Odom AR, Stahlberg A, Wente SR, York JD (2000) A role for nuclear inositol 1,4,5-trisphosphate kinase in transcriptional control. Science 287: 2026-2029.

13. Saiardi A, Caffrey JJ, Snyder SH, Shears SB (2000) Inositol polyphosphate multikinase (ArgRIII) determines nuclear mRNA export in Saccharomyces cerevisiae. FEBS Lett 468: 28-32.

14. Ives EB, Nichols J, Wente SR, York JD (2000) Biochemical and functional characterization of inositol 1,3,4,5, 6-pentakisphosphate 2-kinases. J Biol Chem 275: 36575-36583.

15. Raboy V (2003) myo-Inositol-1,2,3,4,5,6-hexakisphosphate. Phytochemistry 64: 1033-1043.

16. Shears SB (2001) Assessing the omnipotence of inositol hexakisphosphate. Cell Signal 13: 151-158.

17. Shears SB (2017) Intimate connections: Inositol pyrophosphates at the interface of metabolic regulation and cell signaling. J Cell Physiol.

18. Kersting MC, Boyette M, Massey JH, Ryals PE (2003) Identification of the inositol isomers present in Tetrahymena. J Eukaryot Microbiol 50: 164-168.

19. Choi JH, Williams J, Cho J, Falck JR, Shears SB (2007) Purification, sequencing, and molecular identification of a mammalian PP-InsP5 kinase that is activated when cells are exposed to hyperosmotic stress. J Biol Chem 282: 30763-30775.

20. Taylor JR, Chen PH, Chou CC, Patel J, Jin SV (2012) KCS1 deletion in Saccharomyces cerevisiae leads to a defect in translocation of autophagic proteins and reduces autophagosome formation. Autophagy 8: 1300-1311.

21. Mulugu S, Bai W, Fridy PC, Bastidas RJ, Otto JC, et al. (2007) A conserved family of enzymes that phosphorylate inositol hexakisphosphate. Science 316: 106-109.

22. Saiardi A, Caffrey JJ, Snyder SH, Shears SB (2000) The inositol hexakisphosphate kinase family. Catalytic flexibility and function in yeast vacuole biogenesis. J Biol Chem 275: 24686-24692.

23. Glennon MC, Shears SB (1993) Turnover of inositol pentakisphosphates, inositol hexakisphosphate and diphosphoinositol polyphosphates in primary cultured hepatocytes. Biochem J 293 (Pt 2): 583-590.

24. Menniti FS, Miller RN, Putney JW, Jr., Shears SB (1993) Turnover of inositol polyphosphate pyrophosphates in pancreatoma cells. J Biol Chem 268: 3850-3856.

25. Steidle EA, Chong LS, Wu M, Crooke E, Fiedler D, et al. (2016) A Novel Inositol Pyrophosphate Phosphatase in Saccharomyces cerevisiae: Siw14 PROTEIN SELECTIVELY CLEAVES THE beta-PHOSPHATE FROM 5-DIPHOSPHOINOSITOL PENTAKISPHOSPHATE (5PP-IP5). J Biol Chem 291: 6772-6783.

26. Lonetti A, Szijgyarto Z, Bosch D, Loss O, Azevedo C, et al. (2011) Identification of an evolutionarily conserved family of inorganic polyphosphate endopolyphosphatases. J Biol Chem 286: 31966-31974.

27. Pohlmann J, Risse C, Seidel C, Pohlmann T, Jakopec V, et al. (2014) The Vip1 inositol polyphosphate kinase family regulates polarized growth and modulates the microtubule cytoskeleton in fungi. PLoS Genet 10: e1004586.

28. Wang H, Nair VS, Holland AA, Capolicchio S, Jessen HJ, et al. (2015) Asp1 from Schizosaccharomyces pombe binds a [2Fe-2S](2+) cluster which inhibits inositol pyrophosphate 1-phosphatase activity. Biochemistry 54: 6462-6474.

29. Gokhale NA, Zaremba A, Shears SB (2011) Receptor-dependent compartmentalization of PPIP5K1, a kinase with a cryptic polyphosphoinositide binding domain. Biochem J 434: 415-426.

30. Pohlmann J, Fleig U (2010) Asp1, a conserved 1/3 inositol polyphosphate kinase, regulates the dimorphic switch in Schizosaccharomyces pombe. Mol Cell Biol 30: 4535-4547.

31. Fridy PC, Otto JC, Dollins DE, York JD (2007) Cloning and characterization of two human VIP1-like inositol hexakisphosphate and diphosphoinositol pentakisphosphate kinases. J Biol Chem 282: 30754-30762.

32. Pulloor NK, Nair S, McCaffrey K, Kostic AD, Bist P, et al. (2014) Human genome-wide RNAi screen identifies an essential role for inositol pyrophosphates in Type-I interferon response. PLoS Pathog 10: e1003981.

33. Saiardi A, Cockcroft S (2008) Human ITPK1: a reversible inositol phosphate kinase/phosphatase that links receptor-dependent phospholipase C to Ca2+-activated chloride channels. Sci Signal 1: pe5.

34. Streb H, Irvine RF, Berridge MJ, Schulz I (1983) Release of Ca2+ from a nonmitochondrial intracellular store in pancreatic acinar cells by inositol-1,4,5-trisphosphate. Nature 306: 67-69.

35. York SJ, Armbruster BN, Greenwell P, Petes TD, York JD (2005) Inositol diphosphate signaling regulates telomere length. J Biol Chem 280: 4264-4269.

36. Dubois E, Scherens B, Vierendeels F, Ho MM, Messenguy F, et al. (2002) In Saccharomyces cerevisiae, the inositol polyphosphate kinase activity of Kcs1p is required for resistance to salt stress, cell wall integrity, and vacuolar morphogenesis. J Biol Chem 277: 23755-23763.

37. Burton A, Azevedo C, Andreassi C, Riccio A, Saiardi A (2013) Inositol pyrophosphates regulate JMJD2C-dependent histone demethylation. Proc Natl Acad Sci U S A 110: 18970-18975.

38. Wundenberg T, Mayr GW (2012) Synthesis and biological actions of diphosphoinositol phosphates (inositol pyrophosphates), regulators of cell homeostasis. Biol Chem 393: 979-998.

39. Worley J, Luo X, Capaldi AP (2013) Inositol Pyrophosphates Regulate Cell Growth and the Environmental Stress Response by Activating the HDAC Rpd3L. Cell Rep 3: 1476-1482.

40. Onnebo SM, Saiardi A (2009) Inositol pyrophosphates modulate hydrogen peroxide signalling. Biochem J 423: 109-118.

41. Gibney PA, Lu C, Caudy AA, Hess DC, Botstein D (2013) Yeast metabolic and signaling genes are required for heat-shock survival and have little overlap with the heat-induced genes.

Proc Natl Acad Sci U S A 110: E4393-4402.

42. Shively CA, Kweon HK, Norman KL, Mellacheruvu D, Xu T, et al. (2015) Large-Scale Analysis of Kinase Signaling in Yeast Pseudohyphal Development Identifies Regulation of Ribonucleoprotein Granules. PLoS Genet 11: e1005564.

43. Azevedo C, Saiardi A (2006) Extraction and analysis of soluble inositol polyphosphates from yeast. Nat Protoc 1: 2416-2422.

44. Klig LS, Homann MJ, Carman GM, Henry SA (1985) Coordinate regulation of phospholipid biosynthesis in Saccharomyces cerevisiae: pleiotropically constitutive opi1 mutant. J Bacteriol 162: 1135-1141.

45. Cullen PJ, Sprague GF, Jr. (2012) The regulation of filamentous growth in yeast. Genetics 190: 23-49.

46. Ye C, Bandara WM, Greenberg ML (2013) Regulation of inositol metabolism is fine-tuned by inositol pyrophosphates in Saccharomyces cerevisiae. J Biol Chem 288: 24898-24908.

47. Bharucha N, Ma J, Dobry CJ, Lawson SK, Yang Z, et al. (2008) Analysis of the yeast kinome reveals a network of regulated protein localization during filamentous growth. Mol Biol Cell 19: 2708-2717.

48. Gietz RD (2014) Yeast transformation by the LiAc/SS carrier DNA/PEG method. Methods Mol Biol 1205: 1-12.

49. Aslanidis C, de Jong PJ (1990) Ligation-independent cloning of PCR products (LIC-PCR). Nucleic Acids Res 18: 6069-6074.

Figure 3.1 Inositol polyphosphate synthesis pathway in *Saccharomyces cerevisiae.*
The known inositol polyphosphate and inositol pyrophosphate molecules are depicted below with the name of the molecule used throughout the study in the center of each cartoon depiction. The first molecule represented (IP_3) has each position on the *myo*-inositol ring labeled and the same numbering pattern is used in all subsequent molecules. The kinases are listed in black next to the arrow for the step in which they act as the catalytic enzyme. The phosphatases are listed in gray next to the step in which they have been shown to remove a phosphate group.

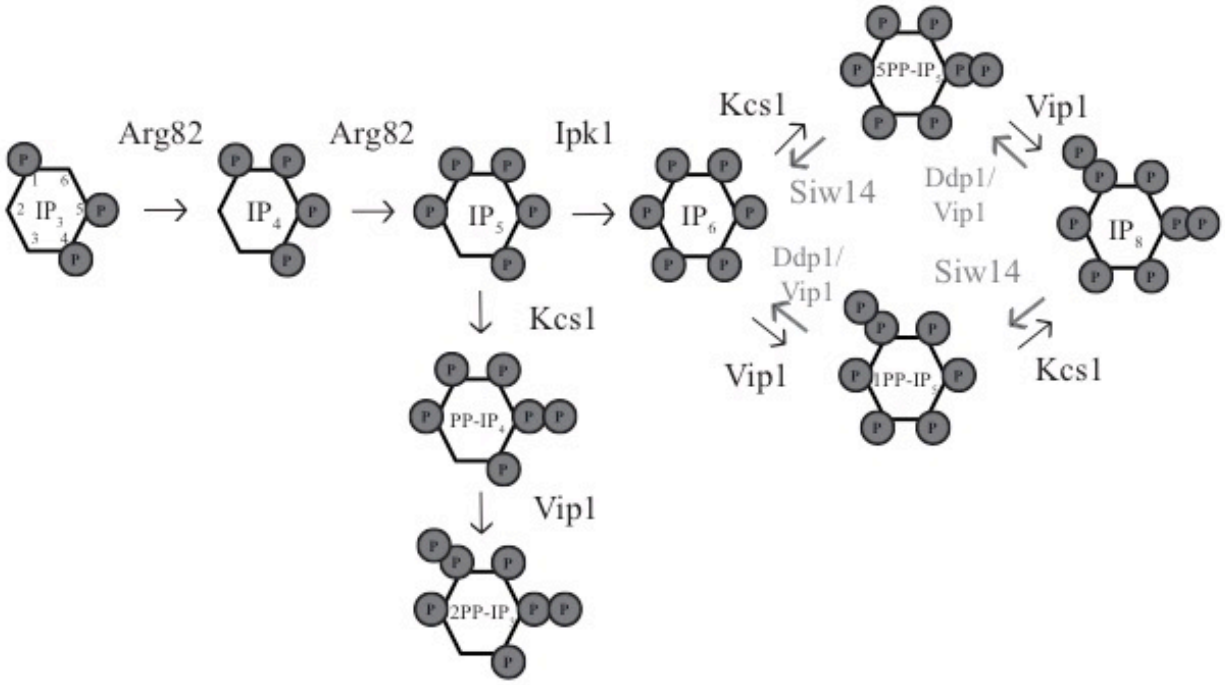

Figure 3.2 Inositol polyphosphate kinases are required for wild-type pseudohyphal growth.
A) Invasive growth phenotypes for haploid deletion strains and B) pseudohyphal growth phenotypes for homozygous diploid strains of the indicated inositol polyphosphate kinases (*ARG82, IPK1, VIP1,* and *KCS1*) are shown. The amount of invasive growth is indicated in white boxes with "-" representing a decrease in filamentous growth and "+" representing an increase in filamentous growth. Boxes without a "-" or "+" indicate wild-type growth.

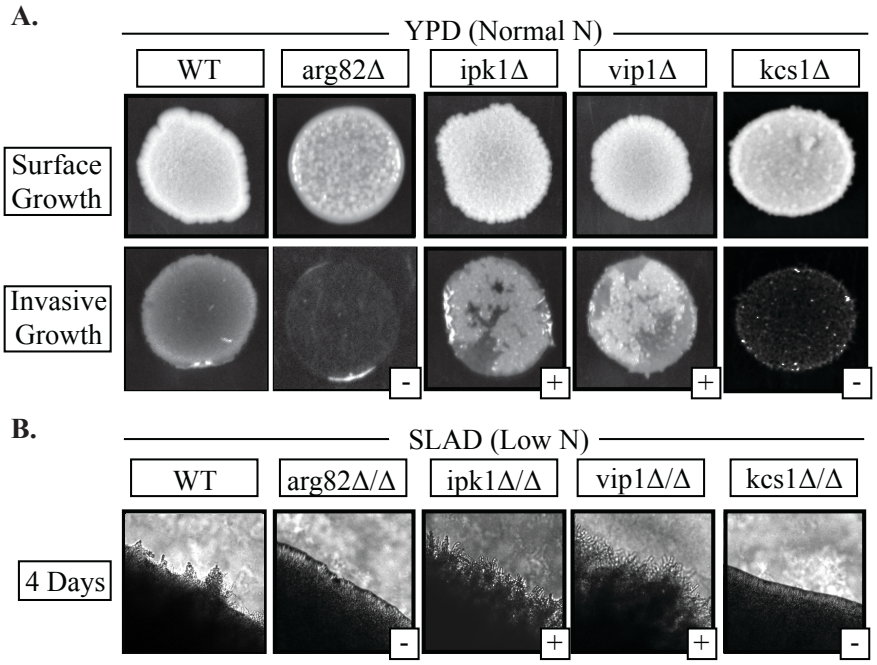

Figure 3.3 Inositol polyphosphate profiles under low nitrogen conditions.
A) Representative images of inositol polyphosphate profiles of a wild-type diploid filamentous strain grown in standard growth conditions (Σ1278b), a wild-type filamentous strain grown in low nitrogen media for 8 hours (Σ1278b SLAD), and a non-filamentous wild-type strain grown in low nitrogen media for 8 hours (BY4743 SLAD). Two isoforms of IP_7 are observed along with a decrease in IP_5 and PP-IP_4 levels when comparing WT and WT SLAD B) Representative images of *vip1*Δ/Δ and *kcs1*Δ/Δ strains grown in low nitrogen media compared to WT. C) A zoomed in portion of indicated region in panel B to better visualize the distinct separation of IP_7 isoforms that become apparent under nitrogen starvation and through deletion of the kinases that produce the IP_7 molecules. Known inositol polyphosphate and pyrophosphate peaks are indicated by labels in all panels.

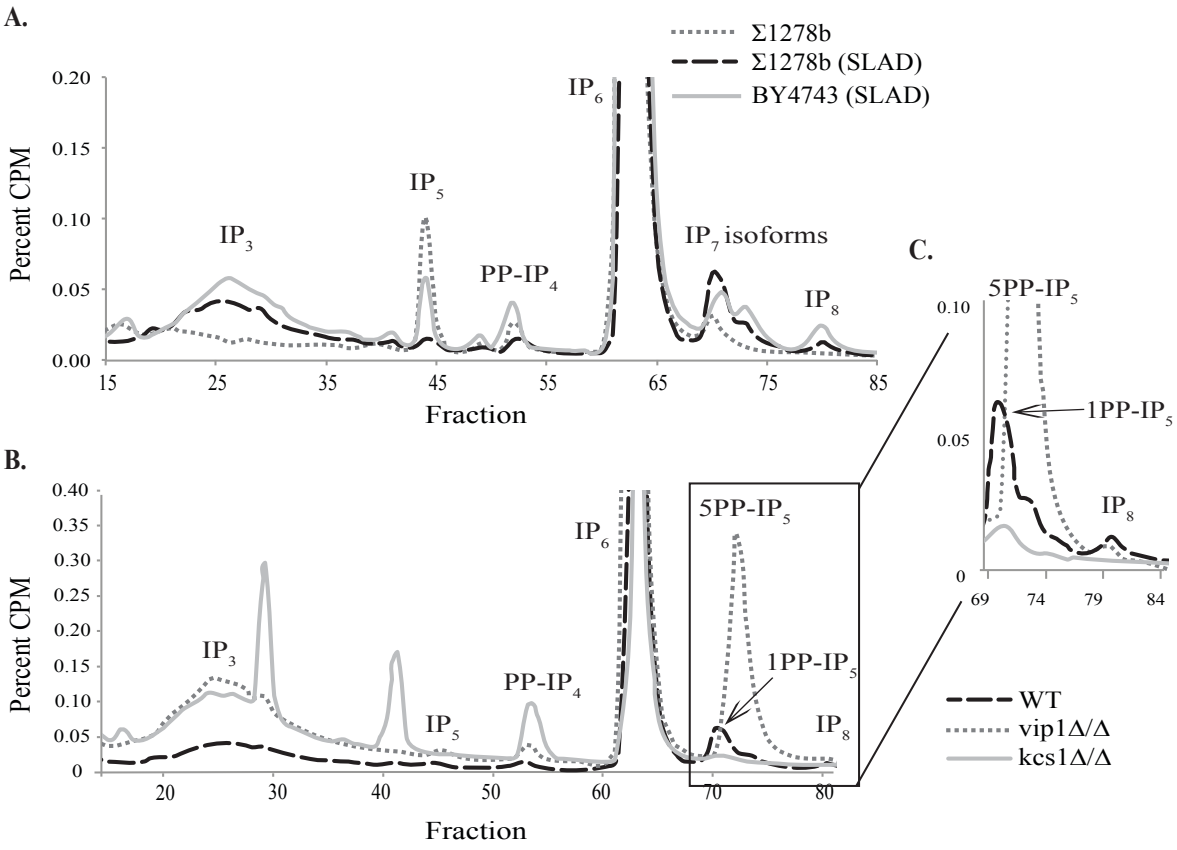

Figure 3.4 Deletion of the *VIP1* kinase domain causes pseudohyphal growth defects.
A) Diagram indicating domains of *S. cerevisiae* Vip1p. Amino acids essential for kinase and phosphatase catalytic activity are indicated below. B) Invasive growth phenotypes and C) pseudohyphal surface spread phenotypes are shown for a kinase-deficient (D487A) and phosphatase-deficient (H548A) *VIP1*. Wild-type strains and *VIP1* deletions are shown for comparison. The amount of invasive growth is indicated in white boxes with "-" representing a decrease in filamentous growth and "+" representing an increase in filamentous growth. Boxes without a "-" or "+" indicate wild-type growth. D) Representative images of the inositol polyphosphate profiles of kinase and phosphatase-deficient *VIP1* strains grown in low nitrogen for 8 hours. A wild-type filamentous strain and *vip1Δ/Δ* strain grown in low nitrogen are shown for comparison.

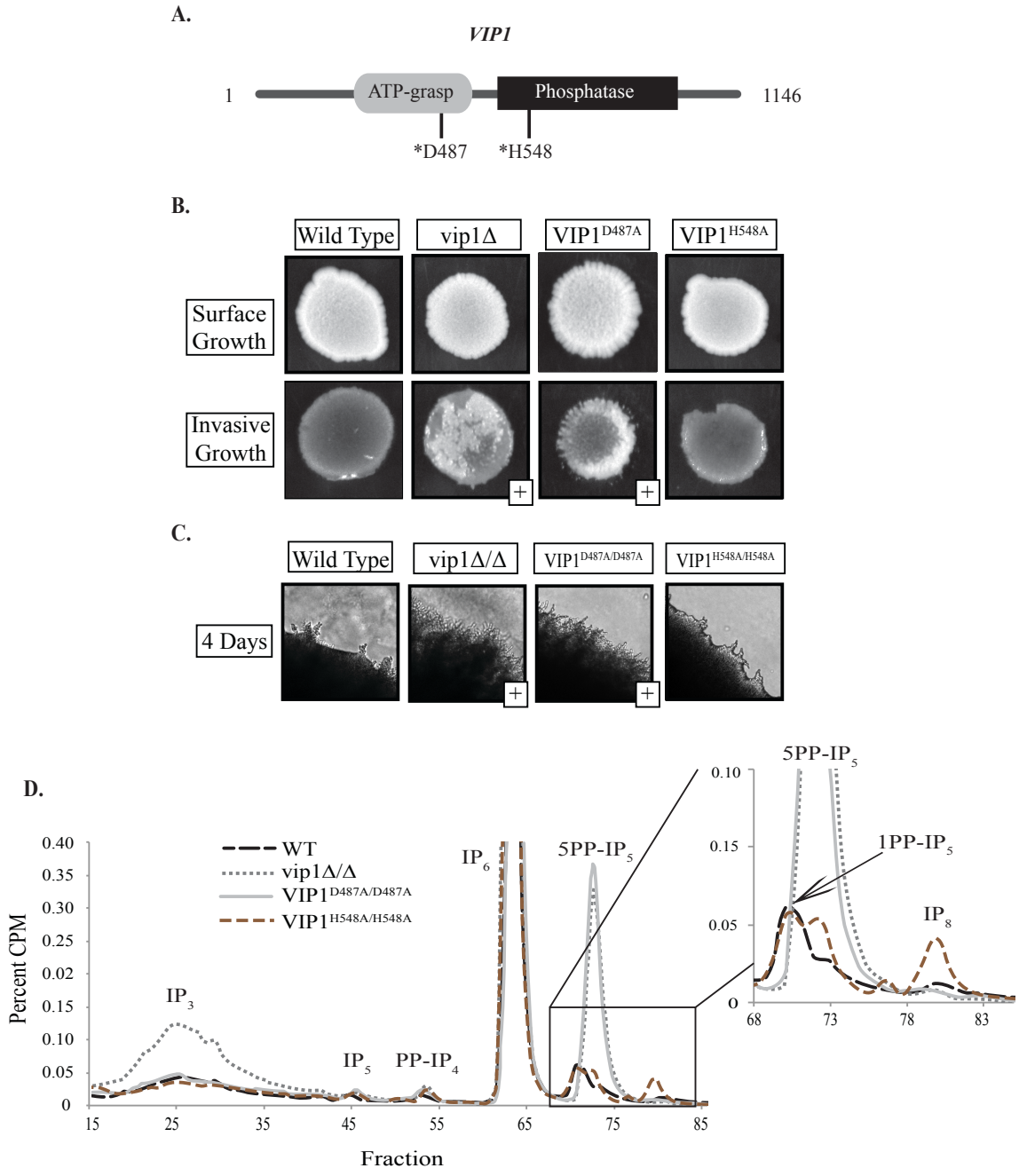

Figure 3.5 Deletion of IP phosphatases causes build up of IP_7 isomers.
A) Representative inositol polyphosphate profiles of mutated phosphatase strains grown in SLAD for 8 hours. B) Surface spread phenotypes of strains with mutated phosphatases grown on SLAD for 4 days.

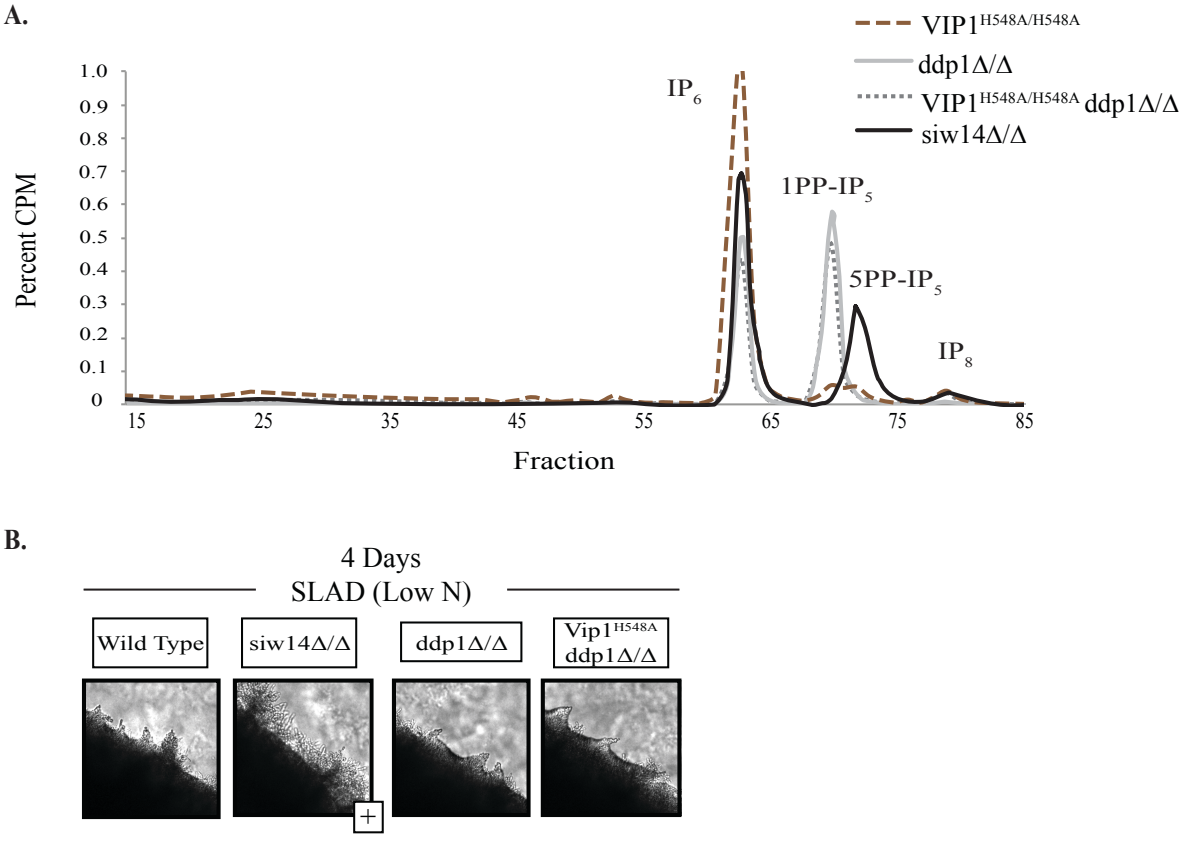

Figure 3.6 Overexpression of *KCS1* and *VIP1*

A) Representative inositol polyphosphate profiles of strains carrying overexpression plasmids for *VIP1* or *KCS1* as indicated compared to a wild-type (WT) strain. All strains were grown for 8 hours in SLAD. B) Pseudohyphal growth phenotypes of overexpression strains. "+" indicates increased surface spread filament formation while "-" indicates decreased surface spread filamentation only compared to a wild-type control. C) Strains grown on rich media for 7 days show increased surface spread filamentation. "+" indicates increased surface spread while "-" indicates decreased surface spread compared to the vector only control of that strain. D) Representative inositol polyphosphate profile of *VIP1* overexpression in a *siw14*Δ/Δ strain with a *siw14*Δ/Δ mutant strain as a comparison to change in peaks.

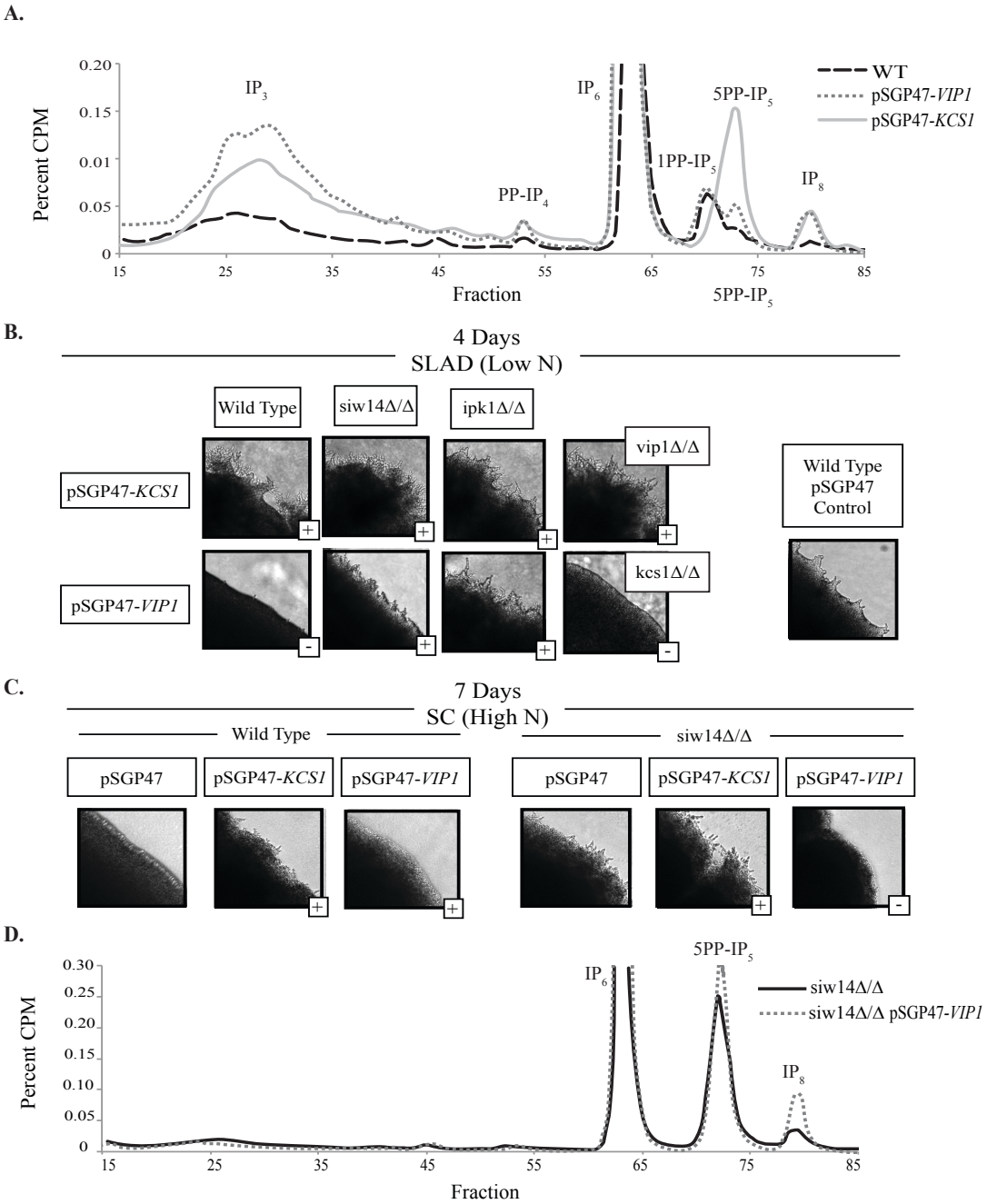

Figure 3.7 Key regulatory kinases affect inositol polyphosphate profiles.

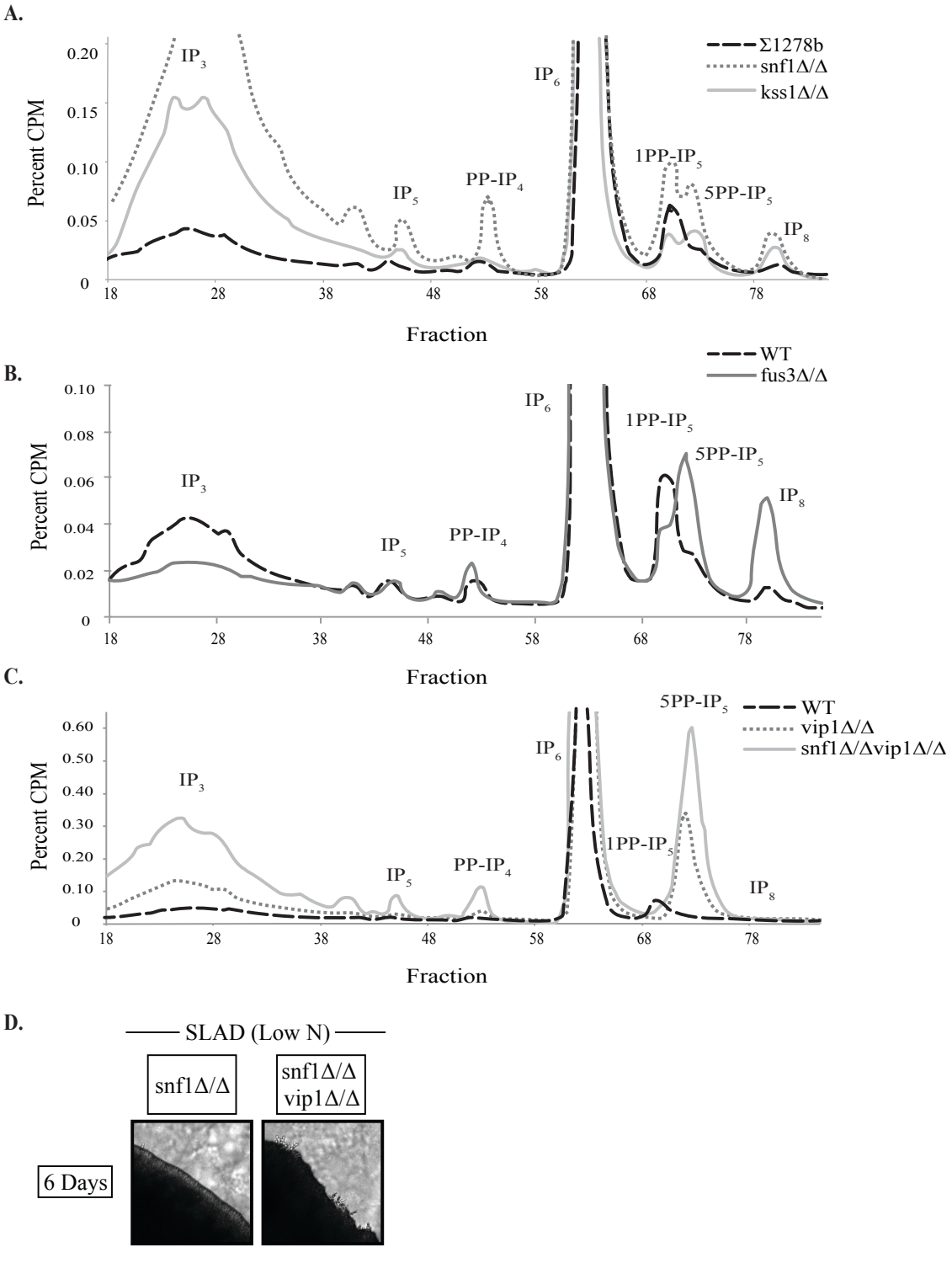

Table 3.1 List of differentially phosphorylated proteins.
Differentially phosphorylated phosphopeptide sequences were found in a previous study using SILAC and mass spectrometry. A ratio of greater than one indicates increased phosphorylation upon mutation of the kinase domain under filamentous growth conditions at the indicated sites. A ratio of less than one indicates a decrease in phosphorylation.

Protein	Modified Sequence	Ratio	Significance	Kinase Dead Data Set Found in
ARG82	_LSDS(ph)TDNLDSIPVK_	2.68	0.022	SNF1
	LSDS(ph)TDNLDSIPVK	2.30	0.032	SNF1
VIP1	_EFNNAEKVDPS(ph)KIS(ph)ELYDTM(ox)K_	0.22	0.015	SNF1
	LPPPGIQDDHS(ph)EENLTVHDTLQR	0.22	0.011	KSS1
	LPPPGIQDDHSEENLT(ph)VHDTLQR	0.24	0.015	KSS1
KCS1	_ISNALDGSHS(ph)VMDLK_	0.24	0.021	SNF1

Table 3.2 List of strains used in this study.

Strain	Genotype	Source
Y825	*ura3-52 leu2Δ0 MAT***a**	M. Snyder (Stanford, CA)
HLY337	*ura3-52 trp1-1 MAT*α	G. Fink (MIT, MA)
Y825xHLY337	*ura3-52/ura3-52 leu2Δ0 trp1-1 MATa/α*	
BY4743	*MATa/α his3Δ1/his3Δ1 leu2Δ0/leu2Δ0 LYS2/lys2Δ0 met15Δ0/MET15 ura3Δ0/ura3Δ0*	This study
yKN12	*arg82Δ::KanMX6 ura3-52 leu2Δ0 MAT***a**	This study
yKN13	*arg82Δ::KanMX6 ura3-52 trp1-1 MAT*α	This study
yKN14	*arg82Δ::KanMX6/arg82Δ::KanMX6 ura3-52/ura3-52 leu2Δ0 trp1-1 MATa/α*	This study
yKN15	*ipk1Δ::KanMX6 ura3-52 leu2Δ0 MAT***a**	This study
yKN16	*ipk1Δ::KanMX6 ura3-52 trp1-1 MAT*α	This study
yKN17	*ipk1Δ::KanMX6/ ipk1Δ::KanMX6 ura3-52/ura3-52 leu2Δ0 trp1-1 MATa/α*	This study
yKN18	*vip1Δ::KanMX6 ura3-52 leu2Δ0 MAT***a**	This study
yKN19	*vip1Δ::KanMX6 ura3-52 trp1-1 MAT*α	This study
yKN20	*vip1Δ::KanMX6/vip1Δ::KanMX6 ura3-52/ura3-52 leu2Δ0 trp1-1 MATa/α*	This study
yKN21	*kcs1Δ::KanMX6 ura3-52 leu2Δ0 MAT***a**	This study
yKN22	*kcs1Δ::KanMX6 ura3-52 trp1-1 MAT*α	This study
yKN23	*kcs1Δ::KanMX6/kcs1Δ::KanMX6 ura3-52/ura3-52 leu2Δ0 trp1-1 MATa/α*	This study
yKN24	*ddp1Δ::KanMX6 ura3-52 leu2Δ0 MAT***a**	This study
yKN25	*ddp1Δ::KanMX6 ura3-52 trp1-1 MAT*α	This study
yKN26	*ddp1Δ::KanMX6/ddp1Δ::KanMX6 ura3-52/ura3-52 leu2Δ0 trp1-1 MATa/α*	This study
yKN27	*siw14Δ::KanMX6 ura3-52 leu2Δ0 MAT***a**	This study
yKN28	*siw14Δ::KanMX6 ura3-52 trp1-1 MAT*α	This study

yKN29	*siw14Δ::KanMX6/siw14Δ::KanMX6 ura3-52/ura3-52 leu2Δ0 trp1-1 MATa/α*	This study
yKN30	*ura3-52/ura3-52 leu2Δ0 trp1-1 MATa/α* + pSGP47-*KCS1*	This study
yKN31	*ura3-52/ura3-52 leu2Δ0 trp1-1 MATa/α* + pSGP47-*VIP1*	This study
yKN32	*fus3Δ::HphMX4/fus3Δ::KanMX6 ura3-52/ura3-52 leu2Δ0 trp1-1 MATa/α*	This study
yKN33	*kss1Δ::HphMX4/kss1Δ::KanMX6 ura3-52/ura3-52 leu2Δ0 trp1-1 MATa/α*	This study
yKN34	*snf1Δ::KanMX6 vip1Δ::HphMX4 ura3-52 leu2Δ0 MAT***a**	This study
yKN35	*snf1Δ::KanMX6 vip1Δ::HphMX4 ura3-52 trp1-1 MAT*α	This study
yKN36	*snf1Δ::KanMX6/ snf1Δ::KanMX6 vip1Δ::HphMX4/ vip1Δ::HphMX4 ura3-52/ura3-52 leu2Δ0 trp1-1 MATa/α*	This study
yKN37	*snf1Δ::KanMX6/snf1Δ::KanMX6 ura3-52/ura3-52 leu2Δ0 trp1-1 MATa/α* + pSGP47-*VIP1*	This study
yKN38	*snf1Δ::KanMX6/snf1Δ::KanMX6 ura3-52/ura3-52 leu2Δ0 trp1-1 MATa/α* + pSGP47-*KCS1*	This study
yKN39	*ipk1Δ::KanMX6/ ipk1Δ::KanMX6 ura3-52/ura3-52 leu2Δ0 trp1-1 MATa/α* + pSGP47-*KCS1*	This study
yKN40	*ipk1Δ::KanMX6/ ipk1Δ::KanMX6 ura3-52/ura3-52 leu2Δ0 trp1-1 MATa/α* + pSGP47-*VIP1*	This study
yKN41	*vip1Δ::KanMX6/vip1Δ::KanMX6 ura3-52/ura3-52 leu2Δ0 trp1-1 MATa/α* + pSGP47-*KCS1*	This study
yKN42	*kcs1Δ::KanMX6/kcs1Δ::KanMX6 ura3-52/ura3-52 leu2Δ0 trp1-1 MATa/α* + pSGP47-*VIP1*	This study
yKN43	*siw14Δ::KanMX6/siw14Δ::KanMX6 ura3-52/ura3-52 leu2Δ0 trp1-1 MATa/α* + pSGP47-*KCS1*	This study
yKN44	*siw14Δ::KanMX6/siw14Δ::KanMX6 ura3-52/ura3-52 leu2Δ0 trp1-1 MATa/α* + pSGP47-*VIP1*	This study
yCS1	*snf1Δ::KanMX6 ura3-52 leu2Δ0 MAT***a**	This study
yCS2	*snf1Δ::KanMX6 ura3-52 trp1-1 MAT*α	This study
yCS3	*snf1Δ::KanMX6/snf1Δ::KanMX6 ura3-52/ura3-52 leu2Δ0 trp1-1 MATa/α*	This study

Table 3.3 List of plasmids used in this study.

Strain	Genotype	Source
pSGP47	*URA,* high copy, Amp^r	DNASU Plasmid Repository (Tempe, AZ)
pSGP47-*KCS1*	P_{ADH2}-*KCS1 URA,* high copy, Amp^r	This Study
pSGP47-*VIP1*	P_{ADH2}-*VIP1 URA,* high copy, Amp^r	This Study

CHAPTER 4

Complex haploinsufficiency-based genetic analysis of the NDR/Lats kinase Cbk1 provides insight into its multiple function in *Candida albicans*

4.1 Abstract

Methods for synthetic genetic analysis have proven useful for the dissection of eukaryotic signaling networks in many organisms, and here we describe the use of directed genetic interaction studies based on complex haploinsufficiency to probe the function of the **R**egulation of **A**ce2 and **M**orphogenesis (RAM) pathway in the pathogenic yeast *Candida albicans*. Complex haploinsufficiency is observed when a mutant heterozygous at two alleles exhibits a phenotype that is more severe than that observed in strains containing either mutation in isolation. For this study, we utilized a library of 5200 *Tn7*-mutagenized derivatives of a parental strain of *C. albicans* heterozygous at the *CBK1* locus; Cbk1p is the key kinase in the RAM pathway. The heterozygous *cbk1* double mutants were screened for alterations in serum-induced filamentation. We confirmed these phenotypes and identified a set of 36 unique double heterozygous strains showing complex haploinsufficiency. Follow-up analysis led to the first demonstration that the RAM pathway is required for oxidative stress tolerance in a manner related to the two-component-regulated kinase Chk1 and revealed a potential direct connection between the RAM pathway and the essential Mps1 spindle pole-related kinase. In addition,

genetic interactions with *CDC42*-related genes and *MSB1* were identified.

4.2 Introduction

While *Candida albicans* is a component of the normal gastrointestinal flora of humans, it is also one of the most important human fungal pathogens and causes disease in both immunocompetent and immunocompromised individuals [1]. Superficial mucosal disease predominates in persons with normal immune function and those with altered T-cell function, while invasive, deep-seated infections occur in patients with more profound immune deficits affecting innate and adaptive immunity. The ability of *C. albicans* to cause disease has been linked to its characteristic transition between three distinct morphological forms: yeast, pseudohyphae, and hyphae [2]. *C. albicans* mutants locked in either yeast or hyphal morphological forms fail to cause disease [3]: the yeast forms are able to infect mice but cannot cause disease, while those locked as hyphae fail to disseminate and establish infection. Although this dichotomous model for the role of filamentation is consistent with much of the literature, it is almost certainly an oversimplification. Indeed, a large-scale screen of *C. albicans* mutants comparing the ability to infect mice with morphological phenotypes found that normal filamentation was neither necessary nor sufficient to establish infection [4]. These observations are not necessarily contradictory to the data from morphologically locked stains, since the ability to cause disease was not studied in the large-scale experiment. One broad but generally accurate interpretation of the vast amount of data regarding *C. albicans* filamentation is that it is a crucial aspect of this organism's biology. Considered in converse, it also seems broadly accurate that genetic perturbations of many biological processes directly or indirectly result in alterations in *C. albicans* morphology. As such, phenotypes related to filamentation provide a sensitive assay for

the detection of mutations that have some effect on *C. albicans* biology.

Recently, the use of complex haploinsufficiency has been described as an approach to studying genetic interactions between, and within, pathways in *C. albicans* [5]. Complex haploinsufficiency involves the generation of heterozygous mutations in two loci and comparing the phenotypes of that strain with the single heterozygotes. If the double heterozygote has a more profound phenotype than either of the single heterozygotes, then this indicates that the two genes interact. This approach is similar in concept to nonallelic, noncomplementation as developed in *Saccharomyces cerevisiae* [6] and has been used to study the genetic interactions of essential genes in *S. cerevisiae* as well [7]. Although the recent discovery and, emerging development, of haploid genetics in *C. albicans* may allow the simple construction of double haploid mutants at some point [8], the generation and study of complex heterozygotes remains a facile and expedient approach to genetic interaction screening and analysis in *C. albicans*.

The utility of this approach, however, is dependent on the identification of a sensitive phenotypic read-out to detect the effects of altered gene dosage on *C. albicans* physiology. Based on the pioneering simple haploinsufficiency screen of [9], morphological phenotypes are such a phenotype. Accordingly, we have used filamentation-related phenotypes and complex haploinsufficiency to probe the role of the **R**egulation of **A**ce2 and **M**orphogenesis (RAM) in *C. albicans* biology [5]. The RAM pathway is centered on the Ndr/Lats family protein kinase Cbk1 (FungiDB: orf19.4909) and its transcription factor substrate Ace2 (FungiDB: orf19.6124). In addition to these two effector proteins, the RAM network includes Mob2, a Cbk1-binding protein required for kinase activity; Kic1, a kinase of unclear function; and the accessory proteins Tao3, Hym1, and Sog2 [10]. Recent work has shown that Cbk1 also phosphorylates Bcr1 (FungiDB: orf19.723), a transcription factor involved in biofilm formation [11], and the

Fkh2, a forkhead transcription factor [12], involved in morphogenesis.

Others and we have been interested in identifying other signaling pathways that interact with Cbk1 during filamentation. Gutierrez-Escribino *et al.* (2011) have shown that Cdc28 phosphorylates Mob2 and Cdc28 also regulates Fkh2 [12], indicating that the RAM pathway, as well as its output, is interconnected with this important cell cycle regulator. In a previous application of complex haploinsufficiency screening to Cbk1 [5], it was found that the RAM and PKA–cAMP pathways interact and subsequent mechanistic studies revealed that Efg1 (FungiDB: orf19.610), the main transcription factor regulated by the cAMP–PKA pathway, suppresses *ACE2* expression early in morphogenesis [13]. The previous complex haploinsufficiency screen was performed using Spider medium as the filament-inducing conditions [5] and, in addition to revealing the PKA pathway interaction, identified a large number of Ace2 targets. Ace2 is required for normal filament formation in Spider medium but is dispensable when serum is used [14]; Cbk1, on the other hand, is required for filament formation under either conditions [15,16]. To identify additional, potentially Ace2-independent interactors with Cbk1 during filamentation, Saputo *et al,* screened a library of transposon-mutagenized *cbk1*Δ/*CBK1* complex heterozygotes for strains with decreased filamentation on serum medium [17]. This screen identified a distinct set of Cbk1-interacting genes relative to the Spider medium screen with a large number of these genes also being Ace2 related [18], suggesting that, although not essential for filamentation, Ace2 remains an important effector of the RAM pathway during serum-induced morphogenesis. In contrast to the metabolic and nutrition-related genes identified in the Spider medium screen [5], genes related to cell cycle and polarity as well as other processes not previously connected to RAM pathway function were isolated. Additional analyses of these interacting genes provided links between Cbk1 and the

master polarity regulator Cdc42, the mitotic spindle kinase Msp1, and the two-component regulator kinase Chk1.

4.3 Results and Discussion

4.3.1 Independent verification of transposon mutagenized cbk1Δ/CBK1 heterozygote strains deficient for filamentation on serum-containing medium

A transposon library of 5200 strains mutagenized with *Tn7* in a *cbk1*Δ/CBK1 *C. albicans* background strain was produced and tested for phenotypic deficiencies in filamentous growth on Spider medium [5]. This same library was again tested to see if different targets could be found by screening on 1% serum using the concept of complex haploinsufficiency [17]. The serum screen led to a total of 121 strains that had a complex haploinsufficient phenotype. These strains were then sequenced for transposon insertions and 36 strains were found to have complex haploinsufficiency due to transposon insertion [17]. From this set of 36 strains, we independently reconstructed 13 double heterozygote strains (Table 4.1) and confirmed filamentous phenotypes on 1% serum; a representative set of reconfirmed strains is shown in Figure 4.1.

4.3.2 CBK1 is required for oxidative stress tolerance and expression of CHK1

Chk1 is a two-component system histidine kinase that overlaps functionally with many of the processes regulated by the RAM pathway including filamentation, cell wall integrity, and cell separation [19]. In addition, *CHK1* appears to interact with the cAMP/PKA pathway based on the requirement for Chk1 activity in farnesol inhibition of filamentation; farnesol has been shown to inhibit the activity of the cAMP-based signaling in *C. albicans* [20]. Previous studies have shown that the RAM and PKA pathways interact [5]. In addition, *CHK1* is induced by

overexpression of the transcription factor *BCR1* in **a**/**a** biofilms [21]; Bcr1 is a known target of Cbk1 in biofilms. Based on these previous observations, the genetic interaction between *CHK1* and *CBK1* seemed quite reasonable.

To further explore the interaction between *CBK1* and *CHK1*, we asked whether it might manifest under conditions for which *CHK1* was known to function. One of the best-characterized functions of Chk1 is in protecting *C. albicans* from oxidative stress [22]. Although the RAM pathway has been shown to be required for a variety of stress responses in *C. albicans*, it has not been previously linked to oxidative stress tolerance. We therefore, hypothesized that *CHK1* may interact with *CBK1* under oxidative stress conditions. Consistent with that hypothesis, the *chk1*Δ/*CHK1 cbk1*Δ/*CBK1* double heterozygote showed a CHI interaction relative to the two single heterozygotes on medium containing hydrogen peroxide (Fig 4.2 A). This role is further supported by the fact that the *cbk1*Δ/*CBK1 ace2*Δ/*ACE2* strain also shows complex haploinsufficiency in the presence of hydrogen peroxide. To further explore a potential mechanism for this interaction, we determined the effect of *CBK1* and *CHK1* mutations on *CHK1* expression in the presence of hydrogen peroxide. As shown in Figure 4.2 B, the expression of *CHK1* was reduced ~2.5- and 3-fold in the *cbk1*Δ and *chk1*Δ heterozygotes relative to WT, respectively. *CHK1* expression was reduced by fourfold in the *chk1*Δ/*CHK1 cbk1*Δ/*CBK1* double heterozygote, providing a potential explanation for the CHI interaction between *CHK1* and *CBK1* in the presence of oxidative stress. A role for Cbk1 in the regulation of *CHK1* expression during oxidative stress is further supported by the fact that *CHK1* expression is dramatically reduced (~20-fold) in the *cbk1*Δ/Δ relative to WT (Fig 4.2 B). This observation suggests that intact RAM pathway signaling is required to maintain *CHK1* expression at levels sufficient to protect the cell from oxidative stress.

The promoter of *CHK1* does not contain consensus sequences for Ace2 binding and, thus, it seems unlikely that Cbk1 regulates *CHK1* expression through Ace2. As discussed above, overexpression of the Cbk1 target *BCR1* increases expression of *CHK1* [21]. In addition, Cbk1 has been shown to phosphorylate Bcr1 in the setting of biofilm formation [11]. Based on these considerations, Bcr1 appeared to be a reasonable candidate as a potential Cbk1-dependent regulator of *CHK1*. Further supporting this possibility is the fact that *bcr1*Δ/Δ mutants are hyper-susceptible to neutrophil-mediated killing, a process intimately related to oxidative stress tolerance [23]. To test this hypothesis, we determined the effect of a *bcr1*Δ/Δ mutation of *CHK1* expression during oxidative stress; as shown in Figure 4.2 C. *CHK1* expression is fivefold lower in the *bcr1*Δ/Δ mutant relative to WT. This is consistent with previous data indicating that overexpression of *BCR1* increases *CHK1* expression [21]. However, the *cbk1*Δ/Δ mutant has a larger effect (20-fold) on *CHK1* expression than the *bcr1*Δ/Δ mutant, suggesting that other transcriptional regulators may also contribute to Cbk1-regulated expression of *CHK1*. Thus, our data are consistent with a model in which Cbk1 regulates *CHK1* expression during oxidative stress in a manner partially dependent on Bcr1, a transcription factor previously shown to be a substrate of Cbk1.

4.3.3 Mitotic defects of mps1 mutants are exacerbated by loss of Cbk1 function

Three genes with functions in cell cycle-related processes were isolated: *CDC13*, an essential gene that functions in telomere maintenance; an ortholog of *S. cerevisiae CDC16* with ubiquitin ligase activity that functions in the anaphase-promoting complex (APC); and *MPS1*, a kinase that is part of the spindle assembly checkpoint complex. Recently, Kamthan *et al.* (2014) characterized *MPS1* in *C. albicans* and showed that it was essential [24]. In addition,

they found that, like the *S. cerevisiae* ortholog, it plays an important role in mitosis. In *S. cerevisiae*, Cbk1 plays functions in the mitotic exit network (MEN) and in the regulation of cytokinesis [25]. In addition, *C. albicans* cells lacking components of the RAM pathway show increased levels of multinucleate cells [16]. *MPS1* expression is increased by hyphae-inducing conditions in a PKA/Efg1-dependent manner [24]. Previous data shows that Efg1 activity is increased in *cbk1* mutants with elevated expression of many Efg1 targets [5]. We therefore, hypothesized that *MPS1* may be important for maintaining mitotic stability in the absence of RAM pathway activity.

If *CBK1* and *MPS1* were interacting in a manner that affected mitosis, we suspected that this might also affect overall growth rate. Indeed, the *mps1*Δ/*MPS1 cbk1*Δ/*CBK1* mutant showed significantly reduced growth rate in liquid culture relative to either of the single heterozygotes, confirming a complex haploinsufficient interaction between *MPS1* and *CBK1* (Fig 4.3 A). Kamthan *et al.* (2014) observed that depletion of *MPS1* through the use of a methionine-regulated allele led to actively dividing cells with buds lacking nuclei, indicating that *MPS1* is required for proper mitosis. Song *et al.* (2008) had also previously shown that mitotic defects were present in *cbk1*Δ/Δ strains. We therefore examined the nuclear segregation of the corresponding single and double heterozygous *cbk1* and *mps1* strains. Although neither of the single heterozygous mutants showed a statistically significant increase in large daughter cell buds without nuclei relative to WT, the double heterozygous *mps1*Δ/*MPS1 cbk1*Δ/*CBK1* mutant showed such an increase, indicating an interaction between these two genes with respect to mitosis (Fig 4.3 B and C). Taken together with our screening results, these data confirm a genetic interaction between *MPS1* and *CBK1*during filamentation and during vegetative growth. Because mitotic processes are essential during both of these growth phases, it is likely that the effect of

the mutations is to prevent smooth progression through mitosis, leading to a reduction in the rate of growth and filamentation.

Our observations in *C. albicans* are also consistent with previous data indicating that the RAM pathway interacts with *MPS1* genetically in *S. cerevisiae*. Specifically, Luca and Winey (1998) showed that double mutants of *mps1-1* and *mob2*Δ, the binding partner of Cbk1, showed increased ploidy relative to each single mutant [26]. Inspection of the protein sequence of Cbk1 revealed the presence of a consensus Mps1 phosphorylation site (E/D/N/Q at the −2 position relative to S or T; [27]) at S98 (*E*M**S**) and data from a recent phosphoproteomic study indicate that this position is phosphorylated in *C. albicans* [28]. In addition, *C. albicans* Mob2 contains five consensus Mps1 sites that are also phosphorylated (*N*L**S**^{35}; *N*L**S**^{44}; *Q*D**S**^{83}; *Q*S**S**^{86}; and *Q*S**S**^{93}) according to this study [29]. RAM pathway function in *C. albicans* has been previously shown to be regulated through Cdc28 phosphorylation of Mob2, providing precedent for signaling pathway cross-talk to the RAM pathway involving Mob2 [11]. It should be noted that Mps1 and polo-like kinases have similar phosphorylation sites and it is possible or even likely that the *C. albicans* polo-like kinase Cdc5 may regulate Mob2–Cbk1. Although additional experiments will be required to confirm the direct interaction between Mps1 and the Mob2–Cbk1 complex in *C. albicans*, our data suggest that the function of the RAM pathway during mitosis may be modulated through Mps1-mediated phosphorylation of both Mob2 and Cbk1.

4.3.4 Decreased CBK1 gene dosage leads to increased levels of the putative polarity scaffold protein Msb1

We first tested the phenotypes of the independently constructed *msb1*Δ/*MSB1* and *msb1*Δ/*MSB1 cbk1*Δ/*CBK1* mutants on serum-containing medium (data not shown); surprisingly,

these strains showed no phenotype relative to WT or the *cbk1*Δ/*CBK1*simple heterozygote, suggesting that the phenotype of the transposon-derived mutant was not reflective of a simple loss-of-function mutation. In contrast, the *msb1*Δ/*MSB1* showed no peripheral invasion outside of the colony Spider medium at 37°, while the *cbk1*Δ/*CBK1* heterozygote showed the previously reported [5,9] modest reduction in peripheral invasion relative to WT (Fig 4.4 A). Introduction of the *cbk1*Δ/*CBK1* mutation into the *msb1*Δ/*MSB1* background partially restored invasion to the mutant, indicating that deletion of an allele of *CBK1* partially suppressed the invasion defect of *msb1*Δ/*MSB1* (Fig 4.4 A). These observations suggest that reduced gene copy of either *CBK1* or *MSB1* leads to modulation of the other gene's ability to support filamentation.

MSB1 has not been characterized in *C. albicans* previously. Therefore, we generated a GFP-tagged allele in both WT and *cbk1*Δ/Δ strains and examined its localization under both yeast (YPD, 30°) and hyphae phase growth (Spider medium, 37°). Interestingly, we could detect almost no GFP signal in WT strains under yeast phase growth conditions (Fig 4.4 B) In contrast, Msb1–GFP was readily detectable in WT cells under hyphae-inducing conditions (Spider medium, 37°). As shown in Figure 4.4 B, Msb1–GFP signal was apparent in both the cytosol and, in more dense concentrations, at the septa of hyphal cells. Although studies in *S. cerevisiae* indicated that Msb1 localizes to the bud tip, we were unable to conclusively observe localization to the hyphal tip; however, the signal is rather low and we cannot rule out this possibility. The relatively low signal also made it difficult to assess localization in *cbk1*Δ/Δ cells; additionally, it seemed that Msb1 levels were higher in the *cbk1*Δ/Δ under yeast conditions but it was difficult to conclusively quantitate this by microscopy (data not shown).

To characterize the effect of hyphae-inducing conditions and decreased RAM pathway activity on Msb1 protein levels, we performed Western blot analysis. Consistent with the

microscopy data, Msb1 protein levels are increased in hyphal cells and *cbk1*Δ/Δ relative to WT in yeast phase (Fig 4.4 C). These data indicate that *MSB1* expression is normally increased by hyphal induction in Spider medium and is required for normal invasion (Fig 4.4 A). Furthermore, our data are also consistent with a model whereby decreased RAM pathway activity leads to a compensatory increase in Msb1 protein levels that, in turn, suppress the haploinsufficiency of the *msb1*Δ/*MSB1* heterozygote. As discussed above, the function of *MSB1* in *S. cerevisiae* appears dependent on its level of expression, since most of the phenotypes described for it involve overexpression [30]. These data also suggest that increased expression of *MSB1* may compensate for reduced function of polarity-related proteins such as Cbk1.

4.4 Summary

We have used a complex haploinsufficiency-based genetic interaction approach to explore the role of the RAM pathway in *C. albicans* filamentation. One of the motivations for this analysis is that *C. albicans* morphogenesis is affected by a wide variety of genes that are both directly and indirectly related to the process of filamentous growth [2]. As such, we propose that filamentation can function as a general readout of normal *C. albicans* biology in much the same way that colony growth is used to assess synthetic genetic interactions in *S. cerevisiae*. As has been well discussed in the literature, a wide range of factors appear to effect *C. albicans* filamentation, both subtly and dramatically, under filamentation-inducing conditions [2]

At present, it is not completely understood why genes from diverse functional groups affect filamentation. Indeed, this association is, to a certain extent, based on empiric observation. One general model for this association is that some genes are required for the establishment of a physiologic state that sets the stage for filamentation but may have functions that are not directly

related to filamentation. Once this state has been established, a distinct set of genes is required to specifically execute the morphological transition to filamentous growth. Our genetic interaction data and transcriptional profiling results indicate that the specific genes indirectly related to filamentation vary with the conditions under which filamentation occurs. Screens designed to identify genes required for filamentation will not discriminate between these two groups of genes. However, the dependence of filamentation on both directly and indirectly related genes provides a sensitive phenotype for genetic interaction analysis. Thus, we propose that filamentation is a particularly useful phenotype for complex haploinsufficiency-based analysis of *C. albicans* genes because its sensitive nature allows one to detect the relatively subtle consequences of partial loss-of-function mutations.

Understandably, most screens under filament-inducing conditions were focused on identifying genes specific to the process of filamentation. We assert that the filamentation phenotype is also useful for identifying genes and pathways that interact with a query gene but only indirectly affect filamentation. These interactions allow one to infer nonmorphogenesis related functions of genes such as *CBK1*. For example, the screen conducted by Saputo *et al.* (2016) identified functional genetic evidence for the interaction of Cbk1 with a variety of pathways and processes, including the PKA pathway, cell cycle, two-component signaling (Chk1 and Srr1), mitosis through a potential direct interaction with the kinase Mps1, and cell polarity through two proteins related to Cdc42 function[17]. We fully investigated and characterized some of these interactions here. We also uncovered a role for the Cbk1 pathway in the ability of *C. albicans* to withstand oxidative stress. Taken together, these results provide new insights into the multidimensional function of the RAM pathway in *C. albicans* biology and provide further support for the use of complex haploinsufficiency-based genetic analysis as a tool for

understanding the biology of this predominantly diploid human pathogen.

4.5 Materials and Methods

4.5.1 Strains, media and materials

Strains were generated using standard PCR-based methods and correct integrations were confirmed by PCR. For epitope-tagged strains, candidate strains that showed proper integration by PCR were further evaluated by Western blotting to ensure the presence of a band at the expected molecular weight. Yeast culture media were prepared according to published recipes [31]. Filamentation was induced by dilution of a starter culture (overnight growth at 30° in yeast peptone dextrose (YPD) medium starting from a single colony) into fresh inducing medium and incubation at 37° unless otherwise stated. Plates containing hydrogen peroxide were prepared the day prior to use. All chemical reagents were obtained from Sigma-Aldrich (St. Louis, MO) and used without further purification. Oligonucleotides were synthesized by IDT Technologies (Corralville, IA) and used as received.

4.5.2 Plate-based phenotyping

The indicated strains were grown to stationary phase overnight in YPD at 30°, harvested, and adjusted to cell density of 1 OD_{600} in sterile water. Tenfold dilution series were prepared and spotted on the indicated medium using a manual pinning tool. The plates were incubated at 30° or 37° for 1–7 days depending on specific conditions. Plates were photographed and the images were processed using Photoshop with equal brightness and contrast applied to all parts of a given image. At least two independent isolates of each mutant were tested and phenotypes shown in figures are representative of the phenotypes displayed by each isolate.

4.5.3 RNA preparation and quantitative RT-PCR analysis

Yeast strains were inoculated in 5 ml YPD supplemented with uridine and incubated overnight at 30° with shaking at 250 rpm. Cell cultures were diluted to an OD_{600} of ~0.2 in fresh YPD and grown with shaking until OD_{600} of ~1.0 was reached. Alternatively, strains were back diluted in to YPD supplemented with uridine and 10% serum and grown at 37° for 8 hr. Cell cultures were pelleted by spinning at 3000 × *g* for 5 min and the supernatant was removed. When applicable, pelleted cells were washed and then resuspended in PBS with 6 μM of H_2O_2 and incubated at 37° with shaking at 250 rpm for 1 hr. At this point, cells were once again pelleted at 3000 × *g* for 5 min and the supernatant was removed. Pelleted cells were flash frozen in a dry ice/ethanol bath and stored at −80° until ready for use. RNA was extracted using the RiboPure Yeast Kit (Ambion/Life Technologies, Grand Island, NY) following the manufacturer's protocol. Superscript II Reverse Transcriptase Kit (Invitrogen/Life Technologies) was used for complementary DNA (cDNA) synthesis with 2 μg of total RNA as template and Oligo $d(T)_{12–18}$ as primers according to the manufacturer's protocol. Quantitative real-time (qRT) assays were performed in triplicate with a StepOnePlus (Applied Biosciences/Life Technologies) using SYBR Green 1 dye-based detection (Life Technologies). Each reaction contained 10 μl of the SYBER Green PCR Master Mix, 0.15 μM of the appropriate primers, and 120 ng of cDNA template in a total volume of 20 μl. All primers used in qRT-PCR were first analyzed for qPCR efficiency. The qRT-PCR reactions were performed at 95° for 5 min followed by 40 cycles of 30 sec at 95° and 30 sec at 60°. Relative differences in RNA levels were normalized against *ACT1* levels using the $\Delta\Delta C_T$ method.

4.5.4 Microscopy

Light and fluorescence microscopy was performed using a Nikon ES80 epifluorescence microscope equipped with a CoolSnap CCD camera. Images were collected using NIS-Elements Software and processed in Photoshop. To assess mitotic integrity, exponential phase cells (synthetic complete medium, 30°) were harvested and stained with DAPI. The indicated number of cells was scored for the presence of nuclei within large daughter cell buds as described by Kamthan et al. (2014). For Rgd3–GFP localization, WT and cbk1Δ/Δ strains, with GFP integrated at the C terminus of the chromosomal allele, were grown to stationary phase overnight and then either transferred to hyphae-inducing conditions (Spider medium, 37°) or YPD at 30°. Cells were harvested, washed, and examined under bright field and fluorescence channels.

4.5.5 Fitness assay

Yeast strains were inoculated in 5mL YPD supplemented with uridine and incubated overnight at 30°C with shaking at 250 rpm. Cell cultures were diluted to an OD_{600} of 0.2 in fresh YPD. Taking OD600 measurements every hour for nine hours assessed fitness.

4.5.6 H_2O_2 sensitivity assay

Yeast strains were inoculated in 5mL YPD supplemented with uridine and incubated overnight at 30°C with shaking at 250 rpm. Cell cultures were diluted to an OD_{600} approximately 0.2 in fresh YPD and grown with shaking until an OD_{600} of 1.0 was reached. Cells were pelleted by spinning at 3000g for 5 minutes and washed twice in 1X PBS. Pellets were resuspended in 1X PBS containing either 0 μM, 30 μM, 60 μM, 75 μM, or 100 μM of H_2O_2. Cultures were grown for an hour at 37°C with shaking at 200 rpm. Serial dilutions of cultures were plated for each

concentration.

4.6 References

1. McCarty TP, Pappas PG (2016) Invasive Candidiasis. Infect Dis Clin North Am 30: 103-124.

2. Sudbery P, Gow N, Berman J (2004) The distinct morphogenic states of Candida albicans. Trends Microbiol 12: 317-324.

3. Saville SP, Lazzell AL, Monteagudo C, Lopez-Ribot JL (2003) Engineered control of cell morphology in vivo reveals distinct roles for yeast and filamentous forms of Candida albicans during infection. Eukaryot Cell 2: 1053-1060.

4. Noble SM, French S, Kohn LA, Chen V, Johnson AD (2010) Systematic screens of a Candida albicans homozygous deletion library decouple morphogenetic switching and pathogenicity. Nat Genet 42: 590-598.

5. Bharucha N, Chabrier-Rosello Y, Xu T, Johnson C, Sobczynski S, et al. (2011) A large-scale complex haploinsufficiency-based genetic interaction screen in Candida albicans: analysis of the RAM network during morphogenesis. PLoS Genet 7: e1002058.

6. Stearns T, Botstein D (1988) Unlinked noncomplementation: isolation of new conditional-lethal mutations in each of the tubulin genes of Saccharomyces cerevisiae. Genetics 119: 249-260.

7. Haarer B, Viggiano S, Hibbs MA, Troyanskaya OG, Amberg DC (2007) Modeling complex genetic interactions in a simple eukaryotic genome: actin displays a rich spectrum of complex haploinsufficiencies. Genes Dev 21: 148-159.

8. Hickman MA, Zeng G, Forche A, Hirakawa MP, Abbey D, et al. (2013) The 'obligate diploid' Candida albicans forms mating-competent haploids. Nature 494: 55-59.

9. Uhl MA, Biery M, Craig N, Johnson AD (2003) Haploinsufficiency-based large-scale forward genetic analysis of filamentous growth in the diploid human fungal pathogen C.albicans. EMBO J 22: 2668-2678.

10. Saputo S, Chabrier-Rosello Y, Luca FC, Kumar A, Krysan DJ (2012) The RAM network in pathogenic fungi. Eukaryot Cell 11: 708-717.

11. Gutierrez-Escribano P, Zeidler U, Suarez MB, Bachellier-Bassi S, Clemente-Blanco A, et al. (2012) The NDR/LATS kinase Cbk1 controls the activity of the transcriptional regulator Bcr1 during biofilm formation in Candida albicans. PLoS Pathog 8: e1002683.

12. Greig JA, Sudbery IM, Richardson JP, Naglik JR, Wang Y, et al. (2015) Cell cycle-independent phospho-regulation of Fkh2 during hyphal growth regulates Candida albicans pathogenesis. PLoS Pathog 11: e1004630.

13. Saputo S, Kumar A, Krysan DJ (2014) Efg1 directly regulates ACE2 expression to mediate cross talk between the cAMP/PKA and RAM pathways during Candida albicans

morphogenesis. Eukaryot Cell 13: 1169-1180.

14. Kelly MT, MacCallum DM, Clancy SD, Odds FC, Brown AJ, et al. (2004) The Candida albicans CaACE2 gene affects morphogenesis, adherence and virulence. Mol Microbiol 53: 969-983.

15. McNemar MD, Fonzi WA (2002) Conserved serine/threonine kinase encoded by CBK1 regulates expression of several hypha-associated transcripts and genes encoding cell wall proteins in Candida albicans. J Bacteriol 184: 2058-2061.

16. Song Y, Cheon SA, Lee KE, Lee SY, Lee BK, et al. (2008) Role of the RAM network in cell polarity and hyphal morphogenesis in Candida albicans. Mol Biol Cell 19: 5456-5477.

17. Saputo S, Norman KL, Murante T, Horton BN, Diaz J, et al. (2016) Complex Haploinsufficiency-Based Genetic Analysis of the NDR/Lats Kinase Cbk1 Provides Insight into Its Multiple Functions in Candida albicans. Genetics 203: 1217-1233.

18. Mulhern SM, Logue ME, Butler G (2006) Candida albicans transcription factor Ace2 regulates metabolism and is required for filamentation in hypoxic conditions. Eukaryot Cell 5: 2001-2013.

19. Li D, Williams D, Lowman D, Monteiro MA, Tan X, et al. (2009) The Candida albicans histidine kinase Chk1p: signaling and cell wall mannan. Fungal Genet Biol 46: 731-741.

20. Davis-Hanna A, Piispanen AE, Stateva LI, Hogan DA (2008) Farnesol and dodecanol effects on the Candida albicans Ras1-cAMP signalling pathway and the regulation of morphogenesis. Mol Microbiol 67: 47-62.

21. Srikantha T, Daniels KJ, Pujol C, Kim E, Soll DR (2013) Identification of genes upregulated by the transcription factor Bcr1 that are involved in impermeability, impenetrability, and drug resistance of Candida albicans a/alpha biofilms. Eukaryot Cell 12: 875-888.

22. Calera JA, Calderone R (1999) Histidine kinase, two-component signal transduction proteins of Candida albicans and the pathogenesis of candidosis. Mycoses 42 Suppl 2: 49-53.

23. Luo G, Ibrahim AS, Spellberg B, Nobile CJ, Mitchell AP, et al. (2010) Candida albicans Hyr1p confers resistance to neutrophil killing and is a potential vaccine target. J Infect Dis 201: 1718-1728.

24. Kamthan M, Nalla VK, Ruhela D, Kamthan A, Maiti P, et al. (2014) Characterization of a putative spindle assembly checkpoint kinase Mps1, suggests its involvement in cell division, morphogenesis and oxidative stress tolerance in Candida albicans. PLoS One 9: e101517.

25. Weiss EL (2012) Mitotic exit and separation of mother and daughter cells. Genetics 192: 1165-1202.

26. Luca FC, Winey M (1998) MOB1, an essential yeast gene required for completion of

mitosis and maintenance of ploidy. Mol Biol Cell 9: 29-46.

27. Gogl G, Schneider KD, Yeh BJ, Alam N, Nguyen Ba AN, et al. (2015) The Structure of an NDR/LATS Kinase-Mob Complex Reveals a Novel Kinase-Coactivator System and Substrate Docking Mechanism. PLoS Biol 13: e1002146.

28. Willger SD, Liu Z, Olarte RA, Adamo ME, Stajich JE, et al. (2015) Analysis of the Candida albicans Phosphoproteome. Eukaryot Cell 14: 474-485.

29. Dou Z, von Schubert C, Korner R, Santamaria A, Elowe S, et al. (2011) Quantitative mass spectrometry analysis reveals similar substrate consensus motif for human Mps1 kinase and Plk1. PLoS One 6: e18793.

30. Bender A, Pringle JR (1991) Use of a screen for synthetic lethal and multicopy suppressee mutants to identify two new genes involved in morphogenesis in Saccharomyces cerevisiae. Mol Cell Biol 11: 1295-1305.

31. Burke D, Dawson D, Stearns T (2000) Methods in Yeast Genetics. Woodbury, NY: Cold Spring Harbor Laboratory Press.

Figure 4.1 Representative set of strains to confirm CHI phenotypes.
The indicated strains were incubated on YPD + 1% serum at 37°. The double heterozygotes show decreased central wrinkling relative to either the parental *cbk1*Δ/*CBK1* strain or the heterozygous deletion of the interacting gene.

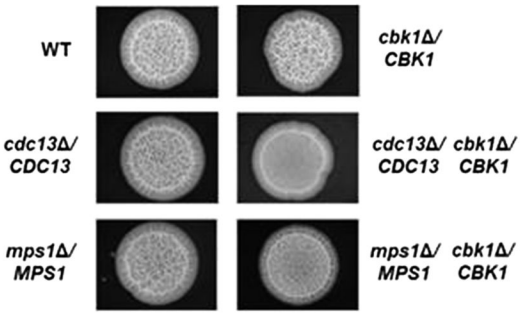

Figure 4.2 Cbk1 is required for oxidative stress tolerance through its regulation of *CHK1* *expression.*

A) The indicated strains were plated (5 µl of cell suspensions at densities of 1 OD_{600} and 0.1 OD_{600}) on YPD or YPD containing 4.5 mM hydrogen peroxide and incubated at 30°. The left legends indicate the parental genotype and right indicate whether the strain is homozygous (+/+) or heterozygous (−/+) at the *CBK1* locus. The phenotypes are representative of independent isolates tested in duplicate. (B) The effect of the indicated mutations on the expression of *CHK1* in the presence of H_2O_2 was determined by RT-PCR using the $\Delta\Delta C_T$ method. The relative transcript levels are expressed as fold change relative to H_2O_2-exposed WT. Bars indicate the mean of biological replicates performed in triplicate and error bars indicate standard deviation.

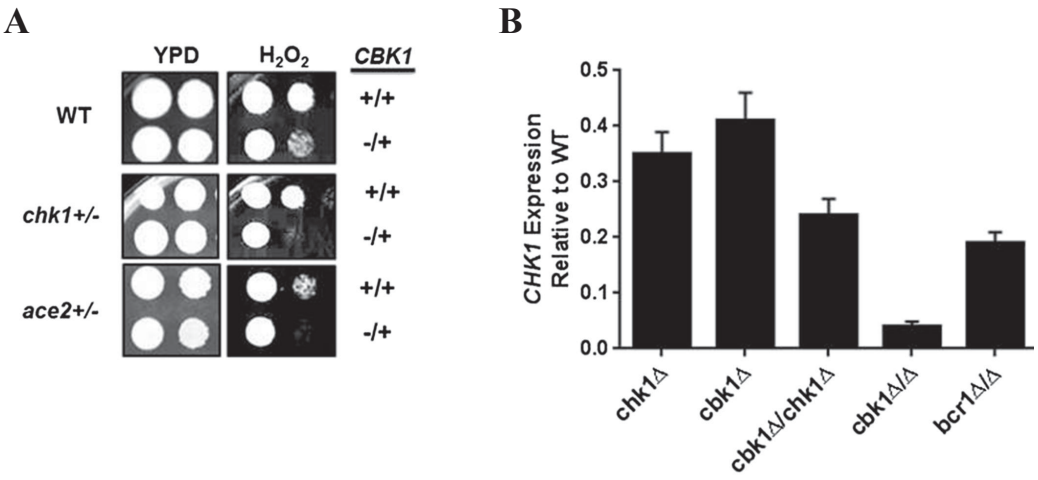

Figure 4.3 *CBK1* interacts with the essential kinase *MPS1* as part of mitosis.
(A) The complex heterozygote *cbk1*Δ/*CBK1 mps1*Δ/*MPS1*has a growth defect in liquid culture at 30° relative to WT and the single heterozygous mutants. The curves were generated from duplicate experiments with technical replicates; error bars indicate standard deviation. (B) Exponential phase WT and *cbk1*Δ/*CBK1 mps1*Δ/*MPS1* cells were stained with DAPI. These images show normal segregation of the nucleus into a large daughter bud for WT and a *cbk1*Δ/*CBK1 mps1*Δ/*MPS1*, demonstrating a cell in a similar stage of cell cycle lacking a nucleus. (C) The proportion of large daughter cells showing the phenotype described in A was determined for each of the indicated strains. The number of cells that were counted is indicated in parentheses on the *y*-axis. The data were analyzed by χ^2 test with $P < 0.05$ used to establish statistical significance.

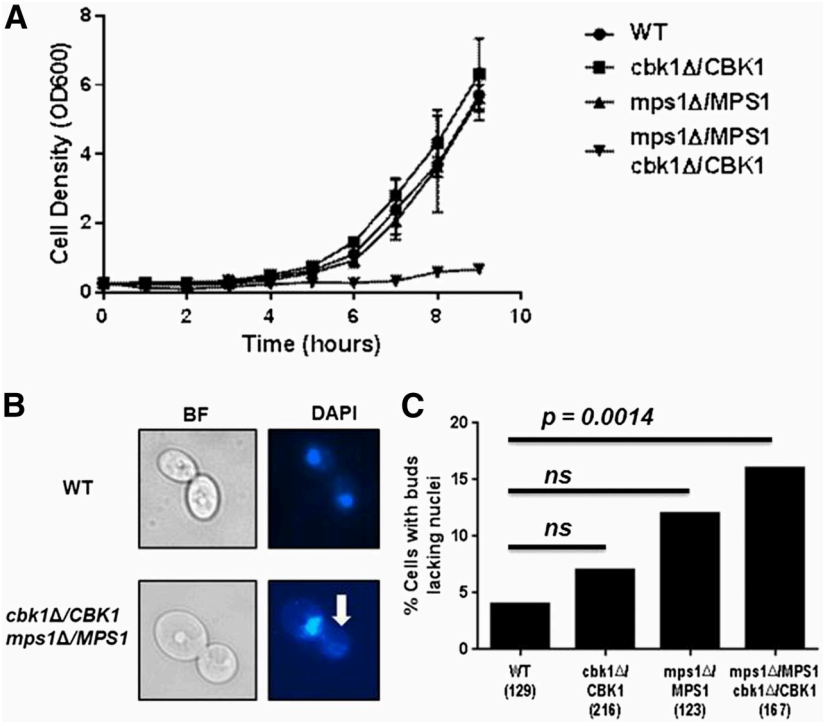

Figure 4.4 *MSB1* interacts with *CBK1* during filamentation on SM.
(A) The indicated strains were incubated on SM at 37° for 6 days and photographed. The heterozygous *MSB1* deletion strain shows decreased peripheral invasion relative to WT and the *CBK1* heterozygote that is suppressed by deletion of *CBK1*. (B) WT strain containing an allele of *MSB1* with a C-terminal GFP tag was incubated in YPD at 30° or SM at 37°; cells were harvested, washed, and immediately photographed at ×40 using the indicated channels. The arrowheads show increased signal focused at septal regions of cells under hypha-inducing conditions. (C) The indicated strains were harvested from yeast (YPD, 30°) or hypha-inducing (SM, 37°) conditions, lysed, and processed for Western blotting with anti-GFP antibodies. The loading control was a nonspecific background band present in nontagged strains.

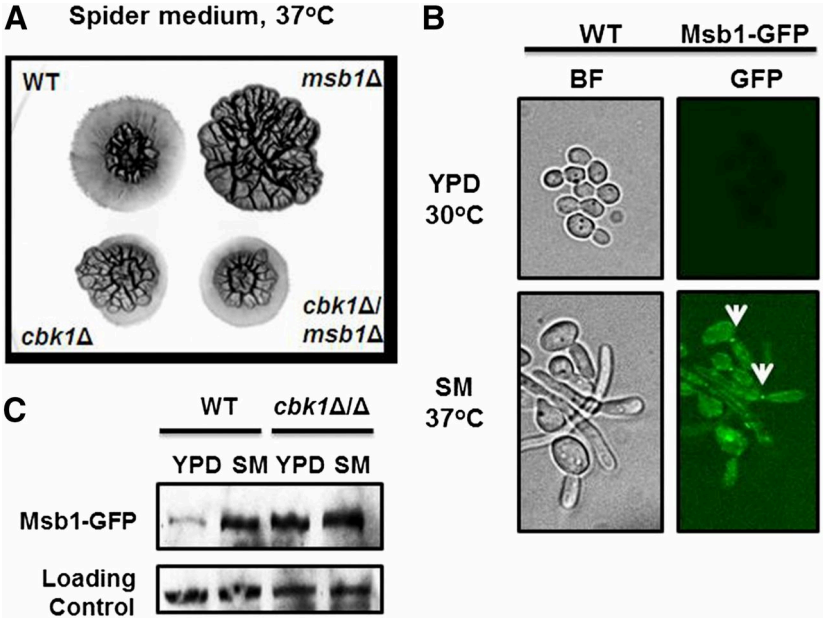

Table 4.1 Genes with complex haploinsufficient genetic interactions with *cbk1*Δ/CBK1 during morphogenesis induced by 1% serum

[a] Assembly 19/21 identifier
[b] Candida Genome Database name
[c] presence of consensus motif *aaCCAgC*
[d] Altered expression in Mulhern *et al.* (2006)
[3] Boldface type indicates essential genes

ORF[a]	Gene name[b]	Description[c]	Ace2p binding site[d]	Altered expression in *ace2*Δ/Δ[e]
FungiDB: orf19.4629	*BUL1*	Ortholog(s) has ubiquitin–ubiquitin ligase activity, role in mitochondrion inheritance.	Yes	No
FungiDB: orf19.6072	***CDC13***[e]	Essential protein, involved in telomere maintenance.	Yes	No
FungiDB: orf19.896	*CHK1*	Histidine kinase; two-component signaling, cell-wall synthesis; hyphal growth defect.	No	No
FungiDB: orf19.4937	*CHS3*	Major chitin synthase of yeast and hyphae; transcript induced at yeast–hyphal transition.	Yes	No
FungiDB: orf19.7612	*CTM1*	Putative cytochrome c lysine methyltransferase; regulated by Gcn2 and Gcn4; transcript induced under weak acid stress.	Yes	No
FungiDB: orf19.7512	*DIT2*	Has domain(s) with predicted electron carrier activity, heme binding, iron ion binding, and oxidoreductase activity.	No	No
FungiDB: orf19.780	*DUR1,2*	Urea amidolyase; hydrolyzes urea to CO_2; use of urea as N source and for hyphal switch in macrophage.	Yes	No
FungiDB: orf19.610	*EFG1*	bHLH transcription factor; hyphal growth, cell-wall gene regulation; roles in adhesion and virulence.	Yes	No
FungiDB: orf19.6160	*EIS1*	Ortholog(s) has role in eisosome assembly and membrane raft, mitochondrion, and plasma membrane localization.	No	Yes
FungiDB: orf19.3066	*ENG1*	Endo-1,3-beta-glucanaseog of *S.*	Yes	Yes

ORF[a]	Gene name[b]	Description[c]	Ace2p binding site[d]	Altered expression in *ace2*Δ/Δ[e]
		cerevisiae Dse4 needed for needed separation.		
FungiDB: orf19.3695	*EPT1*	Ortholog(s) has roles in phosphatidylcholine biosynthetic process.	No	No
FungiDB: orf19.1117	*FDH1*	Protein similar to formate dehydrogenase.	Yes	No
FungiDB: orf19.7293	***MPS1***	Monopolar spindle protein, a putative kinase; essential for growth; periodic mRNA expression, peak at cell-cycle S/G2 phase.	No	No
FungiDB: orf19.1133	*MSB1*	Putative regulator of transcription; role in regulation of adhesion factors.	Yes	No
FungiDB: orf19.2685	*PGA54*	GPI-anchored protein; induced in *CYR1* and *EFG1* mutants or in hyphae; regulated by Tec1p, Egf1p, Ntd80p, Rob1p, and Brg1p.	Yes	Yes
FungiDB: orf19.2619	***PHO113***	Putative constitutive acid phosphatase; Rim101 repressed; possibly an essential gene, disruptants not obtained by UAU1 method.	Yes	Yes
FungiDB: orf19.6134	***SEC39***	Ortholog(s) has role in ER-dependent peroxisome organization, retrograde vesicle-mediated transport.	Yes	Yes
FungiDB: orf19.454	*SFL1*	Transcription factor involved in negative regulation of morphogenesis, flocculation, and virulence.	Yes	No
snR5d	*snR5d*	H/ACA box small nucleolar RNA (snoRNA).	No	No
FungiDB: orf19.6222	*SPO22*	Ortholog(s) has role in regulation of synaptonemal complex assembly and condensed nuclear chromosome localization.	No	No

ORF[a]	Gene name[b]	Description[c]	Ace2p binding site[d]	Altered expression in *ace2Δ/Δ*[e]
FungiDB: orf19.7136	*SPT6*	Putative transcription elongation factor; transposon mutation affects filamentous growth.	No	No
FungiDB: orf19.5843	*SRR1*	Two-component system response regulator; involved in stress response; Plc1 regulated.	Yes	Yes
FungiDB: orf19.6367	***SSB1***	HSP70 family heat shock protein; mRNA in yeast and germ tubes; at yeast cell surface, not hyphae; antigenic in human/mouse infection.	Yes	No
FungiDB: orf19.5175	*SSM4*	Ortholog(s) have ubiquitin-protein ligase activity, role in ER-associated ubiquitin-dependent protein catabolic process.	Yes	Yes
FungiDB: orf19.5297	***TFB1***	Ortholog(s) have phosphatidylinositol-3-phosphate binding, phosphatidylinositol-5-phosphate binding activity.	Yes	No
FungiDB: orf19.7570	*UGA3*	Zn(II)2Cys6 transcription factor; required for utilization of gamma-aminobutyrate (GABA) as a nitrogen source.	Yes	No
FungiDB: orf19.5820	*UGA6*	Putative GABA-specific permease.	Yes	No
FungiDB: orf19.1792	***CDC16***	Ortholog(s) have ubiquitin-protein ligase activity.	Yes	No
FungiDB: orf19.5019	orf19.5019	Uncharacterized ORF.	Yes	Yes
FungiDB: orf19.5070	orf19.5070	Similar to cell-wall mannoproteins; induced in low iron	Yes	No
FungiDB: orf19.7341.1	orf19.7341.1	Uncharacterized ORF; Spider biofilm induced.	No	No
FungiDB: orf.19.7551	*ALO1*	D-Arabinono-1,4-lactone oxidase involved in biosynthesis of dehydro-D-arabinono-1,4-lactone.	No	Yes

ORF[a]	Gene name[b]	Description[c]	Ace2p binding site[d]	Altered expression in *ace2Δ/Δ*[e]
FungiDB: orf19.4231	*PTH2*	Putative cAMP-independent regulatory protein; constitutive expression independent of MTL or white-opaque state.	Yes	No
FungiDB: orf19.1596	***FGR28***	Protein lacking an ortholog in *S. cerevisiae*; transposon mutation affects filamentous growth; possibly an essential gene.	Yes	No
FungiDB: orf19.5759	*SNQ2*	Protein similar to *S. cerevisiae* Snq2p transporter; member of PDR subfamily of ABC family; transposon mutation affects filamentation.	No	Yes
FungiDB: orf19.5992	*WOR2*	Zn(II)2Cys6 transcription factor; regulator of white-opaque switching; required for maintenance of opaque state.	No	No

CHAPTER 5

Future Directions

5.1 Introduction

The future directions presented here are ideas and hypotheses based on work done in Chapter 3. While I will no longer be in the Kumar laboratory to conduct this work, Amberlene De La Rocha has taken up the studies indicated here.

Our data gathered thus far strongly implicate the inositol polyphosphate signaling pathway as being necessary for filamentous growth. Perturbations of any of the IP kinases results in either hyper- or hypo-pseudohyphal growth compared to a wild-type strain. However, there still remain two large questions surrounding the involvement of IPs in pseudohyphal growth regulation: 1) what is regulating the IP kinases and 2) what are the targets of IPs and PP-IPs during the filamentous growth transition. Below is a short list of experiments that I would conduct if I were continuing with this project.

5.2 *In vitro* kinase assays

Data presented in Chapter 3 connects several major kinase cascades as possible regulators of the IP pathways since deletion of the MAPK *KSS1*, *SNF1*, and *FUS3* all result in changes to the inositol polyphosphate pathway under low nitrogen conditions. Specifically, the major changes, as well as the major factors influencing filamentous growth, seem to stem from

the relative ratios of IP_7 isomers and IP_8. Therefore, we hypothesize that upstream regulation of the IP pathway is targeting the down stream IP kinases Kcs1p and Vip1p. It is also possible that upstream kinase cascades may also regulate the phosphatases Ddp1p and Siw14p or a combination of both the kinases and the phosphatases.

It is possible that this regulation is direct, and Kss1p, Snf1p, or Fus3p could directly phosphorylate IP kinases and phosphatases. To determine if these interactions are through direct phosphorylation, I propose that we purify the kinases Kss1p, Fus3p, and Snf1p as well as the potential targets Kcs1p, Vip1p, Ddp1p and Siw14p. We will clone the corresponding gene sequences in to the same plasmid used in Chapter 3 for our overexpression analysis (pSGP47). This will result in the gene of interest under control of a constitutively active *ADH2* promoter with a C-terminal 10x-his tag which we will purify with TALON resin as previously described [1]. We will then conduct *in vitro* kinase assays with all combinations of kinases and substrates. When analyzing the protein sequence of the IP kinases and phosphatases, there are several predicted putative MAPK and AMPK phosphorylation sites making it possible that there are direct interactions. It is also possible that these *in vitro* kinase assays reveal no direct phosphorylation by Kss1p, Snf1p, or Vip1p, suggesting instead that regulation is indirect. Indirect regulation may occur through phosphorylation by another unknown intermediate, which could make finding a direct interaction more difficult.

5.3 Analysis of gene expression through qRT-PCR and protein expression through Western blotting

We cannot eliminate the possibility that regulation is occurring at the transcriptional level as well as the translational level. To determine this, I propose that we utilize qRT-PCR to first

evaluate expression levels of all IP kinases and phosphatases after 8 hours of growth in low nitrogen media to determine if some of the differences in IPs and PP-IPs are due to higher expression levels of certain IP proteins. Additionally, it would be interesting to look at expression levels in low nitrogen upon deletion of *KSS1*, *SNF1*, and *FUS3.* Changes in gene expression do not always equate to changes in protein levels. Therefore, I suggest checking the levels of protein expression through Western blot analysis. There are currently no specific antibodies that recognize the proteins within the IP pathway and it will be necessary to tag each protein with chromosomal sequence encoding a His or HA epitope; chromosomal insertion of the sequence should not dramatically affect the level of protein production relative to inserting a gene copy on a plasmid. Protein expression levels can be compared in regular media and low nitrogen media. Additionally they can also be compared in strains lacking *KSS1, SNF1,* and *FUS3.*

5.4 Summary

We hope that these experiments will help identify if IP kinases and phosphatases regulated at the transcriptional level, translational level, through post-translational modifications, or through a combination of multiple types of regulation. We also hope to identify if this regulation is Kss1p, Snf1p, or Fus3p-dependent. Optimistically, we also hope to identify a direct regulatory link through phosphorylation events by these kinases. Currently, we are unclear how to determine downstream targets of the IP pathway. It is known that IPs and PP-IPs signal by: 1) binding and causing a conformational change, and also 2) through pyrophosphorylation of other proteins. While there are some known domains that often bind these molecules, proteins with these domains are few and do not play an obvious role in regulating pseudohyphal growth.

Recently, a study utilized synthetically made PP-IPs to conduct pull-down assays of an IP_7 isomer to identify binding partners. We believe that this technique could be utilized to conduct a pull-down assay under low nitrogen conditions and we would expect to observe different binding partners. However, these techniques necessitate the ability to synthetically produce IPs and PP-IPs. While this is still a possibility in the future, it is not a realistic experiment to run in the short-term future.

In sum, the mechanisms through which inositol polyphosphate signaling regulates pseudohyphal growth remain to be elucidated. The proposed kinase assays and studies should be productive steps towards understanding these mechanisms, holding potential impact towards defining the molecular basis underlying the pseudohyphal growth transition as well as the processes of inositol polyphosphate signaling under conditions of nitrogen limitation. This metabolic analysis of stress-responsive signaling is likely to be an important area for ongoing study in the budding yeast and other eukaryotes.

5.5 References

1. Szymanski EP, Kerscher O (2013) Budding yeast protein extraction and purification for the study of function, interactions, and post-translational modifications. J Vis Exp: e50921.

APPENDIX

A. HPLC Use and Maintenance in the Kumar Lab

In order to complete chapter three of my thesis work, I required access to a high-performance liquid chromatography machine (HPLC). It was not feasible to borrow another laboratory's equipment for these purposes as this was a new technique to our lab that was going to be instrumental for branching into studies regarding inositol polyphosphate signaling. Additionally, and probably more importantly, the analysis of inositol polyphosphate species requires the use of the radioactive isotope tritium. This document is being added in to my thesis to be used as a guide and handbook for future members of the Kumar Lab who may need to analyze inositol polyphosphate species.

It is important to remember that the space around the HPLC is considered a radioactive space, though it is checked often to make sure no radioactive activity remains. However, because tritium is used heavily within this area standard radioactive precautions must be taken and proper radioactive training must be completed as dictated by the University of Michigan.

A.1 The machine

Our lab utilizes an old HPLC model, Hewlett Packard 1100 series quaternary pump. This model has long been discontinued and HP actually no longer makes HPLC equipment at all. However, this model is the same as Agilent 1100 series and the user manuals are the same[1].

Our HPLC is set up with the quaternary pump (cat. no. G1311A) on bottom with the degasser (G1322A) stacked on top and the buffer shelf on top of that (Fig A.1). The entire system is heavy and if it does need to be moved has to be moved one section at a time making sure to disconnect all interconnected parts. Many of the standard operating procedures on these parts such as locations of power buttons, status lamps, and how the machines are connected by tubing is all available in the manual and it is highly suggested that it is read when needing to remove, clean, or move the equipment.

A.2 Using the HPLC for inositol polyphosphate analysis

A.2.1 Setting up the pumps

Since we have a quaternary pump, we have the ability to use attach four different solutions to four different pumps. The actual process of running our program for separation of inositol polyphosphates only requires the use of two pumps. The standard configuration we use for our pumps is as follows: Buffer A on pump A, Buffer B on pump B, 50% HPLC grade methanol on pump C, and filtered water on pump D. All of our buffers, besides solutions that are bought at HPLC grade, must be filtered and degassed (see section…). HPLC grade methanol is stored in the flammable cabinet and must be labeled with HPLC only otherwise other lab members may accidentally use it instead of standard methanol and HPLC grade methanol is substantially more expensive since it has been purified.

Before the standard configuration can be set up, the pump lines need to be cleaned. A full tube cleaning should always be done prior to attaching the column if the system has been sitting for a long period of time. However, if the column has only been disconnected for a few days or a couple of weeks, a full cleaning may not be necessary. To fully clean each pump, first open the

purge valve (black knob at the front of the quaternary pump) by twisting it to the left. You will notice the knob gets looser. Turning the knob to the left opens up the purge valve and directs liquid to the waste tube instead of the pump outlet capillary. The waste tube is the large diameter white tube attached to the underside of the purge valve while the pump outlet capillary is the very small green tube coming from the top right side of the purge valve. Helpful pictures indicating what each piece is, are found in the manual under the repair section. As long as the purge valve is loose and open, no liquid is moving towards the column area. At this point the flow rate can be increased to anywhere from 2-5 ml/min. It is extremely important to NEVER have the flow rate more than 1 ml/min when the purge valve is closed or this can potentially blow the small capillaries as they have a smaller pressure allowance.

Now that the purge valve is open, flush filtered water through each pump (making sure to clean the pump inlet with water before moving to a new solution). Each pump is flushed individually at 100% A, 100% B, 100% C and 100% D. The control module's default is always to have pump A be the predominate pump. Therefore, when looking at the analysis screen, when B, C, and D all say 0% you are at 100% of pump A. Roughly 25 mL of filtered water should be used for each pump. Once all pumps have been thoroughly cleaned with water, they will all need to be cleaned with 25 mL of HPLC grade isopropanol at a flow of 5 mL/min for 5 min. This high flow rate along with the isopropanol pushes any air out of the system that often builds up in the system after inactivity. Any excess air in the system will cause pressure fluctuations that can be seen on the control module and will ultimately affect the gradient run on the column. If at any time you see large pressure fluctuations, and you have ruled out any leaks, it is good to try an isopropanol flushing.

After isopropanol flushing has been completed on all four pumps (you can't just do one

or two, all pumps need to be done in order to remove air), flush each pump line again with 25 mL of water. When switching between any buffers on a single pump line, it is important to flush the pump line with water in-between any two buffers. For example, if you had a high salt buffer (such as Buffer B), and immediately put methanol or isopropanol through this line without water between the two solutions, the salt would precipitate and clog your line. If this were to happen, you would have to remove your tubing, thoroughly clean it or replace it if the salt precipitate has clogged one of the small filter connections. If salt precipitate reaches the column (or forms inside the column), there is no way to remove this and the pressure will increase beyond safe levels resulting in a ruined column. Therefore, whenever switching buffers always use water in between.

After the second round of water flushing, the pump lines can be primed with their respective solutions as defined in our "standard" set-up above. To be safe, I would flush each pump with at least 25 mL of their respective solution with the purge valve open to make sure all tubing is now fully in the solution you desire.

A.2.2 Attaching the column

The column that we use for inositol polyphosphate analysis is a Partisphere 5 μm SAX cartridge column 125 x 4.6 mm (HiCHROM cat. no. 4621-0505). It comes stored in methanol and when not attached to the HPLC system should always be stored in methanol. A lay out of how the column pieces attach to the HPLC system can be found in Figure A.2 A. Set the system to a flow rate of 0.1 mL/min and a 100% pump D (filtered water). The column will be attached to the blue capillary that comes from the back of the injection device. Before the column, we will first attach the anion guard cartridge (HiChrom cat. no. 4641-0005). This is used to protect the

column and hopefully catch any particles before they hit the column. If pressure builds up, it is best to check if pressure is still relatively high when just attached to the guard cartridge. If so, then this will need to be changed. The guard cartridges come in a pack of 5 and are less expensive than an entire new column so it is better to have these clogged then the actual column.

Place an anion guard cartridge with the silver flat fritted end in to the WVS integral guard cartridge holder (Whatman cat. no. 4631-1003). Attach the guard cartridge holder in to the inlet fitting. Manually tighten until just barely tight, you don't want to over tighten. If any leaks occur in this area, you can tighten more if necessary. The inlet fitting can now be attached to the blue capillary. Run enough water through the system so that you see it coming out of the guard cartridge holder. Now, remove the bottom black cap from the column. The column is used in one direction only and there are arrows on the side that indicate the direction of flow. Once the bottom cap is removed, quickly attach the WVS column end fitting that is attached to the outlet tube. Remove the top black cap of the column and make sure to fill with the water coming out of the guard cartridge holder so there is no air in the column. Tighten the column on to the guard cartridge holder just until tight. Again, you do not want to over tighten anything on the HPLC. At this point, the entire system should be connected and liquid should be starting to flow out of the outlet tube. At a flow rate of 0.1 mL/min it may take a minute or two to start seeing the flow from the outlet tube. Once enough liquid has gone through the tube and you no longer see air bubbles, you are ready to move on. If you do see air bubbles, it is likely there is a leak in the column system, lightly tighten all of the connections until you have gotten rid of all air pockets and there are no leaks.

A.2.3 Ramping up the system

Before completing any runs, you must ramp up the system to a flow rate of 1.0 mL/min.

Once the column is attached, liquid must constantly be flowing over it. If the column sits attached to the HPLC system without any liquid moving over it, the column will dry out. Therefore, we keep a constant flow rate of 0.05 mL/min when not actively doing a run. Normally, we flow Buffer A over the system when it is in between runs. However, when first attaching the column you want to use water to wash out the methanol.

It is important that you do not ramp up flow rate too quickly as this can increase the pressure too drastically and compress or blow out the column. Therefore, the safest way to ramp up the system is by going from 0.05 mL/min to 1.0 mL/min over a minimum period of 30 minutes. I usually use the following strategy: 0.05 mL/min – 0.1 mL/min – 0.25 mL/min – 0.40 mL/min – 0.55 mL/min – 0.70 mL/min – 0.85 mL/min – 1.0 mL/min with a minimum of five minutes at each flow rate. While doing the ramp up, it is important to monitor pressure. When at 0.05 mL/min is water or Buffer A the pressure should be around 2.5-2.8 Bar. When first flushing a column to remove the methanol after it has been in storage it may be slightly more as methanol causes a higher pressure. At a flow of 1.0 mL/min with water or Buffer A the pressure should be around 54-56 Bar. It is important to note the pressure every time. As the pressure gets higher, it may be time to replace the guard cartridge or possibly the column if replacing the guard cartridge does not fix the pressure problem.

A.2.4 Using the column for analysis

Once the column has been properly attached, you need to flush the methanol out of the system. You will need to run 10 mL of water over the system to accomplish this. Since you will have ramped up with pump D at 100% as explained in the section above, you will most likely have gotten all of the methanol out but to be safe, I would run 10mL of filtered water over the

column once more at a flow of 1.0 mL/min. The column is now ready to be equilibrated in Buffer A. Run 10 mL of Buffer A over the system (10 minutes at 1.0 mL/min 100% Buffer A).

A.2.4.1 Blank run

To properly equilibrate the column further as well as to check for proper pressure, and to make sure there are no leaks, a blank run should be done after attaching the column to the system, as well as after any washing of the column (see section…). First, set the injection device to load, where the knob is pushed all the way to left. Remove the injection needle only when in the "load" position. Flush the injection needle three times with water. Fill the injection needle with 300-400 µl of autoclaved water and load this in to the injection device slowly. As long as the injection device stays in the "load" position, your sample (or in this case the water) stays within the injection sample tube and does not go toward the column. On the control panel, the gradient should already be set as desired and can be viewed by pushing the timetable button. If for some reason the gradient has been deleted it is as follows: 0-5 min, 0% buffer B; 5-10 min, 0-10% buffer B; 10-90 min, 10-100% Buffer B; 90-100 min, 100% Buffer B; 100-101 min, 0% buffer B; 101-110 min 0% buffer B. The gradient is run at a flow rate of 1.0 ml/min. Push start to initiate the protocol. A screen will pop up about vial injections. Simply push "OK" and at the exact time you push "OK" also move the injection device in to the "Inject" position by moving the knob all the way to the right. This will move the sample from the injection capillary tube to the column. Do not remove the injection needle when it is in the injection position. The run takes 110 minutes to complete and the protocol is set up so it automatically resets itself to 0.05 ml/min of 0% Buffer B (which is 100% Buffer A). If you wish to continue with another run directly after the blank run, you will need to ramp up the system again to 1.0 mL/min.

While the blank run is going, you do not need to collect samples, simply let the waste collect in the waste bottle. Make sure to monitor the column and the pressure. If you see any leaks in the column, properly tighten. You may not have seen a leak initially but may see it when the percentage of Buffer B gets higher as this also causes a rise in the pressure. Since Buffer B has large amounts of salt, you will see the precipitate form on the outside of the column if leaks do occur. Make sure to wash off residue as soon as possible with water. The run should start roughly at a pressure of 54-56 Bar. This pressure should remain stable for about 5 minutes and then there will be a small spike in pressure as Buffer B goes from 0%-10% from minute 5 to minute 10. From this point on, the pressure will increase steadily over the entire protocol but should never increase drastically. It should max out at a pressure of about 130 Bar when it reaches 100% Buffer B. If you find the pressure is getting much higher then this, make sure to check the anion guard cartridge as well as the column. Also, make sure the pressure ripple always stays below 1% ripple. You can check the ripple by pressing the "m" button on the right side when in the analysis screen. Then press the "status" button that appears. This screen will show you the percentage of ripple that is occurring. If the ripple rises above 1% it means the pressure is fluctuating quickly up and down. This can often be caused by air in the system. If you have tightened everything and this continues to occur, you will need to re-do the pump flushing with isopropanol (see section A.2.1).

Only move on to a real run once your pressure is stabilized and at the correct levels and there are no leaks in the system.

A.2.4.2 Actual run

Before starting an actual run, set up the collection tubes. Fill the collection rack with 90

scintillation tubes, making sure they are all at the same height. Place the collection rack in the fraction collector (Frac-100 from Pharmacia Biotech) and clear the fraction collector of all old protocols by pressing in succession 9-1-store/return. Set the fraction collector to move the collection rack one spot every minute by pressing in succession 7-1-store/return. Move the injection knob to "Load," remove the needle, and flush the needle three times with water. Suction up roughly 100 µl of water, and then suction up your entire sample. Move the column outlet tube in to the arm of the fraction collector so it drips in to the first scintillation tube. Adjust column outlet tube and collection rack if necessary. You are now ready to start your full run. You will need to do three things in quick succession, almost at the same time. Push start to initialize the protocol. This will cause the vial screen to pop up. From here you will need to push "OK," move the injection device to "Inject," and press start on the fraction collector all basically at the same time. Once you have done this, watch the first two collections to make sure the fraction collector is moving at the same time you reach the next minute on the HPLC to make sure they are in sync. You will periodically need to check the fraction collector to make sure that it didn't accidentally skip a scintillation tube (some times it does this for no apparent reason). You will also want to periodically check the HPLC pressure to make sure there are no sudden increases in pressure as well as the column to make sure there are no leaks.

A.2.4.3 Reading samples

Once fractions have been collected, the tubes can be moved in sequential order to the blue scintillation racks, making sure the knob of the scintillation rack is on the left side. One run of 90 should use 5 blue racks. Add 4 mL of Ultima-Flo AP liquid scintillation cocktail (Perkin-Elmer cat. no. 6013599) and shake vigorously. If tubes are not shaken, they will not mix with the

scintillation cocktail and radioactivity cannot be read. Load racks in to the scintillation counter and read levels of tritium radioactivity for 4 minutes per sample. This takes about 6-7 hours to read all 90 samples of one run.

A.2.4.4 Washing the column

After every 3-4 runs, the column must be washed to keep it in optimal shape. At a flow of 0.5 mL/min run **warm** filtered water over the column for 30 minutes. This helps break up precipitates as well as starts to sanitize the column so nothing will grow on it. At a flow of 0.5 mL/min run 50% HPLC grade methanol over the column for 30 minutes to help kill anything that may be stuck on the column. You do not want to run methanol solutions at more than 0.5 mL/min because the pressure will become too high. Again, run filtered water over the column for 30 minutes. The column is now prepped and will need to be equilibrated by running a blank run (see section A.2.4.1).

A.2.4.5 Removing the column

To remove the column, complete a full wash of the column (see section A2.4.4) except stop after the methanol flushing. Once the column is in methanol, lower the flow to 0.05 mL/min. Remove the column from the guard cartridge holder and place a black cap on top. Remove the WVS outlet fitting and place a black cap on the bottom. It is now safe to turn off the entire HPLC system.

A.3 Inositol Polyphosphate Extraction Protocol

* Note: This protocol is adapted from a previously published protocol from the Sairaidi lab [2]. It

is presented here with modifications.

A.3.1 Buffers

Extraction Buffer

- 1M Perchloric Acid ($HClO_4$) – Sigma Aldrich cat. no. 244252
- 3 mM EDTA - add EDTA directly before use
    - The addition of EDTA helps prevent IPs salt insoluble complexes from forming

Neutralization Buffer

- 1M Potassium carbonate (K_2CO_3) - Sigma Aldrich cat. no. P5833
- 3 mM EDTA – add EDTA directly before use

Buffer A

- 1 mM EDTA
    - Usually make in 4 L batches
- Filter sterilize with a 0.2 μm pore filter and degas for an hour
- Gently poor in to autoclaved bottles

Buffer B

- 1 mM EDTA
- 1.3 M Ammonium phosphate dibasic ($(NH_4)_2HPO_4$)
- pH to 3.8 with phosphoric acid (H_3PO_4)
- Make in a 4 L volume as every time you make a batch of Buffer B, you may need to

check standards as peaks can run slightly differently.

- Filter sterilize with a 0.2 μm pore filter and degas for an hour
- Gently poor in to autoclaved bottles

A.3.2 Standards

To determine peak location, standard strains can be run which have a consistent profile reported in the literature. Use strains *plc1Δ, arg82Δ, ipk1Δ, kcs1Δ*, and if possible *ipk1Δkcs1Δ*. Diploid versions can also be used.

A.3.3 Labeling with Tritiated Inositol

- Inoculate 5 mL of appropriate media with strain of interest and grow overnight at 30°C with shaking at 250rpm.
- On the next day, in the late afternoon, add 5 mL of synthetic media without inositol (supplemented with necessary amino acids) to a plastic 50 mL conical tube.
    - Poke 3-4 holes with a needle in the cap of the tube to make sure that they cultures can aerate.
- Place 5 μl of saturated overnight culture in to media
- Add 25 μl of *myo*[1,2-^{3}H]inositol 30 Ci/mmol 1mCi/ml to the culture and let grow at 30°C shaking at 250 rpm for 12-16 hours or until almost at an OD_{600} of 1.0
    - Some strains will take longer to reach this point.
    - **NOTE:** From this point forward, everything will have radioactivity in it.
        - Dispose of all materials properly including tubes used to grow cultures.
        - Use appropriate protective wear.

        - Work only in the designated radioactive areas.
- Spin down cells at 3000 rpm for 5 min and discard supernatant in radioactive waste.
- Wash pellet 2 times with 5 ml of water discarding water in to radioactive waste.
- If no nitrogen stress will be utilized:
    - Freeze pellet at -80°C for future use.
        - Pellets are stable for several months at -80°C.
    - Or continue on to inositol polyphosphate extraction.
- If nitrogen stress will be utilized:
    - Resuspend washed pellet in 5 ml of SLAD minus inositol supplemented with necessary amino acids
    - Grow at 30°C with shaking at 250 rpm for 8 hours
    - Spin down cells at 3000 rpm for 5 min and discard supernatant in radioactive waste
    - Wash pellet 2 times with 5 ml of water discarding water in to radioactive waste
    - Freeze pellet at -80°C for future use
        - Pellets are stable for several months at -80°C
    - Or continue on to inositol polyphosphate extraction

A.3.4 Extraction of Inositol Polyphosphate

- Thaw frozen pellets on ice
- Resuspend pellets in 300 µl of Extraction Buffer and move to a screw top tube
- Add 425-600 µm acid washed glass beads (Sigma Aldrich cat. no. G8772) to just below the liquid level (usually 2-3 scoops).

- Break cells by bead beating in cold room at 4°C using the Vortex Genie 2 for 5 minutes.
- Cool cells on ice for 1 minute.
- Centrifuge at full speed for 5 min at 4°C.
- Transfer supernatant to a new 1.5 ml eppindorf tube making sure not to disturb the pellet.
- Neutralize the sample to a pH between 6 and 8
    - Start by adding 135 µl of Neutralization Buffer.
        - Add slowly as solution will fizz.
    - Flick cells to mix and let sit on ice until clear layer starts to separate on top of the sample
    - Test the pH to make sure it is between 6-8. Use 5.0-9.0 Plastic pH Indicator Strips (Fisherbrand cat. no. 13-640-519). Add 2 µl from cleared liquid on top to pH strips to test.
        - If it is not, add either Neutralization Buffer or Extraction Buffer (as appropriate) in 2-5 µl increments until the pH has been reached
- Leave the tubes open on ice for 2 hours flicking the tubes to mix at least every 30 minutes.
    - Alternatively, neutralization can go over night by closing cap of tube and poking a hole in the middle of the cap with a needle and placing at 4°C.
- Centrifuge the samples at full speed at 4°C for 10 minutes.
- Very carefully transfer the supernatant to a new tube.
    - Spin down again to make sure none of the pellet was taken as this will clog the column
- Samples can be kept at 4°C for two weeks.

- Run on the HPLC as directed in section A.2.4.2

A.4 References

1. (1999) Agilent 1100 Series Quaternary Pump: Reference Manual. Agilent Technologies. Germany.

2. Azevedo C, Saiardi A (2006) Extraction and analysis of soluble inositol polyphosphates from yeast. Nat Protoc 1: 2416-2422.

Figure A.1 HPLC system set up

Figure A.2 Order of column pieces from top to bottom (shown left to right)